Size Controlled Fabrication of Starch Acetate Nanoparticles and Assessment of their Potential Applications as Hydrophobic Drug Carriers

Getahun Paulos Teka

A Thesis submitted to

The Department of Pharmaceutics and Social Pharmacy

School of Pharmacy, College of Health Sciences, Addis Ababa University

Presented in Partial Fulfilment for the Requirements of the Degree of Doctor of Philosophy in Pharmaceutics

Addis Ababa University

Addis Ababa, Ethiopia

March 2019

Addis Ababa University

School of Graduate Studies

This is to certify that the thesis prepared by Getahun Paulos, entitled: "Size Controlled Fabrication of Starch Acetate Nanoparticles and Assessment of their Potential Applications as Hydrophobic Drug Carriers" and submitted in partial fulfilment of the requirements for the Degree of Doctor of Philosophy (Pharmaceutics) complies with the regulations of the University and meets the accepted standards with respect to originality and quality.

Signed by the Examining Committee:

External Examiner: Prof. Dr. Alfred Fahr Signature: …….…….…….. Date: …….

Internal Examiner: Dr. Anteneh Belete Signature: ……..….……Date: …….

Advisor: Prof. Tsige Gebre-Mariam Signature: ……..……Date: ……

Advisor: Prof. Dr. Dr. Reinhard HH. Neubert Signature: …….…….Date: ……

_____

Chair of Department or Graduate Program Coordinator

Abstract

Size Controlled Fabrication of Starch Acetate Nanoparticles and Assessment of their Potential Applications as Hydrophobic Drug Carriers

Getahun Paulos,

Addis Ababa University, 2019

Over the past few decades, there has been considerable interest in developing biodegradable polymer-based nanoparticles (NPs) to effectively deliver a drug to a target site. Polymeric materials used for preparing NPs for drug delivery must be biocompatible and preferably biodegradable. Starch has been a focus of increasing attention in recent years for the design and engineering of novel nanoparticulate drug delivery systems due to its desirable attributes including plentiful availability, renewability, biocompatibility, biodegradability, nontoxicity and ease of modification. The objectives of this study were to fabricate NPs from acetylated starches having particle size less than 200 nm with minimum polydispersity index (PDI); to investigate if the origin of starch has effect on the particle size and PDI of starch acetate (SA) NPs; to investigate the potential applications of SA as nano drug carrier with respect to drug loading (DL) capacity, encapsulation efficiency (EE) and release profile; and to determine the influence of solubility and partition coefficient of different drugs on the characterstics of starch-based NPs. To meet these objectives, acetylated starch was first synthesized by reacting native (cassava, dioscorea, enset and maize) starches with acetic anhydride (AA) in the presence of sodium hydroxide as a catalyst. Starch acetate nanoparticles (SANPs) were then fabricated via spontaneous emulsification solvent evaporation method (using, chloroform, dichloromethane or ethyl acetate; surfactants - Pluronic® F68, Pluronic® F127, Polyvinyl Alcohol (PVA) or Tween® 80) and nanoprecipitation method (using Pluronic® F127). A systematic investigation of independent variables revealed that solvent type, surfactant type and concentration, and homogenization speed and time have significant influence on the size and PDI of SANPs. Hence, response surface methodology (RSM) based on central composite design (CCD) was employed to fabricate the desired SANPs (particle size less than 200 nm and PDI < 0.2) under optimized condition. According to RSM based on CCD, the predicted optimum responses (particle size and

PDI) of SANPs of cassava starch were found to be 94.48 ± 1.622 nm and 0.107 ± 0.024, respectively, whereas, the experimentally determined responses were found to be 96.37 nm ± 1.208 nm and 0.131 ± 0.021, respectively using emulsification solvent evaporation method. The predicted optimum responses and experimentally determined responses obtained under optimal fabrication conditions of independent variables (consisting of ethyl acetate, 1.51% of Pluronic® F127, homogenization speed of~15,000 rpm and homogenization time of ~16 min) were therefore found to be in reasonable agreement. Hence, judicious selection of solvent system and surfactant as well as optimizing formulation and process variables is crucial in order to fabricate the desired NPs. Based on the optimized conditions for fabrication of NPs, comparative study was conducted to determine if the origin of starch has effect on particle size and PDI of SANPs. The size and PDI of SANPs fabricated by emulsification solvent evaporation method were found to be 94.48 nm ± 1.622, 0.107 ± 0.024 (cassava), 90.27 nm ± 4.257, 0.133 ± 0.031 (dioscorea), 98.74 nm ± 2.975, 0.176 ± 0.011 (enset) and 104.61nm ± 2.766, 0.076 ± 0.001 (maize), respectively. SANPs fabricated by nanoprecipitation method were found to be 211.52 nm ± 7.42, 0.356 ± 0.016 (cassava), 201.74 nm ± 9.53, 0.243 ± 0.051 (dioscorea), 207.63 nm ± 5.75, 0.283 ± 0.035 (enset) and 216.691nm ± 6.80, 0.203 ± 0.027 (maize), respectively. The size and PDI of cassava SANPs fabricated either by emulsification solvent evaporation or by nanoprecipitation methods were significantly different from those NPs obtained from dioscorea, enset or maize SAs ($p < 0.05$). Similar differences were also observed among the NPs of dioscorea, enset and maize SAs, indicating the origin of starch has significant effect on fabrication of SANPs. Based on ICH guideline, SANPs stored for 3 months at different storage conditions (5°C ± 3°C, 25°C ± 2°C/60% ± 5% RH and 40°C ± 2°C/75% ± 5% RH) remained stable. SANPs prepared from various SAs with different degrees of substitution (DS) were loaded with ibuprofen or oat ceramides (CERs) and their properties, namely, size, PDI, DL, EE, release profiles were studied. Like unloaded SANPs, ibuprofen or oat CERs loaded SANPs were also fabricated with desired particle size (< 200 nm) and PDI (< 0.2). The DL and EE of SANPs increased with an increase in the DS. The average DL of ibuprofen and oat CERs loaded SANPs increased from 9.3 to 26.6% and 8.8 to 21.2%, respectively as DS of SAs increased from low (0.91) to high (2.74). Similarly EEs of ibuprofen and oat CERs increased from 44.7 to 78.3% and 2.2 to 85.2%, respectively. *In vitro* drug release of ibuprofen was sustained over 8 h of study period. Drug release profile of SANPs followed Higuchi Model. *In vitro* a comparative artificial membrane penetration study,

the release and penetration of oat CERs from microemulsion (ME) was higher than from SANPs. Over 90% of oat CERs incorporated in ME, and 59-63% oat CERs in the SANPs were released and penetrated into multilayer membrane system after 60 min. Thus, compared to ME, SANPs retarded the release of oat CERs into the artificial membrane. Hence, this study provides insight into the potential applications of SANPs as sustained release nano drug carrier. Finally, the effects of solubility and partition coefficient of different model drugs based on Biopharmaceutics Classification System (BCS) Class II (ibuprofen), BCS Class III (acyclovir) and BCS Class IV (furosemide) on DL, EE and release profile of SANPs were investigated. The results showed that the DL and EE of ibuprofen and furosemide-loaded SANPs increased consistently with an increase in the DS of SA. On the contrary, DL and EE of acyclovir-loaded NPs decreased as DS of SA increased. Due to their poor solubility and high partition coefficient, the EEs of ibuprofen (77.9%) and furosemide (80.5%) in SANPs fabricated from SA with high DS were much greater than that of acyclovir (50.9%). Furthermore, as DS of SA increased, the cumulative release of ibuprofen from SANPs was retarded whereas the release of acyclovir was enhanced. On the other hand, furosemide, the most lipophilic drug of all, exhibited the lowest extent of release over the study period. Hence, along with the hydrophobic nature of SA, the DL, EE and drug release profile from SANPs were dependent on the solubility and partition coefficient of the incorporated drug molecule. In conclusion, the favourable particle size, PDI, DL and EE with sustained drug release profile suggest that SANPs could be regarded as promising carriers in nano drug delivery systems.

Keywords: Acetylated starch, Central composite design, Drug loading capacity, Emulsification solvent evaporation, Encapsulation efficiency, Nanoprecipitation, Particle size, Polydispersity index, Release profile, Response surface methodology, Starch acetate nanoparticles

Acknowledgements

First of all, I must praise the only Beloved Son of Almighty God, Lord and Saviour, Jesus Christ for the marvellous things He has done for me. I can do nothing without His great mercy and unending love.

Next, I feel honoured to acknowledge my advisors, Prof Tsige Gebre-Mariam and Prof. Reinhard Neubert for their suggestions, guidance, patience, encouragement and support throughout my study. Dear Prof Tsige, I have been searching for premium words to articulate your passion to help; your scientific maturity and wisdom to guide and your determination to enable one realize his goals. One could seldom find an advisor like you who always finds the time for listening to the little problems and roadblocks that unavoidably crop up in the course of performing research. When I had been in Halle for lab works, I came to understand that you are not only my advisor, but elder brother who cares. Dear Prof., you have been investing on me since my undergraduate studies. Your dynamism, professionalism, sincerity and patience always give me the strength to progress.

My thanks and gratitude also go to Dr. Yahya Mrestani, for his technical assistance during FT-Raman spectroscopic determination of the samples. I thank Dr. Frank Heyroth for his help in determination of starch acetate morphology. I must show appreciation to my close friends and colleagues Dr. Efrem Nigussu and others for encouragement and comments. I thank all members of the Department of Pharmaceutics and Social Pharmacy, friends and technicians. I am grateful to Addis Ababa University for financial support, Institute of Pharmacy, Martin Luther University, Halle for technical support and Jimma University for sponsorship. I am highly indebted to the "welcome to Africa-DAAD project", Alexander Von Humboldt Foundation for sponsoring this work and arranging my visit to MLU.

Last but not Least, I must thank my beloved sisters and brothers for their love and empathy. My beloved wife Feven Fiseha, my baby Emmanuel; your love has given me strength and determination. God bless your years! Finally, I would like to dedicate this dissertation to my mom, Nigist Belayneh and my dad Paulos Teka.

Table of contents

List of Tables

List of Figures

Acronyms/Abbreviations

AA:	Acetic Anhydride
AAU:	Addis Ababa University
ACY:	Acyclovir
ANOVA:	Analysis of Variance
BCS:	Biopharmaceutics Classification System
CCD:	Central Composite Design
CER:	Ceramide
DS:	Degrees of Substitution
DMSO:	Dimethyl Sulfoxide
ESEM:	Environmental Scanning Electron Microscope
FITC:	Fluorescein Isothiocyanate
FRS:	Furosemide
HA:	Hyaluronic acid
IBU:	Ibuprofen
ME:	Microemulsion
NP:	Nanoparticle
NSAID:	Non-steroidal Anti-Inflammatory Drug
PBS:	Phosphate Buffer Solution
PCL:	Poly-ε-caprolactone
PDI:	Polydispersity Index
PEG:	Polyethylene Glycol
PLA:	Polylactic acid
PLGA:	Poly-D-L- lactide-co-glycolide
PVA:	Polyvinyl Alcohol
SA:	Starch Acetate
SANP:	Starch Acetate Nanoparticle
SLNs:	Solid Lipid Nanoparticles
SNNPR:	Southern Nations and Nationalities People Region
RSM:	Response Surface Methodology
TDDS:	Transdermal Drug Delivery System
UV:	Ultra-Violet

CHAPTER 1: INTRODUCTION

Nanotechnology is the design, characterization, synthesis and application of materials, structures, devices and systems by controlling shape and size at nanometer scale (Bhowmik *et al.,* 2009; Drexler, 1987). Recent years have witnessed the unprecedented growth of research and applications in the area of nanotechnology. There is increasing optimism that nanotechnology, as applied to medicine, will bring significant advances in the diagnosis and treatment of diseases (Ochekpe *et al.,* 2009). Anticipated applications in medicine include drug delivery, *in vitro* and *in vivo* diagnostics, nutraceuticals, and production of improved biocompatible materials (Arayne *et al.,* 2007; Mahapatro and Singh, 2011).

Nanomaterials are solid or liquid materials at the nanoscale. Several literatures regard materials ranging between 1 nm and 100 nm as nanomaterials (Lövestam *et al.,* 2010). The most widely used term for solid nano-sized material is known as nanoparticles (NPs). NPs are particulate dispersions or solid particles of polymers, lipids, or inorganic materials. In pharmaceutical applications, typically, the drug of interest is dissolved, entrapped, adsorbed, attached and/or encapsulated into or onto a nano-matrix (Barratt, 2000).

The reason why these NPs have been attractive for medical purposes is based on their important and unique features, such as their much larger surface to mass ratio than other particles (Ochekpe *et al.,* 2009; Jong and Borm, 2008; Mahapatro and Singh, 2011). When drugs are loaded into NPs through physical encapsulation, adsorption or chemical conjugation, the pharmacokinetics of the drugs can be significantly improved in contrast to the conventional formulations (Zhang *et al.,* 2004; Jain *et al.,* 2011).

Some of the additional reasons of designing NPs as drug delivery devices include: Particle size and surface characteristics of NPs can be easily manipulated to achieve both passive and active drug targeting after administration through different routes such as parenteral, oral, nasal, intra-ocular etc. (Singh *et al.,* 2010); NPs control and sustain the release of drug during the transportation and at the site of localization so as to increase drug therapeutic efficacy and reduce side effects (Parveen *et al.,* 2012); NPs enable the delivery of drugs that are poorly water soluble. The technology increases oral bioavailability of drugs due to their specialized uptake mechanisms such as absorptive endocytosis and can provide means of bypassing the liver, thereby preventing the first pass metabolism (Rieux *et al.,* 2006); NPs are also able to penetrate tissues and are easily taken up by cells, allowing for efficient delivery of drugs to

target sites of action, i.e., they can pass through the smallest capillary vessels because of their ultra-tiny volume and avoid rapid clearance by phagocytes so that their duration in blood stream is greatly prolonged; they can penetrate cells and tissue gap to arrive at target organs such as liver, spleen, lung, spinal cord and lymph (Parveen *et al.*, 2012).

1.1. Types of NPs as drug delivery vehicles

Over the past few decades, many types of NPs have been developed as drug delivery vehicles. Besides their unique size and surface properties, each nanomaterial offers additional functionalities to improve the pharmacokinetics and pharmacodynamics of loaded drugs. Herein, three widely investigated nanocarriers, namely, polymeric NPs, lipid-based NPs and inorganic NPs are introduced.

1.1.1. Polymeric NPs

Polymeric NPs are colloidal solid particles that are developed from non-biodegradable and biodegradable polymers (Hughes, 2005; Singh and Lillard, 2009). Polymeric NPs are promising vehicles for drug delivery to specific targets (Birrenbach and Speiser, 1976). Polymer based NPs effectively carry drugs, proteins, and DNA to target cells and organs. Their nanometer size promotes effective permeation through cell membranes and stability in the blood stream. Polymeric NPs can be conveniently prepared either from natural or synthetic polymers. Some of natural and synthetic polymers used in the fabrication of NPs include chitosan, alginate, albumin, gelatin, polyacrylates, polycaprolactones, poly (D, L-lactide-co-glycolide) and poly (D, L-lactide) (Ochekpe, *et. al.*, 2009; Mora-Huertas *et al*., 2010).

1.1.2. Lipid based NPs

The other important materials for preparation of NPs are lipids. The most widely used lipoidal NPs are liposomes and solid lipid NPs. Liposomes are lipid vesicles (50-100 nm) entrapping compounds in the inner phase or bilayers depending on their physicochemical property and potentially loading all kinds of active agents. Liposomes have been applied as drug carriers due to their ability to prevent degradation of drugs, reduce side effects and target drugs to site of action. They are developed from phospholipids such as phosphatidylcholine, phosphatidylglycerol, phosphatidylethanolamine and phosphatidylserine (Singh and Lillard, 2009).

Solid lipid nanoparticles (SLNs) are nanostructures made from solid lipids such as glyceryl behenate (Compritol), stearic triglyceride (tristearin), cetyl palmitate and glycerol tripalmitate (tripalmitin). SLNs combine the advantages of polymeric NPs, emulsions, and liposomes (Subedi *et. al.,* 2009; Zhang *et al.,* 2011). They have attracted increased attention because of their unique structure and properties, such as good biocompatibility, product protection against degradation, site-specific drug targeting and controlled drug release.

1.1.3. Inorganic NPs

Inorganic NPs are prepared usually from materials such as ceramic, metal and carbons (Xu *et al.,* 2006). Ceramic NPs are particles fabricated from inorganic compounds with porous characteristics such as silica, alumina and titania. They can be prepared with the desired size, shape and porosity. Their sizes are less than 50 nm and are able to avoid uptake by the reticulo-endothelial system as foreign bodies. Similarly, their large surface area provides the ability to carry a relatively higher dose of drugs. However, these particles are not biodegradable and hence may accumulate in the body and cause harmful effects (Koo *et al.,* 2005). Metallic NPs include iron oxide, gold, silver, gadolinium and nickel which have been studied for targeted cellular delivery (Hughes, 2005).

Carbon nanomaterials include carbon nanotubes and fullerenes. Fullerenes are carbon allotrope made up of 60 or more carbon atoms with a polygonal structure. Nanotubes have been used for their high electrical conductivity and excellent strength. These materials are being studied for therapeutic applications. Fullerenes can be functionalized for delivery of drugs and biomolecules across cell membrane to mitochondria. Carbon nanotubes' unique properties include low cytotoxicity and good biocompatibility attracting attention for their use as vectors in targeted delivery of drugs, proteins and genes (Bianco, 2005).

1.2. Biodegradable polymers used in nano drug delivery

Many types of nanomaterials have been developed as drug delivery vehicles over the past few decades. Although each type of drug-carriers has its unique advantages and drawbacks, their safety as carriers in drug delivery systems causes great concern. Some inorganic nanomaterials possess optical and magnetic properties, but it is hard to ignore their inflammatory effect and toxicity on cells after repeated administration (Guzmán *et al.,* 2006). For example, studies have shown that NPs of titanium oxide can induce DNA damage and cell death (Nakagawa *et al.,* 1997). Carbon nanotubes, as emerging drug delivery platforms,

have been reported to cause granulomas in lungs of laboratory animals (Lam *et al.,* 2004). As a result, research has focused on developing more biocompatible and biodegradable polymeric NPs as effective drug delivery devices. A few of the most extensively used biodegradable polymer matrices for preparation of NPs are summarized below.

1.2.1. Albumin

Albumin is synthesized in the liver and is the main human blood plasma protein which constitutes about 55-60% of all plasma proteins. Albumin is a versatile protein carrier with several characteristics that make it an ideal candidate for drug delivery (Elsadek and Kratz, 2012). It has been shown to be biodegradable, nontoxic, metabolized *in vivo* to produce innocuous degradation products, non-immunogenic, easy to purify and soluble in water. Among the different nano-devices that have been developed in recent years, protein-based NPs have gained considerable interest from scholars to be used as ideal candidates for NP preparation (Elzoghby *et al.,* 2012).

1.2.2. Alginate

Alginate is an anionic polysaccharide comprising of linear copolymers of guluronic and mannuronic acid residues and is now known to be a whole family of safe and haemocompatible polymers which do not show any significant accumulation within major organs and have provided evidence of *in vivo* degradation (Gazori *et al.,* 2009). Alginate-based NPs are hydrophilic carriers which prolong the drug release and enhance its therapeutics activity (Sarei *et al.,* 2013).

1.2.3. Chitosan

Chitosan is a naturally occurring linear polysaccharide composed of primarily of repeating units of D-glucosamine. It is structurally similar to cellulose, and the presence of highly reactive amino groups renders the polymer a net positive charge (Dutta *et al.,* 2004). Chitosan is the most common polymer currently used for drug/gene delivery because of its biocompatibility, mucoadhesive nature, and permeation enhancement potential. It can be enzymatically degraded *in vivo* into oligomers and finally to N-glucosamine, which is endogenously present in the human body (Huang *et al.,* 2004). The use of chitosan NPs offers many advantages, providing targeted delivery of drugs, improving the bioavailability and stability of the therapeutic agents against chemical/enzymatic degradation (Shi *et al.,* 2011).

1.2.4. Gelatin

Gelatin is a naturally occurring protein polymer with relatively low antigenicity and is extensively used in food and medical products. Its biodegradability, biocompatibility, non-toxicity, ease of chemical modification and cross-linking make gelatin-based NPs an efficient carrier in delivery and controlled release of drugs. It is known that the mechanical properties such as swelling behaviour and thermal properties of gelatin NPs depend significantly on the degree of crosslinking between cationic and anionic groups. These properties of gelatin can be manipulated to prepare the desired type of NPs (Ofokansi, *et al.*, 2010).

1.2.5. Hyaluronic acid (HA)

HA is a glycosaminoglycan disaccharide occurring as a natural hydrophilic polyanionic linear polymer composed of glucuronic acid and N-acetylglucosamine repeats via a β-1→4 linkage. HA is one of the main components of the extracellular matrix, present abundantly in various organs including connective, epithelial and neural tissues (Cho *et al.*, 2011). It is a biocompatible and biodegradable linear polysaccharide with good chemical stability (Jin *et al.*, 2010). The carboxylic acid groups in the structure of HA provide one of the best functional moieties to conjugate drugs or targeting ligands (Varnamkhasti *et al.*, 2015). During fabrication of NPs, it forms core-shell polymeric structure making it suitable for encapsulating of therapeutic and/or imaging molecules into inner hydrophobic cores (Han *et al.*, 2013).

1.2.6. Pectins

Pectins typically consist of a complex family of structural polysaccharides present in all plant primary cell walls and contain large quantities of poly-(d-galactouronic acid) linked by a-1,4-glycosidic bonds. Pectin has long been emerged in the development of biodegradable carriers for colon-targeted drug delivery (Morris *et al.*, 2010). Pectin NPs are considered as hydrophilic gel NPs which can efficiently encapsulate water-soluble drugs (Zhang *et al.*, 2015).

1.2.7. Polylactic acid (PLA)

PLA is a biocompatible and biodegradable polymer which is broken down to monomeric units of lactic acid in the body. Lactic acid is a natural intermediate/by-product of anaerobic respiration, which is converted into glucose by the liver. The use of PLA NPs is therefore safe and devoid of any major toxicity. PLA NPs have been used to develop protein and

peptide based nanomedicines, nano-vaccines, and genes containing NPs for *in-vivo* delivery systems (Nobs *et al.,* 2004).

1.2.8. Poly-D-L- lactide-co-glycolide (PLGA)

PLGA is aliphatic biodegradable copolymer which is synthesized by means of ring-opening copolymerization of two different monomers, namely lactic and glycolic acids (Lin *et al.*, 2002). The combination of polylactic acid (PLA) and polyglycolic acid (PGA) yields one of the most successfully developed biocompatible and biodegradable polymers, especially in drug delivery. It is widely utilized to manufacture nano- and microparticles (Jagur-Grodzinski, 1999). It undergoes hydrolysis in the body to produce biodegradable metabolite monomers such as lactic acid and glycolic acid. These metabolites are normally found in the body and participate in a number of physiological and biochemical pathways. Hence, there is very minimal systemic toxicity associated with the use of PLGA for the drug delivery or biomaterial applications (Feczkó *et al*., 2011).

1.2.9. Poly-ε-caprolactone (PCL)

PCL is biodegradable and biocompatible synthetic aliphatic polyester that is widely used in drug delivery applications. It is a highly hydrophobic crystalline polymer that degrades by hydrolysis of its ester linkages under the normal physiological conditions in the human body and has minimal or no toxicity. PCL has attracted the attention of researchers as a candidate of choice for use in drug delivery and long-term implantable devices. NPs made from PCL have promising biomedical applications because of their desirable features including: high colloidal stability in a biological fluid, facile cellular uptake by endocytosis, low toxicity *in vitro* and *in vivo*, and controlled release of their cargo (Chawla and Amiji, 2002).

1.2.10. Starch

Starch is the second most abundant biopolymer produced in higher plants after cellulose. It is the major dietary source of carbohydrates and occurs as granules in the chloroplast of green leaves and the amyloplast of seeds, pulses, and tubers (Ellis *et al.,* 1998). Starch granules vary in shape and size with varying physicochemical and functional characteristics depending on its plant origin (Salar *et al.,* 2013). These differences are attributed to the proportion of amylose to amylopectin, molecular weight of amylose, and the branch chain length of amylopectin. Genetic make-up and the activity of the plant have also been reported to contribute to such differences in physicochemical properties (Hizukuri *et al.,* 1981).

Starch has been the subject of intensive research over many decades occupying a vast body of published literature reporting its preparative and analytical methods, molecular structure, physical, chemical and biochemical properties, functionality and uses (Blanshard *et al.*, 1984). The manifestation of diverse native starches and numerous starch modification techniques allowed different starches to be used for different applications (Ellis *et al.*, 1998). Starches from different sources are different, and that not all granules of a single starch behave identically (BeMiller, 1997). The knowledge of the internal organization helps the researcher to understand the functionalities and the transformation behavior of starch, and improve the properties and stability of starch products (Ozean and Jackson, 2005).

Starch consists of two main structural components, the amylose, which is essentially a linear polymer in which glucose residues are α-D-(1-4) linked and amylopectin, which is a larger branched molecule with α-D-(1-4) and α-D-(1-6) linkages and a major component of starch. Most seed storage starches have a final amylose content of 25–30 %. Compared to amylopectin, amylose is a smaller molecule with longer chains and a limited number of branch linkages (Fig. 1.1). Amylose is linear or slightly branched with a degree of polymerization up to 6000, and has a molecular mass of 105–106 g/mol. The chains can easily form single or double helices.

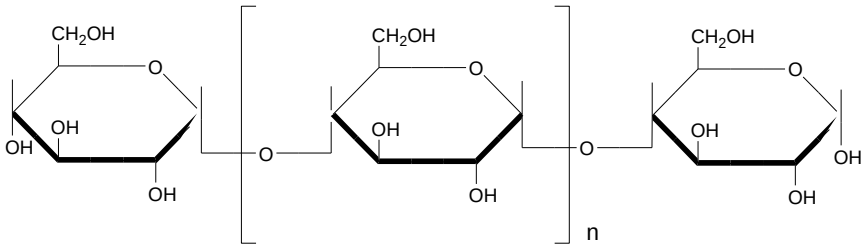

Fig.1.1: Representative partial structures of amylose (On average n = ca. 1000).

The basic unit of the starch granule is a branched polymer of glucose called amylopectin. In contrast to amylose, each branched chain of amylopectin contains many short chains of glucose molecules (only up to 30 glucose units). The multitude of branching in amylopectin gives it a molecular weight that is 1000 times that of amylose. These 1,4-linked chains are joined together by 1,6 branch points and the chains are arranged into clusters in which adjacent chains form double helices. Hence Amylopectin is formed by non-random α-1⟶6 branching of the amylose-type α-(1⟶4)-D-glucose structure (Fig. 1.2). About 70% of the mass of starch granule is regarded as amorphous and about 30% as crystalline. The

amorphous regions contain the main amount of amylose, and a considerable part of the amylopectin. The crystalline region consists primarily of the amylopectin (Hizukuri, 1986; Lansky *et al.,* 1949).

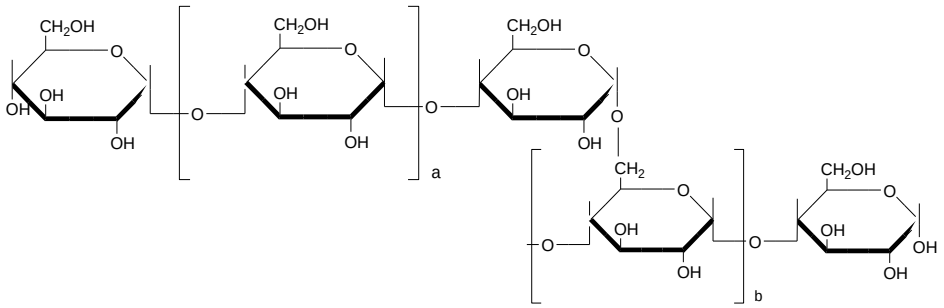

Fig.1.2: Representative partial structures of amylopectin (a = ca. 12-23 for exterior chains and b = ca. 20-30 for interior chains).

1.3. Hydrophobically modified starch based NPs

NPs fabricated from starch have prominently been noticed due to their unique properties, low cost, abundance, and biodegradability. Most starch based NPs are fabricated from chemically modified starches. Modified starches have been used to produce water-resistant materials and are capable in forming self-assembled NPs for biomedical uses (Berski *et al.,* 2011). On top of that, hydrophobic starch NPs are one of the up-coming drug carriers as they possess prominent characteristics such as controlled solubility and *in vivo* biocompatibility (Hermawan *et al.,* 2015; Kshirsagar and Singhal, 2007; Namazi *et al.,* 2011).)

Hydrophobically modified polymers have also attracted much attention in drug delivery applications due to their subtle balance of hydrophilic–hydrophobic nature and biodegradability (Daoud *et al.,* 2007). They spontaneously self-associate forming hydrophobic cores with considerable potential in drug/gene delivery research and other biomedical applications. These NPs are utilized for drug delivery applications because of their high stability, prolonged residence time, high drug encapsulation, better storage life (Couillet, *et al.,* 2005).

1.3.1. Hydrophobic modification of starches

Starch has been indicated as an interesting potential carrier and is relatively unexplored. It is biocompatible, biodegradable, nontoxic polymer, abundantly occurring in nature as the major

polysaccharide storage in higher plants (Zhang and Sun, 2004). However, due to the abundance of hydroxyl groups, the hydrophilic nature of the starch seriously limits the development of native-starch based materials. The major limitations are its deliquescent nature, high viscosity and incongruousness with some hydrophobic polymers. On the other hand, the presence of numerous hydroxyl groups on the molecules of starch granules can be used as advantage for anchoring hydrophobic side chains. Currently, hydrophobic modification is one of the most exploited solutions to the aforementioned limitations (Dandekar *et al.,* 2012).

1.3.1.1. Derivatization by etherification

One of the hydrophobic starch derivatizations is etherification into propyl starches. Propyl starch is the most widely used derivatives of starch to produce hydrophobically modified NPs. The hydroxyl groups of the glucose residues in starch, exhibiting reactivity typical for alcohols, could undergo conversion into ethers by various alkylation agents such as methyl, ethyl and propyl starch ethers; bromopropane (Fig. 1.3) and other alkyl halides could etherify starch granules into propyl starch derivatives (Jain *et al.,* 2011; Dandekar *et al.,* 2012).

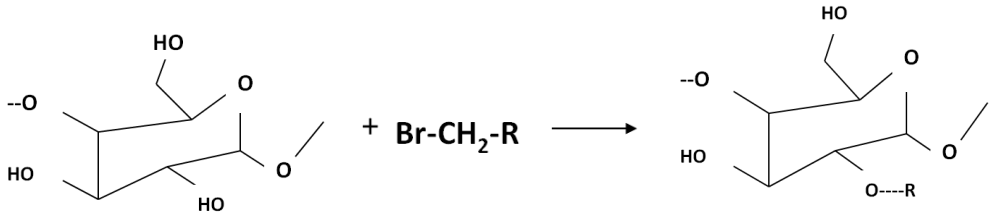

Fig.1.3: Starch derivatization by etherification to starch propyl

1.3.1.2. Derivatization by esterification

Esterification is another method to produce hydrophobic starch. The most common esters of hydrophobic starch are SA (with vinyl acetate and acetic anhydride (AA)) and fatty acid modified starches.

Acetylation: Acetylation of starches is an important modification that has been applied to the native starches to impart thickening and this is known for more than a century (Roper H, 1996). In the acetylation, parts of the hydroxyl groups of the α-D-glucopyranose units have been converted by esterification to acetyl groups. Acetylation of starch takes place by an addition-elimination mechanism (Fig.1.4). Reaction (a - c) is the main rate-controlled

reaction where starch is acetylated with AA and a base catalyst. Xu *et al.*, (2004) reported that the three free OH groups have different reactivities. The primary OH on C_6 is more reactive and is acetylated more readily than the secondary ones on C_2 and C_3 due to steric hindrance. The primary OH located at the exterior surface of the starch molecules reacts readily with the acetic groups, while the two secondary ones located within the interior surface of starch form hydrogen bonds with the OH groups on the neighboring glucose unit. Of the two secondary OH groups, the OH on C_2 is more reactive than the one on C_3, mainly because the former is closer to the hemi-acetal and more acidic than the later (Garga and Jana, 2011).

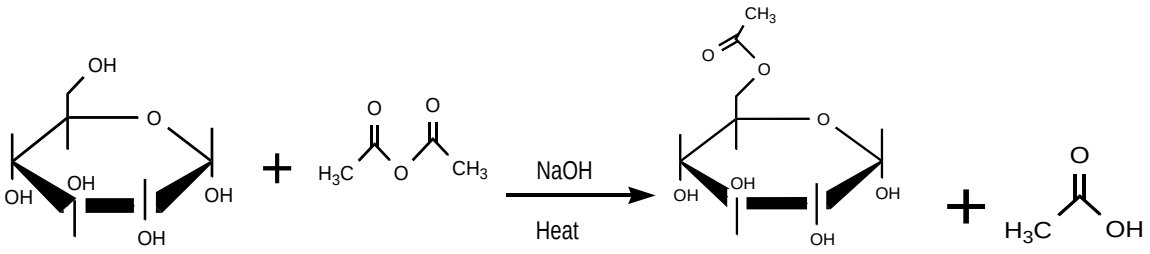

Reaction a

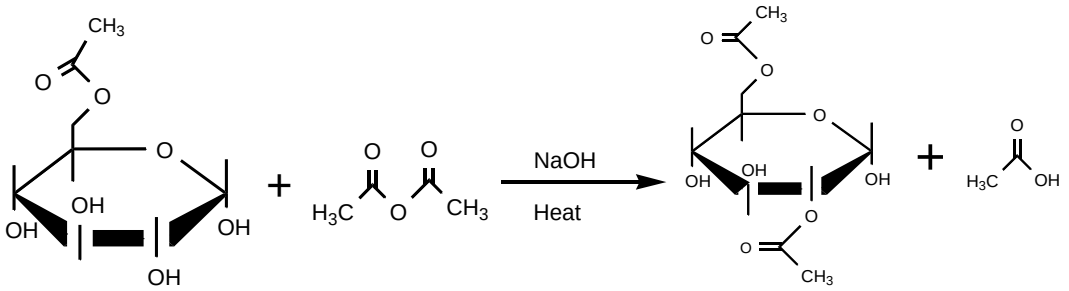

Reaction b

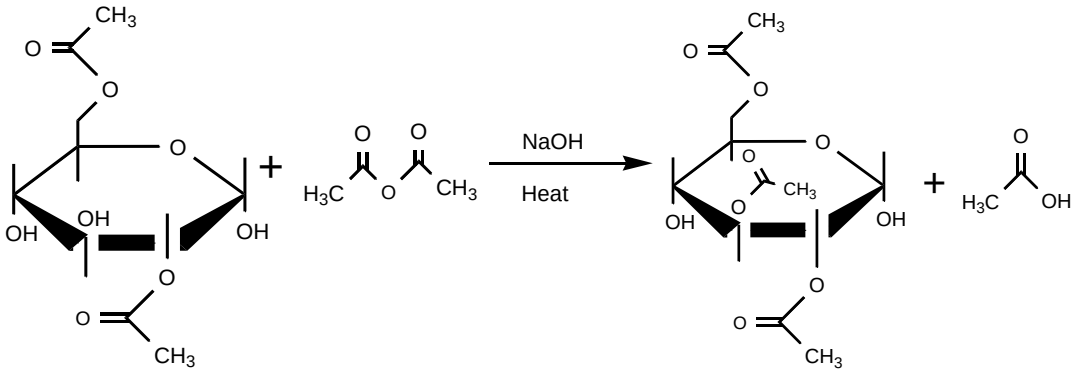

Reaction c

Fig. 1.4: A scheme of the chemical reactions involved during acetylation of starch with AA (reaction a-c) (From Xu *et al.*, 2004).

Fatty acid esters: To improve the mechanical properties as well as degree of hydrophobicity, higher fatty acids (C_{12}-C_{18}) have been used in the modification reaction. The mechanical properties and hydrophobicity of the products are significantly improved when using these longer-chain fatty acid precursors such as oleic, palmitic and stearic acids. The complexation with lipids reduces the solubility of starch in water, alters the rheological properties of pastes, decreases swelling capacity, increases gelatinization temperature, reduces gel rigidity, retards retrogradation and reduces the susceptibility to enzymatic hydrolysis (Copeland *et al.*, 2009).

Succinylation: Modification of starch by succinylation has been found to modify its physicochemical properties (Bhandari and Singhal, 2002). Modification of native starch to its succinate derivatives reduces its gelatinization temperature and the retrogradation, improves the freeze-thaw stability as well as the stability in acidic and salt containing medium. Generally, succinylated starch can be prepared by treating starches with different alkenyl succinic anhydrides, for example, dodecenyl succinic anhydride, octadecenyl succinic anhydride or octenyl succinic anhydride. The incorporation of bulky octadecenyl succinic anhydride grouping to hydrophilic starch molecules has also been found to confer surface active properties to the modified starch (Wang *et al.*, 2015).

1.3.1.3. Dual modification

Dual modification of starches has been demonstrated to introduce desirable properties to starch for specific applications. Cross-linking and substitution of starch are two such methods commonly utilized in industrial applications (Jyothi *et al.*, 2006; Singha *et al*., 2007). The chemical modification is commonly done by partial substitution of hydroxyl groups of cross-linked starches (Mulhbacher *et al.*, 2001). Strengthening bonding between starch chains by cross-linking will increase the resistance of the granule to swelling. Cross-linking greatly increases the stiffness of the gels (Liu *et al*., 1999; (Mulhbacher *et al.*, 2001; Wattanchanta *et al*., 2003).

Dual modification results in starch with improved qualities than those of native starches. However, the effect of dual modification depends upon the preparation procedure. Cross-linking followed by substitution has been reported to yield starches that are more shear and heat stable than the native starch (Onofre *et al.*, 2009). This may be due to the structural change in the granules after the first modification (cross-linking) (Reddy and Seib, 2000; Singha *et al.*, 2007).

1.3.2. Types of starch NPs

1.3.2.1. Propylated starch NPs

The synthesis and characterization of propyl starch with a controlled degree of substitution (DS) to modulate the release of the incorporated hydrophobic drug has been reported by Jain *et al.,* (2011) and Dandekar *et al.,* (2012). The application of this polymer in formulating NPs of anti-cancer agents such as doxorubicin and docetaxel was found to be effective against numerous types of cancers (Santander-Ortega *et al.,* 2009). Docetaxel loaded propyl starch NPs were formulated by the solvent emulsification/diffusion technique and the safety and efficacy of the NPs were confirmed by cellular cytotoxicity assays using Caco-2 cells. Uptake studies with these NPs indicated their enhanced internalization by the cancerous cells and their peri-nuclear localization. The results indicated the potential of the developed docetaxel loaded propyl starch NPs as an effective yet safe anticancer therapy.

1.3.2.2. Acetylated starch NPs

There have been some reports about the synthesis, characterization of acetylated starch and the fabrication of starch-based NPs. These types of NPs could be potentially used for the encapsulation of hydrophobic drugs (Han *et al.,* 2013). Raj and Prabha (2015) reported the potential application of SA copolymer for controlled release of an anticancer drug. They produced SA–PEG–gelatin NPs as controlled drug delivery systems for cisplatin using simple nanoprecipitation method. Minimol *et al.* (2013) also developed controlled release NP formulation using PEGylated SA. In a different study, Tan *et al.* (2009) prepared SA nanospheres using simple nanoprecipitation method and fluorescence spectroscopic studies and proved that these types of nanospheres could be potentially used for the encapsulation of hydrophobic drugs.

1.3.2.3. Fatty acid esters NPs

Namazi *et al.*, (2011) synthesized hydrophobically modified corn and potato starch using long-chain fatty acids and fabricated NPs in the range of 360-500 nm using nanoprecipitation method. Simi and Abraham (2007) also synthesized hydrophobic starch using fatty acids (oleic and stearic acids). The hydrophobic NPs were then fabricated from grafted cassava starches and stabilized by cross-linking with sodium tripolyphosphate. Controlled release of the drug previously loaded in NPs was studied by using indomethacin as a model drug. Fatty acid grafted starch NPs were found to be a good vehicle for controlled oral drug delivery.

1.3.2.4. Butanol complexed starch NPs

Arrowroot starch NPs were fabricated from butanol-complexed derivatives. Their application as an encapsulation matrix for herb extracts has been studied by Winarti *et al.,* (2014). The NPs fabricated by nanoprecipitation method produced particles with size ranging from 78.6 nm to 538.7 nm (average 261.4 nm). The lower particle size and biodegradability made arrowroot starch NPs suitable as controlled release matrix for bioactive compounds.

1.3.2.5. Propionic and hexanoic acid modified starch NPs

Starch NPs can be modified with propionic and hexanoic anhydride in order to increase their hydrophobicity and turn them into amphiphilic Polymers (Ju *et al.,* 2012). The hydrophobic groups of the amphiphilic starch dispersed in water can be aggregated to generate hydrophobic micro-domains and thus to minimize exposure to water. This formation of hydrophobic micro-domains suggests that the hydrophobically modified starch NPs could be used as carriers for drug delivery. Kim *et al.,* 2017 studied hexanoic and propionic acid modified starch NPs. In this study, hexanoic anhydride provided a much better hydrophobicity than propionic acid. Consequently, the hydrophobically modified starch NPs modified with hexanoic acid showed better potential as carrier for drug delivery.

1.3.2.6. Octenyl succinic starch NPs

Octenyl succinic anhydride modified taro starch has been used to fabricate amphiphilic starch NPs. The amphiphilicity of octenyl succinic anhydride starch NPs increases with increase in DS. This modification has therefore provided a route to improve dispersion of modified starch in polar/nonpolar solvent and broaden the potential application as carrier in NP fabrication and as stabilizing agent in many oil-water systems (Jiang *et al.,* 2016).

1.3.3. Preparation of hydrophobic starch NPs

In recent studies, various preparation methods of hydrophobic starch NPs have been carried out. Dispersion of preformed polymers is the most generally used technique to prepare hydrophobic starch NPs (Rao and Geckeler, 2011). The under presented are the most widely used methods in the fabrication of NPs.

1.3.3.1. Emulsification-solvent evaporation method

The oil-in-water (O/W) emulsification method is the most commonly used method for fabrication of starch NPs. In this method, the polymer is dissolved in an organic solvent such

as dichloromethane, chloroform or ethyl acetate. The drug is dissolved or dispersed into the preformed polymer solution, and this mixture is emulsified into an aqueous solution to make an O/W emulsion using emulsifying agents like poly(vinyl alcohol), polysorbate-80, poloxamer-188, etc. Following the formation of a stable emulsion, the organic solvent is evaporated by mounting the temperature/under pressure or by nonstop stirring (Fig. 1.5). The size can be controlled by regulating the stirring rate, type and amount of dispersing agent, viscosity of organic and aqueous phases (Reis *et al.*, 2006a; Soppimath *et al.*, 2001). The O/W emulsification, for example, is used in the fabrication of NPs from SAs and propyl starch derivatives (Paulos *et al.*, 2016; Santander-Ortega *et al.*, 2010).

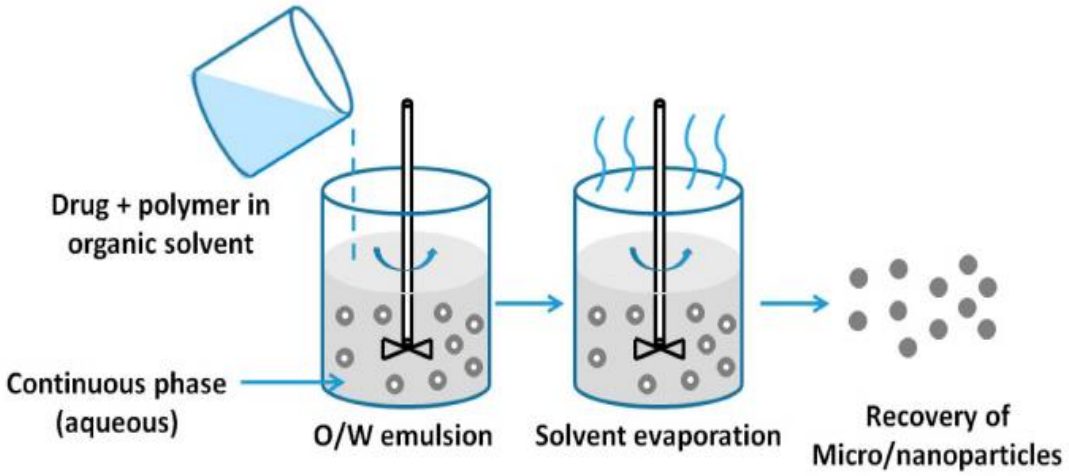

Fig. 1.5: Fabrication of starch NPs by emulsification and solvent evaporation method

1.3.3.2. Emulsification solvent diffusion method

In this method, the organic solvent containing the dissolved polymer and the drug is emulsified in an aqueous surfactant solution by using a high-speed homogenizer. Water is subsequently added under regular stirring to the O/W emulsion system, therefore causing phase transformation and outward diffusion of the solvent from the internal phase, leading to the nano precipitation of the polymer and the formation of colloidal NPs (Fig. 1.6). Finally, the solvent can be removed by vacuum steam distillation or evaporation (D'Mello *et al.*, 2009).

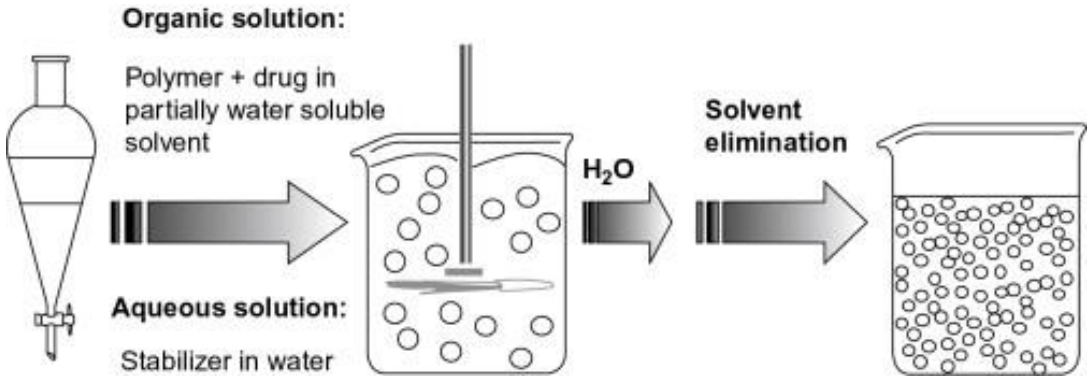

Fig. 1.6: Fabrication of starch NPs by emulsification and solvent diffusion method

1.3.3.3. Nano-precipitation

The nanoprecipitation technique is a one-step process, also known as the solvent displacement method (Fessi *et al.,* 1989). Nanoprecipitation is performed using systems containing three basic components, the polymer, the polymer solvent, and the nonsolvent of the polymer (Thioune *et al.,* 1997). Polymer and drug are dissolved in a polar, water-miscible solvent like acetone, ethanol or methanol. The solution is poured in a controlled manner (drop-by-drop addition) into an aqueous solution with surfactant. NPs are formed immediately by rapid solvent diffusion (Fig. 1.7). Lastly, the solvent is removed under reduced pressure (Chin *et al.,* 2011; Govender *et al.,* 2000; Mahapatro and Singh, 2011). Fluorescence-labeled starch NPs have been prepared by this method. Here, fluorescein-labeled SA is dissolved in water miscible organic solvent (acetone). Distilled water is then added dropwise to the polymer solution. The resulting NP suspensions are stirred at room temperature until acetone is completely vaporized from the aqueous suspension (Li *et al*., 2011).

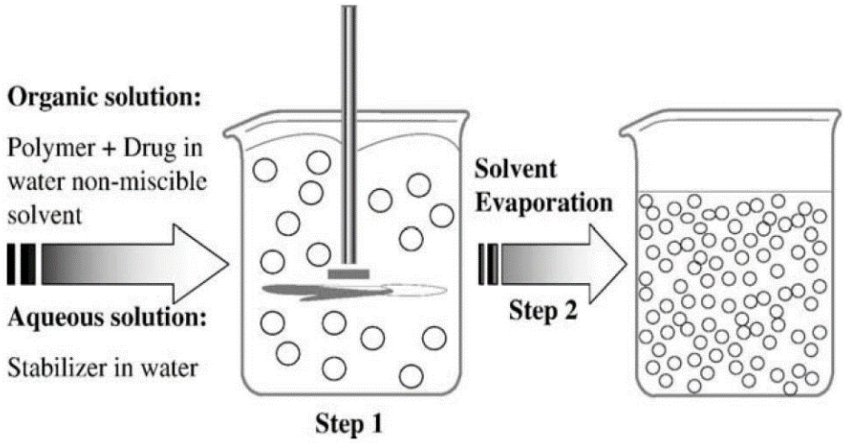

Fig. 1.7: Nanoprecipitation by Solvent evaporation method

1.3.3.4. Membrane dialysis technique

Dialysis offers simple and effective method for the preparation of small, narrow-distributed NPs. Polymer is dissolved in an organic solvent and placed inside a dialysis tube with proper molecular weight cut-off. Dialysis is performed against a non-solvent. The displacement of the solvent inside the membrane is followed by the progressive aggregation of the polymer due to a loss of solubility and the formation of homogeneous suspensions of NPs. The dialysis method has been successfully used for those starches modified by acyl chlorides (octanoyl, lauroyl and palmitoyl chloride) and other long chain fatty acids. Sim and Abraham, (2007) and El-Feky *et al.,* (2016), prepared hydrophobic grafted and crosslinked starch NPs for drug delivery using this method. Namazi *et al.,* 2011, also used this method for fatty acid modified starch.

1.3.4. Characterization of hydrophobic starch NPs

1.3.4.1. Particle Size

NP size is significantly determining factor in the efficacy of the therapeutic agent in terms of tissue penetration and cellular uptake (Gaumet *et al.,* 2008). Starch NPs fabricated so far have particle sizes in the range of 65 nm to 500 nm (Table 1.1). As shown in the Table, variation in size between various studies could be attributed to their method of preparation, chemical modification and crosslinking.

Table 1.1: Sizes of different starch NPs and their methods of preparation

	Starch NP	Preparation method	Size (nm)	References
1	Starch-stearic and	Membrane dialysis	360-500	Namazi *et al.,* 2011
	Starch-oleic acid		65-75	Sim and Abraham, 2007
2	Starch acetate (SA)	Nano-precipitation	150-600	Han et al., 2013
			223-324	Najafi et al., 2016
3	Hexamethylene diisocyanate starch	Acid hydrolysis and conjugation	50-70	Valdokar and Thakore, 2010
4	Propyl starch	O/W emulsion diffusion	150-245	Santander-Ortega *et al.,* 2010
				Dandekar *et al*., 2012
5	Butanol complexed starch	acid hydrolysis	78-538	Winarti *et al.,* 2014

1.3.4.2. Electrical property

NPs with a zeta potential above (+/-) 30 mV have been shown to be stable in suspension, as the surface charge prevents aggregation of the particles. Determining the stability of a sample to minimize aggregation for drug delivery and pharmaceutical applications (high zeta potential) is of great importance in NP research. The zeta potential can also be used to determine whether a charged active material is encapsulated within the centre of the nanocapsule or adsorbed onto the surface (Singh and Lillard, 2009).

Most starch NPs exhibit zeta-potential from low to moderately high value, that is, between -5 and -23 mV. The negative zeta-potential values displayed by starch colloidal systems such as propyl-starch NPs and folate conjugated starch NPs could be attributed to the specific interaction of the NPs surface with the ions present in the medium (Suyao *et al.,* 2006; Santander-Ortega *et al*., 2009). Therefore, the NPs potentially have some tendency to aggregate to each other. For better stability of starch NPs, various non-ionic stabilizers such as poly(vinyl alcohol) are used. The stabilizing effect of poly(vinyl alcohol) may be attributed to its ability to form a macromolecular sheath covering the individual NPs resulting in their mutual repulsion thus imparting a steric stabilization (Dandekar *et al*., 2012).

1.3.4.3. Drug loading

Drug loading and entrapment efficiency of starch NPs have been studied in different researches related to starch based NPs. Drugs are loaded into starch NPs both by incorporating at the time of NPs production (incorporation method) and adsorbing the drug after formation of NPs by incubating the carrier with a concentrated drug solution (adsorption/absorption technique) (Mohanraj and Chen, 2006). The greatest efficiency of drug loading into starch NPs can be accomplished by incorporation method than adsorption techniques. The degree of drug incorporation is found to be as high as 80% (Santander-Ortega *et al.,* 2009).

1.3.4.4. Drug release

Namazi *et al.,* 2011 studied drug release profile of curcumin from starch NPs. Slow release of drug from surface crosslinked cassava starch NPs in buffer of high pH has proved that the starch NP can be used as a good carrier of drugs (Namazi *et al.,* 2011). In another study, folate conjugated starch NPs have shown to sustain the release of drugs such as Doxorubicin (Suyao, *et al*., 2006). It has also been found that drug release study from hydrophobically

modified propyl starch NPs on diffusion cell prolongs the release of docetaxel, flufenamic acid, testosterone and caffeine (Santander-Ortega *et al*., 2010; Dandekar *et al.*, 2012).

1.3.5. Applications of starch NPs

1.3.5.1. Therapeutic applications

A hydrophobic starch derivative is used for safe and enhanced delivery of anticancer drugs and other agents. The synthesis and characterization of propyl and long chain fatty acid starch with a controlled DS to modulate the release of the incorporated hydrophobic drug is reported (Dandekar *et al.,* 2012; Santander-Ortega *et al.,* 2009). The application of this polymer in formulating NPs of anti-cancer agents such as doxorubicin and docetaxel was found to be effective against numerous types of cancers.

1.3.5.2. Imaging applications

Recently, in addition to the fluorescent silica NPs and gold NPs, hydrophobically modified starch-based nanospheres incorporated with fluorescent dye have been studied for its fluorescent stability and effect of the starch on fluorescence spectra of the fluorophores. In this study, it was found that the fluorescent nanospheres exhibit not only a higher fluorescent stability due to the covalent linkage between the dye and the starch matrix but also the incorporation of the indicator dyes in starch matrix has no distinct effect on the fluorescence spectra of the fluorophores, and the fluorescence intensity of the nanospheres increased with increase in pH. Moreover, the fluorescein isothiocyanate (FITC)-labeled SANPs were believed to have a potential application on the intracellular analysis in the area of biomedical or life-sciences (Li *et al.,* 2011).

1.4. Model drugs

In drug delivery studies, model drugs are used to give insight for selecting the most suitable polymer type for drug delivery functions. In this study, acyclovir, furosemide and Ibuprofen were selected as model drugs based on biopharmaceutics classification system (BCS). The low aqueous solubility of BCS class II drugs (such as ibuprofen) is a major obstacle for their clinical applications. . BCS class III (such as acyclovir) drugs are soluble but they have permeability problem. The problem is severe in case of BCS class IV drugs (such as furosemide) suffering low bioavailability because of both low solubility and low permeability

Ibuprofen (Fig. 1.8 a) is a non-steroidal anti-inflammatory drug (NSAID). It has prominent analgesic, anti-inflammatory and antipyretic actions. NSAIDs as ibuprofen work by inhibiting the enzyme cyclooxygenase. Ibuprofen has a short half-life (2 h) and a dose-dependent duration of action of approximately 4–8 h, which is longer than suggested by its short half-life. Due to its low solubility its bioavailability is found to be 47%. The oral dose is 400 mg every 4–6 h, adding up to a usual daily dose of 1200 mg (Kayrak *et al.,* 2003). In spite of these disadvantages, ibuprofen can be formulated in a promising manner by nanotechnology.

Acyclovir aids the body to fight against infections in an impressive way and provides adequate immunity. Acyclovir belongs to a category of antiviral drugs known as synthetic nucleoside analogues (Fig. 1.8 A). It has a bioavailability of 10 –20%, and a plasma half-life of 2.5 h (Shao *et al.,* 2012). Oral acyclovir is mostly used four times a day as 200 mg tablets. Moreover, long term administration of acyclovir (6 months or longer) is essential in an immune-compromised patient with relapsing herpes simplex infection (Gandhi *et al.,* 2014; Emmert, 2000). NPs of Acyclovir can improve the controlled release and efficiency of this molecule in the treatment of herpes simplex with better penetration into the cells which will result in improved targeted delivery and lower side effects (Amsa *et al.*, 2010).

Furosemide, 5-(aminosulphonyl) -4-chloro-2-[(2-fuanyl-methyl) amino] benzoic acid (Fig. 1.8 B), is a potent high ceiling (loop) diuretic, mainly used in the management of edema linked with cardiac, renal, and hepatic failure, and treatment of hypertension.. Furosemide acts by inhibiting the reabsorption of sodium and chloride in the ascending loop of Henle and distal tubules. As a BCS class IV drug (low solubility and low permeability) it exhibits low bioavailability Peak plasma drug concentrations occur between 1 to 1.5 h, with low permeability and variable bioavailability. The dosage form, underlying disease conditions and food substantially influence the rate and extent of bioavailability following oral administration. The permeability and drug delivery related concerns of Furosemide have been addressed using various formulation maneuvers (Derakhshandeh *et al.,* 2016; Wu and Benet, 2005).

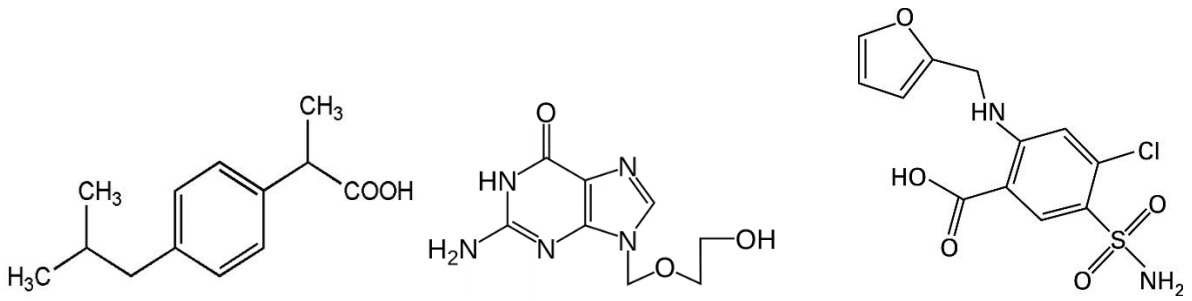

a) b) c)

Fig. 1.8: Chemical structure of model drugs a) ibuprofen b) acyclovir c) furosemide

1.5. Rationale of the study and research questions

A number of published articles attempt to solve questions of whether the properties of carriers are suitable for biomedical applications or not. For instance, liposomes have been used as potential nanodrug carriers instead of conventional dosage forms. However, developmental work on liposomes has been limited due to inherent problems such as low encapsulation efficiency (EE), rapid leakage of water-soluble drug in the presence of blood components and poor storage stability (Singh and Lillard, 2009). Recently, SLNs have been attracting increasing attention because of their unique structure and properties, such as good biocompatibility, protection for the incorporated compound against degradation, site-specific targeting and controlled release of drugs. But they have limitations such as insufficient drug loading and drug expulsion after polymorphic transition on storage (Subedi *et. al.,* 2009).

Furthermore, there emerges a concern about the safety of the nanotechnology products in humans. Some of the nanomaterials are biodegradable while some are not; in addition, the side effects of the by-products present a huge concern (Ochekpe *et al.,* 2009). Inorganic NPs prepared usually from materials such as ceramic, gold, copper, cobalt, titanium and carbons are effective in delivering proteins and genes. However, these particles are not biodegradable and so there is concern that they may accumulate in the body and cause harmful effects. NPs of metals such as copper, cobalt, and titanium, as well as silicon and their oxides have been reported to have inflammatory and toxic effects on cells (Koo *et al.,* 2005).

Scientists are not only attempting to develop new delivery systems that are substantially better than the existing delivery systems, but also seeking for new ways of using old biomaterials. The use of starch-based (native or modified) NPs is an important strategy towards the attainment of this objective. This is because starch, unlike synthetic products, is

biocompatible, nontoxic, biodegradable, eco-friendly and cheap. It is generally a non-polluting renewable source for sustainable supply of cheaper pharmaceutical products (Rodrigues and Emeje, 2012).

However, native starches, irrespective of their sources, cannot fit into controlled drug delivery systems as many drugs are released quickly from such unmodified starch-based systems (Tuovinen *et al.,* 2004) due to considerable swelling and quick enzymatic degradation in biological systems. Therefore, to prepare starch nanostructure which could act as a carrier of different drugs, its backbone structure is modified with hydrophobic molecules resulting in hydrophobized starch copolymer (Besheer *et al.,* 2007; Namazi *et al.,* 2011). When these copolymers are exposed to aqueous environment, they spontaneously form micelles or self-associate to form colloidally stable NPs with inner hydrophobic core (Myrick *et al.,* 2014). This hydrophobic core can easily encapsulate hydrophobic drugs (Gonçalves and Gama 2008).

Hence, in the current study native starches are modified into SAs through acetylation. In acetylation, hydrophilic hydroxyl groups are substituted with hydrophobic acetyl groups making the modified starch hydrophobic (Reddy and Yang 2009; Tuovinen *et al.,* 2003).

Starch generally occurs in the form of granules, varies in shape and size with varying physicochemical and functional characteristics depending on its plant origin (Pérez *et al.,* 2009). These differences attribute to the proportion of amylose to amylopectin, molecular weight of amylose, and the branch chain length of amylopectin (Jane *et al.,* 1999). Genetic make-up and the activity of the source plant have also been reported to contribute to such differences in physicochemical properties of starch from different origins (Chung and Lim 2006).

Studies on cassava, dioscorea, enset and maize starches confirmed that the botanical origin has an effect on the average granule size, amylose content, morphology, swelling capacity and temperature of gelatinization (Gebre-Mariam and Schmidt 1998; Paulos *et al.,* 2009; Sandhu and Singh 2007).

Different studies have previously reported the feasibility of fabricating starch NPs using emulsification and solvent evaporation methods under various process and formulation

variables (Chin *et al.*, 2014; Dandekar *et al.*, 2012; Li *et al.*, 2011). However, there remains a challenge of precisely controlling the particle size and size distribution of NPs. Furthermore polymeric NPs have also limitations with respect to their EE, sustain drug release and storage stability.

Therefore, the current work attempts to address the following research questions:

- What are the optimal conditions to fabricate SANPs with desired particle size and PDI?
- Does the origin of starch influence the fabrication of SANPs?
- What would be the effect of different storage conditions on stability of SANPs?
- What is the capacity SANPs as nano drug carriers?
- Do drugs with different solubility and partition coefficient influence drug loading, EE and release profile of SANPs?

1.6. Objectives

1.6.1. General objective

The objective of the present study was to fabricate size controlled SANPs and evaluate their potential applications as hydrophobic drug carriers.

1.6.2. Specific objectives

- To fabricate SANPs from SAs via emulsification solvent evaporation, and nanoprecipitation methods;
- To evaluate the effect of starch origin on fabrication of SANPs;
- To assess the potential applications of SANPs as nano drug carriers using model drug and
- To study the effect of solubility and partition coefficient of drugs on DL, EE and *in vitro* drug release.

CHAPTER 2: ACETYLATION OF CASSAVA STARCH AND FABRICATION OF SANPS: OPTIMIZATION OF FORMULATION AND PROCESS VARIABLES

2.1. Introduction

Over the past few decades, nanotechnology is making significant advances in biomedical applications, including newer drug delivery techniques (Galindo-Rodriguez *et al.,* 2004). The controlled release of pharmacologically active agents to the specific site of action at optimal rate and dose regimen has been a major goal in designing NPs (Hughes, 2005). In recent years, there has been considerable interest in developing biodegradable polymer-based NPs to effectively deliver the drug to a target site. Polymeric materials used for preparing NPs for drug delivery must be biocompatible and preferably biodegradable (Mahapatro & Singh, 2011). To this aim, many polymeric materials have been explored, including polylactic acid, polyglycolic acid, polycaprolactone, polysaccharides particularly chitosan, polyacrylic acids, proteins or polypeptides such as gelatin, etc. (Chawla & Amiji, 2002; Feczkó *et al.,* 2011; Nobs *et al.,* 2004; Shi *et al.,* 2011).

Polysaccharides are the most commonly used polymeric materials in the preparation of NPs for drug delivery (Li *et al.,* 2011). By and large, the preparation of NPs from polysaccharides was focusing on chitosan carriers (Payne *et al.,* 2005). Recently, however, other polysaccharide based NPs are emerging that may greatly enrich the versatility of NP carriers in terms of category and function. Starch is now being explored for its potential application as a carrier in nanotechnology. Studies have shown that starch NPs could be used as potential carriers of various drugs. A study conducted by Santander-Ortega *et al.,* 2010, showed that propyl starch-based NPs enhanced the permeability of flufenamic acid into human skin. Another study by Yu *et al.,* 2007 revealed that dialdehyde starch NPs were found to be effective for controlled release of doxorubicin on mammary cancer cells. Jain *et al.,* 2008 reported that starch NPs could also be used as an efficient trans-nasal mucoadhesive carrier of insulin.

Starch is an attractive, natural substitute for chemically synthesized polymers due to its abundant availability along with numerous additional attributes including biocompatibility, biodegradability, non-toxicity, non-immunogenicity, stability and compatibility with most

drugs. These advantages along with its availability from renewable resources and its economic benefits make starch an ideal substrate for the preparation of NPs (Liu *et al.*, 2008).

Furthermore, native starch structure can be easily modified by physical, chemical and enzymatic methods. Such modifications play a vital role in improving overall performance and increase the use of starch in various applications including NP carrier systems (Dandekar *et al.*, 2012; Tarvainen *et al.*, 2002; Tarvainen *et al.*, 2004). One of the modifications is acetylation of native starch. Acetylation converts the hydrophilic native starch to hydrophobic SA for applications such as coating and controlled release of water insoluble drugs (Chen *et al.*, 2004; Chowdary *et al.*, 2011; Minimol *et al.*, 2013). Hydrophobically modified starches are soluble in organic solvents and spontaneously self-associate to form NPs by using techniques such as solvent evaporation, nanoprecipitation, emulsion crosslinking and oil in water emulsions (Han *et al.*, 2013; Xu *et al.*, 2010; Shia *et al.*, 2011). Among these, emulsification and solvent evaporation is a widely used method due to its several advantages including high batch to batch reproducibility, amenability to scale-up, and the possibility to control the size and polydispersity of NPs (Santander-Ortega *et al.*, 2010).

In the fabrication of NPs, a precise control over the desired particle size and polydispersity is important for several reasons such as stability, *in vivo* distribution and drug release (Mainardes & Evangelista, 2005). Thus, response surface methodology (RSM) was employed to obtain the optimum conditions of formulation and process variables to fabricate the desired NPs from cassava SAs. RSM is widely used in the development and optimization of NPs (Anarjan *et al.*, 2015; Cheng *et al.*, 2014; Zhang *et al.*, 2013). Computer-aided optimization technique, using the central composite design (CCD), was employed to investigate the effect of independent variables on the desired responses.

This section therefore reports on the fabrication of acetylated cassava starch NPs under optimized formulation and process variables using the emulsification and solvent evaporation method.

2.2. Materials and methods

2.2.1. Materials

Acetic anhydride (May and Baker Ltd, Dagenham, UK); Sodium hydroxide (Loba Chemie Pvt Ltd, Mumbai, India); Sodium metabisulphite (Guangzhou Jinhaunda Chemical Reagents Co. Ltd, Guangzhou, China); Mowiol 4-88-Poly vinyl alcohol (Kuraray Specialties Europe GmbH, Frankfurt/M., Germany); Pluronic® F68 [Poloxamer 188- poly ethylene oxide/poly propylene oxide block copolymer; BASF, Mannheim, Germany]; Pluronic® F127 [Poloxamer 407- poly ethylene oxide/poly propylene oxide block copolymer, BASF, Mannheim, Germany]; Tween® 80 (Carl Roth GmbH, Karlsruhe, Germany); Chloroform (Fisher Scientific UK LTD, Loughborough, UK); Dichloromethane (BDH Lab Supplies, Poole, England), and Ethyl acetate (Sigma Aldrich Chemie GmbH, Taufkirchen, Germany), were used as received.

2.2.2. Methods

2.2.2.1. Isolation of cassava starch

Starch was isolated from cassava tubers (Manihot esculenta) according to the methods described by Paulos *et al.* (2009). About 20 kg of fresh tubers were cleaned, peeled and cut into small pieces and milled in the presence of 0.075% sodium metabisulphite solution. The mass was then strained through muslin and washed with distilled water several times to remove soluble substances, sugars and mucilage. The starch sediment was washed with distilled water until the pH was neutral. It was then sieved, dried at room temperature and milled gently to fine powder.

2.2.2.2. Acetylation of cassava starch

SAs were prepared following the method described elsewhere (Paulos *et al.* 2016). Native starch (100 g) dried in an oven (Kottermann® 2711, Germany) for 24 h at 50 ^{o}C, was mixed with AA (1:4 ratio) in a glass reactor at room temperature over an oil bath. After stirring for 5 min (at 100 rpm), 50% (w/w) aqueous NaOH solution was added as a catalyst drop by drop with constant stirring. The temperature of the oil bath was increased to 90 °C within 15 min, and held at this temperature for different reaction times. At the end of the reaction times, excess cold distilled water was added to the reactor with vigorous mixing to terminate the reaction and to thoroughly rinse the reaction products. The resulting white acetylated starch was dried in an oven at 50 °C.

2.2.2.3. Determination of DS

DS of SA was determined by saponification titration method, as described elsewhere (Elomaa *et al.*, 2004). Accurately weighed 1 g of pulverized SA was added to 50 ml of aqueous solution of ethanol (75%). The slurry was kept in a water bath at 50 ^{o}C for 30 min. The slurry was then cooled down to room temperature and 40 ml of 0.5 N aqueous solution of KOH was added to the mixture. The flask was fitted with a tight stopper and kept at room temperature with occasional shaking for 72 h for complete saponification. The excess of alkali was titrated against 0.5 N HCl with phenolphthalein as indicator. A blank test was performed with native cassava starch following the same procedure. The experiments were done in triplicate.

Acetyl content (% A) was calculated according to the following equation:

$$\%A = \frac{[(\mathrm{Vo}-\mathrm{Vn}) \times \mathrm{N} \times 0.043 \times 100]}{M} \qquad \text{Eq. 2.1}$$

Where V_o is the volume of HCl used to titrate blank, V_n is the volume of HCl used to titrate sample, N is the normality of HCl used, 43 is the weight of acetyl group, M is the sample amount as dry substance (g).

Acetyl content, %A, was used to calculate the DS, according to the following equation:

$$DS = \frac{162 \times \%A}{[4300-(42 \times \%A)]} \qquad \text{Eq. 2.2}$$

Where 162 is the molecular weight of the anhydroglucose unit, 42 is the molecular weight of replaceable acetyl group and 4300 is the molecular weight of the acetyl group attached with 100 anhydroglucose unit.

2.2.2.4. Preparation of SANPs

The preparation of SANPs was based on emulsification-solvent diffusion and evaporation method described by Santander-Ortega *et al*. (2010). In brief, acetylated starch was dissolved in an organic solvent (1 mg/ml), ethylacetate, dichloromethane or chloroform. The organic solution (2 ml) was emulsified in aqueous phase (8 ml) containing a surfactant (1% w/v) (PVA, Tween® 80, Pluronic® F68 or Pluronic® F127) resulting in oil in water (O/W) emulsion. Emulsification of this biphasic system was enhanced by using a high speed homogenizer (Pro Scientific Inc, Oxford, USA). After the formation of stable emulsion, the organic solvent was evaporated under stirring for 5 h at room temperature to transform the nano emulsion into a NP suspension. All experiments were done at least in triplicates.

2.2.2.5. Particle size and polydispersity index (PDI) analysis

Particle size and PDI analysis of the NPs were determined by dynamic light scattering (DLS), also known as photon correlation spectroscopy (PCS), using a 90Plus Particle Size Analyzer (Brookhaven Instruments Corporation, New York, USA). Prior to the measurements, all formulations were diluted using purified water to yield an appropriate scattering intensity. All experiments were done at least in triplicate at 25°C (Namazi *et al.*, 2011).

2.2.2.6. Optimization of starch NPs fabrication

A CCD model coupled with the Design Expert software (Version 8.0.7.1, Stat Ease, Inc, Minneapolis, MN) was used to optimize the formulation (surfactant concentration) and process (homogenization speed and time) variables and to evaluate the main effects, interaction effects and quadratic effects of the independent variables) on the response variables, particle size (Y_1) and PDI (Y_2) of starch NPs. Details of the design are listed in Table 2.1. For each factor, the experimental range was selected on the basis of the results of preliminary experiments and the feasibility of preparing the starch NPs at the extreme values. The value ranges of the variables were: Pluronic® F127 concentration (X_1): 0.6 - 2.0%, homogenization speed (X_2): 6000 - 18000 rpm and homogenization time (X_3): 10.0 - 20.0 min. The design consists of 15 runs (8 factorial points, 6 star points and 1 center point) and 5 replicated runs (center points) yielding 20 experiments in total (Table 2.2). The purpose of replication was to estimate experimental error and increase the precision. Each experimental run was repeated thrice.

Table 2.1: Relationship between coded and actual values of the variables used for starch NP fabrication

	Coded level of variables				
Factors	**-1.68**	**-1**	**0**	**1**	**+1.68**
X_1 = Pluronic® F127 (% w/v)	0.12	0.60	1.30	2.00	2.48
X_2 = Homogenization speed (rpm)	1909.24	6000.00	12000.00	18000.00	22090.76
X_3 = Homogenization time (min)	6.59	10.00	15.00	20.00	23.41
Responses	**Constraints**				
Y_1 = Particle size	Minimize				
Y_2 = PDI	Minimize				

A design matrix comprising of 20 experimental runs was constructed and the responses were modelled by the following polynomial model:

$$Y= b_0 + b_1X_1 + b_2X_2 + b_3X_3 + b_{12} X_1X_2 + b_{13} X_1X_3+ b_{23} X_2X_3+ b_{11}X^2_1 + b_{22}X^2_2 + b_{33}X^2_3 + b \quad \text{Eq. 2.3}$$

Where Y is the measured response associated with each factor level combinations; b_o is the Intercept; b_i's (for i = 1, 2, and 3) are the linear effects, the b_{ii} are the quadratic effects, the b_{ij}'s (for i, j = 1, 2, and 3, i < j) are the interactions between the i^{th} and j^{th} variables.

Table 2.2: Observed responses Experimental setup of CCD for starch NP formulation.

Run	**Point type**	**Factors**		
		Surfactant concentration (%)	Homogenization speed (rpm)	Homogenization time (min)
1	Center	1.30 (0)	12000.00 (0)	15.00 (0)
2	Factorial	2.00 (1)	6000.00 (-1)	20.00 (1)
3	Center	1.30 (0)	12000.00 (0)	15.00 (0)
4	Axial	2.48 (+1.68)	12000.00 (0)	15.00 (0)
5	Center	1.30 (0)	12000.00 (0)	15.00 (0)
6	Factorial	2.00 (1)	18000.00 (1)	20.00 (1)
7	Axial	1.30 (0)	1909.24 (-1.68)	15.00 (0)
8	Factorial	2.00 (1)	18000.00 (1)	10.00 (-1)
9	Axial	0.12 (-1.68)	12000.00 (0)	15.00 (0)
10	Factorial	0.60 (-1)	6000.00 (-1)	20.00 (1)
11	Axial	1.30 (0)	12000.00 (0)	23.41 (+1.68)
12	Factorial	0.60 (-1)	18000.00 (1)	10.00 (-1)
13	Axial	1.30 (0)	12000.00 (0)	6.59 (-1.68)
14	Factorial	2.00 (1)	6000.00 (-1)	10.00 (-1)
15	Factorial	0.60 (-1)	18000.00 (1)	20.00 (1)
16	Axial	1.30 (0)	22090 (+1.86)	15.00 (0)
17	Center	1.30 (0)	12000.00 (0)	15.00 (0)
18	Factorial	0.60 (-1)	6000.00 (-1)	10.00 (-1)
19	Center	1.30 (0)	12000.00 (0)	15.00 (0)
20	Center	1.3 (0)	12000 (0)	15 (0)

2.2.2.7. Statistical analysis

All the data measured and reported in this study are averages of a minimum of triplicate measurements and the values are expressed as mean ± standard deviation. Wherever appropriate, the data were subjected to further statistical analysis making use of software package called IBM SPSS Statistics for Windows, Version 21.0 (IBM Corporation, Armonk, NY, USA). Origin®, version 8.5 (OriginLab Corporation, MA, USA) and MS Excel 2010 (Microsoft Corporation, USA) were also used in plotting graphs with standard error bars.

In optimization process, data were analyzed by using ANOVA which helped determine if the factors and the interactions between factors were significant. To test whether the terms were statistically significant in the regression model, t-tests were performed using a 95% ($\alpha = 0.05$) level of significance. An F-test was used to determine whether there was an overall regression relationship between the response variable Y and the entire set of X variables at a 95% ($\alpha = 0.05$) level of significance. The coefficient of multiple determinations was denoted by R^2, which measured the proportionate reduction of total variation in Y associated with the use of the set of X variables. In addition, the validity of the regression model was assessed according to statistical assumptions and lack of fit test. The statistical analysis was performed using the software Design Expert (Version 8.0.7.1) (Stat-Ease, Inc, Minneapolis, MN).

2.3. Results and discussion

2.3.1. Degree of acetylation

The mean value of acetyl contents and DSs of various SAs are presented in Table 2.3. It can be seen that the DS progressively increases with reaction time due to the favourable effect of time on diffusion and adsorption of the acetyl groups on starch molecules. However, this increase was nonlinear and characterized by an initial faster rate followed by a slower rate. This can be explained by the fact that as the acetylation reaction proceeds, the reactive sites on starch decrease due to structural modification of the starch backbone.

The substitution of hydroxyl moieties with acetate moieties in native starch can provide sufficient hydrophobicity which is important for subsequent fabrication of NPs. The hydrophobicity of SA is related to its DS which refers to the extent to which the hydroxyl groups of the α-D-glucopyranose units of starch molecules are substituted by acetyl groups due to esterification (Ayucitra 2012; Kalita *et al*., 2014; Singh *et al.,* 2007; Xu *et al*., 2010).

The replacement of hydrophilic hydroxyl groups of the native starch by bulk hydrophobic acetyl groups reduces its hydrophilicity and renders the starch to develop hydrophobicity (Shogren and Biswas 2010; Valodkar and Thakore, 2011). Due to this reduction in hydrophilicity SAs can spontaneously self-associate and form NPs with hydrophobic cores that can encapsulate hydrophobic drugs (Minimol *et al.,* 2013).

Table 2.3: Acetyl contents and DSs of acetylated cassava starch, n = 3

Starch type	Time (h)	Acetyl content (% A)	DS
Cassava	1	20.32 (1.29)	0.91
	3	29.87 (0.63)	1.50
	6	36.65 (0.64)	2.15
	9	42.56 (0.25)	2.74

The values in the parentheses indicate standard deviations

2.3.4. Influence of factors on fabrication of NPs

The optimization of various formulation and process variables play an important role in yielding the desired nano sizes (Liu *et al.,* 2008). Hence, factors such as organic solvents, type and concentration of surfactants, SA concentration and DS, speed and duration of homogenization that could possibly have significant effects on the response variables, i.e., particle size and PDI were investigated.

2.3.4.1. Influence of organic solvents

In the formation of SANPs by emulsification-diffusion method, both the organic solvent phase containing SA and the aqueous phase containing stabilizer are in the state of thermodynamic equilibrium. The addition of water to the system destabilizes the equilibrium and it causes the organic solvent to diffuse to the external phase. During such transport of the solvent, SANPs are produced (Song *et al.,* 2006). The size of NPs is therefore dependent upon the type of organic phase solvent used. Hence, solvent optimization is crucial in the preparation of NPs (Santander-Ortega *et al*., 2010). In the current study, the effect of the type of organic solvent on the mean particle size of SANPs was investigated. Based on this investigation, the size of the SANPs produced varied between 146.8 nm to 423.4 nm depending on the type of organic solvent used, keeping all other variables constant. Larger particles above 200 nm mean particle size and PDI > 0.2 were obtained with water-

immiscible solvents such as chloroform and dichloromethane, while smaller particles below 200 nm mean particle size and PDI < 0.2 were obtained with partially water miscible solvent (ethyl acetate) (Fig. 2.1).

Since NPs are formed from the emulsion droplets after organic solvent diffusion, their size is dependent on the stability of the emulsion droplets, which collide and coalesce among themselves. When the stabilizer remains at the liquid–liquid interface during the diffusion process, and its protective effect is adequate, NPs will form (Li *et al.*, 2011). In this study, when chloroform and dichloromethane were used as the organic solvent, nearly every formulation resulted in significant aggregation due to their immiscible nature with water, and hence the stabilizer was unable to completely prevent aggregation of emulsion droplets, leading to large mean particle size. Whereas, small particle size for ethyl acetate was attributed to both the adequacy of the stabilizer's protection against coalescence, and the low interfacial tension between aqueous and organic phases, resulting from their partially water-soluble nature. The results are in agreement with those reported elsewhere (Song *et al.*, 2006).

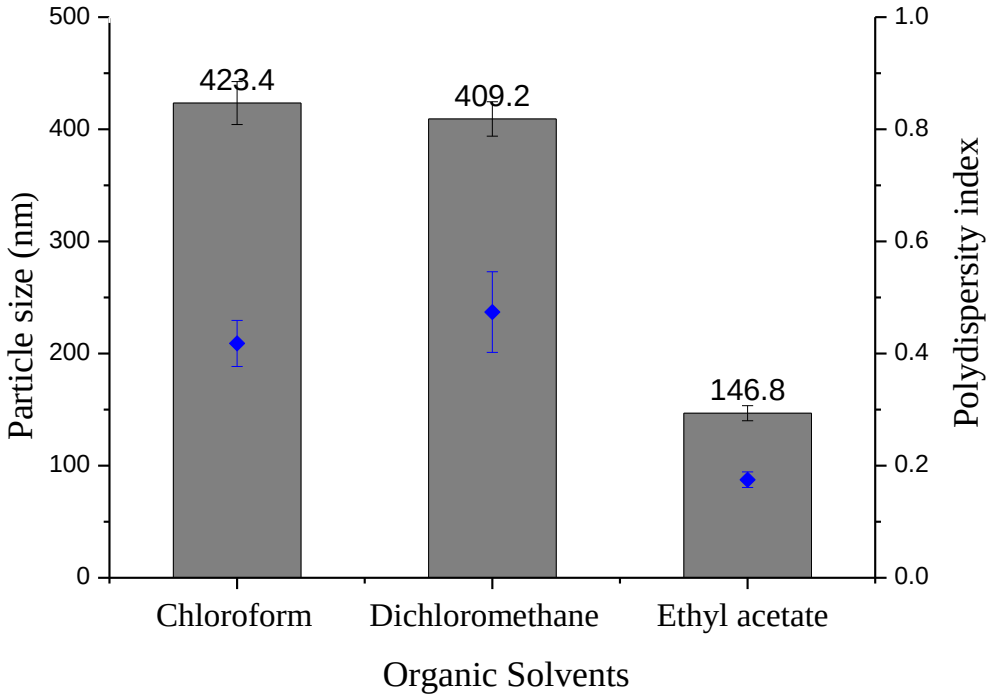

Fig. 2.1: Influence of organic solvents on the size (▭) and PDI (●) of cassava SANPs.

2.3.4.2. Influence of SA concentration in the organic phase

The effect of SA concentration in the organic phase on the size and PDI of NPs is depicted in Fig. 2.2. When the SA concentration is increased from 0.1 mg/ml to 2 mg/ml in the organic solvent the size of the cassava SANPs increased from 160.4 to 224.7 nm. Similarly, PDI increased from 0.18 to 0.23. The effect of the SA concentration on the size and PDI of NPs is probably due to the increase in viscosity of the organic phase which provides resistance to the shear forces applied for emulsification, resulting with coarse emulsions as pointed out by Mainardes & Evangelista (2005).

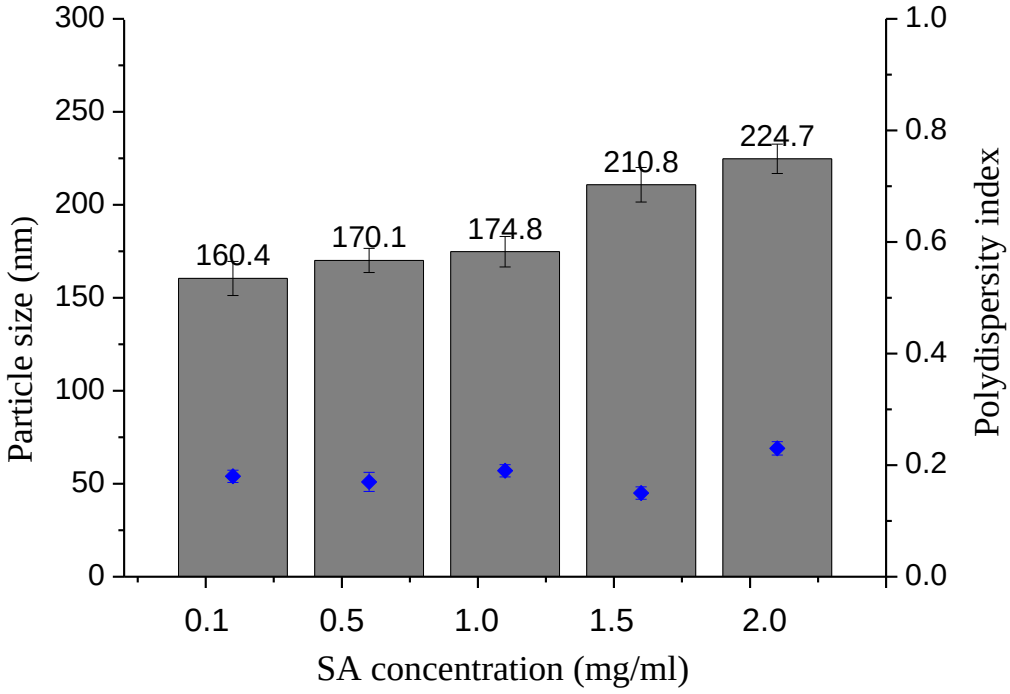

Fig. 2.2: Effect of SA concentrations on size (▭) and PDI (●) of cassava SANPs.

2.3.4.3. Influence of DS

To investigate the effect of DS of SA on mean particle size and PDI of NPs, SAs having low, medium and high DSs were used. Although this increase in DS from low to high was observed to enhance the solubility of SA in organic solvents, the effect on mean particle size was not significant ($p > 0.05$). However, higher PDI was observed with low and medium substituted SAs as depicted in Fig. 2.3. This may be attributed to uncontrolled hydrogen bonding of the less hydrophobic SAs (low and medium substituted) in the aqueous phase. The results are in agreement with those reported by Han, *et al*., 2013. Therefore, SA with

higher DS that renders sufficient hydrophobicity in aqueous medium was used in the subsequent fabrication of NPs.

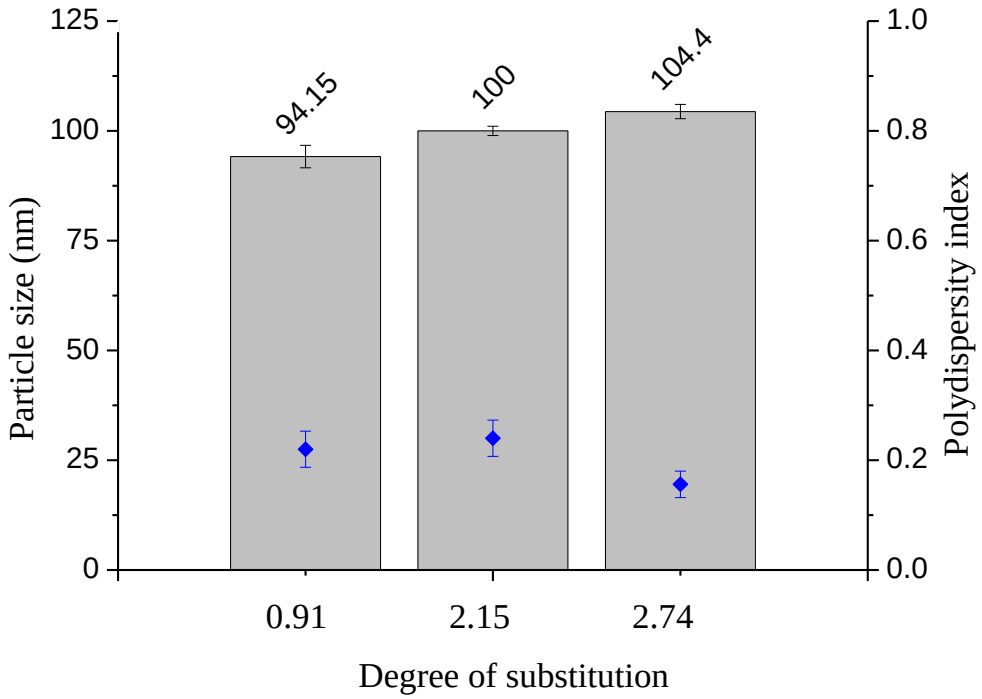

Fig. 2.3: Influence of DS on size (▭) and PDI (●) of the cassava SANPs.

2.3.4.4. Influence of surfactant type

SANPs containing different stabilizing agents were prepared by using emulsification-solvent evaporation method. In this method, emulsion formation step is very critical because the droplet size of the emulsion dictates the final size of NPs. Studies indicate that droplet size largely depends on the type and amount of the stabilizing agents because they disperse the oil-water phases and provide the stabilization of droplets during the emulsification process (Mainardes and Evangelista 2005). Within this context, a series of SANPs containing PVA, Pluronic® F68, Pluronic® F127 and Tween® 80 as stabilizing agents were prepared. The influence of these stabilizers on the size and the PDI of NPs were evaluated. Based on the evaluation, Tween® 80 resulted in smaller particles in the range of 100 - 200 nm, but the PDI of the preparation were too high. Formulations with PVA also resulted in a higher PDI. Whereas Pluronic® F127 provided the smallest particles and low PDI (Fig. 2.4). This may be attributed to more stabilizing effect of the Pluronic® F127 molecules that are adsorbed on the interfaces of emulsion droplets, thereby providing increased protection against coalescence

due to mechanical and steric hindrance as described elsewhere (Chin *et al.*, 2014). Thus, Pluronic® F127 was selected for the fabrication of NPs.

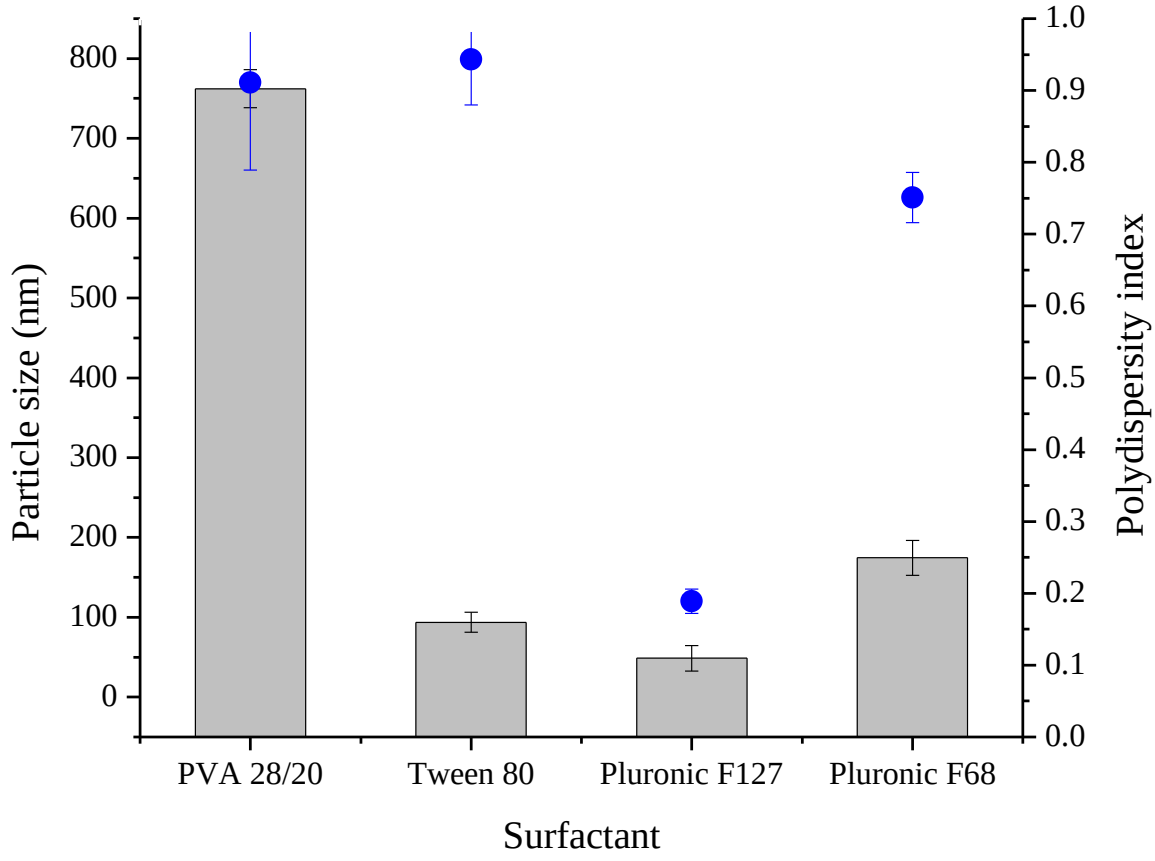

Fig. 2.4: Influence of types surfactants (1%w/v) on size (▭) and PDI (●) of cassava SANPs.

2.3.4.5. Influence of surfactant concentration

The amount of surfactant plays an important role in the emulsification process and in the protection of the droplets, because it can avoid the coalescence of globules. Hence the effect of surfactant concentration on the particle size and PDI of cassava SANPs was further studied using the selected surfactant, Pluronic® F127 at various concentrations.

As shown in Fig. 2.5, increasing the concentration of surfactant from 0.1 to 2.0 % decreases the particle size (from 265.0 nm to 73.3 nm) and PDI (from 0.304 to 0.103) of SANPs. A concentration of 0.5 % (w/v) of Pluronic® F127 was not enough to produce the desired NPs with size less than 200 nm since the amount of surfactant was insufficient to cover the surface area of the droplets. The droplets tend to aggregate to reduce the surface area (Yu *et al.*, 2007). On the other hand, 1.5 % (w/v) concentration of Pluronic® F127 produced NPs with size below 200 nm (Fig. 2.5). More discrete starch NPs are produced due to optimum amount

of surfactant that completely coated the entire surface area of droplets giving high stability against droplets coalescence and thus generating smaller droplet size as described elsewhere (Yu *et al.*, 2007). Besides, low PDIs of NPs were obtained due to the surfactant layer that created the steric stabilization which prevented the aggregation of NPs. Hence, with increasing stabilizer concentration for Pluronic® F127, more stabilizer molecules are adsorbed on the interfaces of emulsion droplets, providing increased protection against coalescence and resulting in smaller emulsion droplets. This in turn enables NP formation with low size and PDI (Sharma *et al.*, 2016).

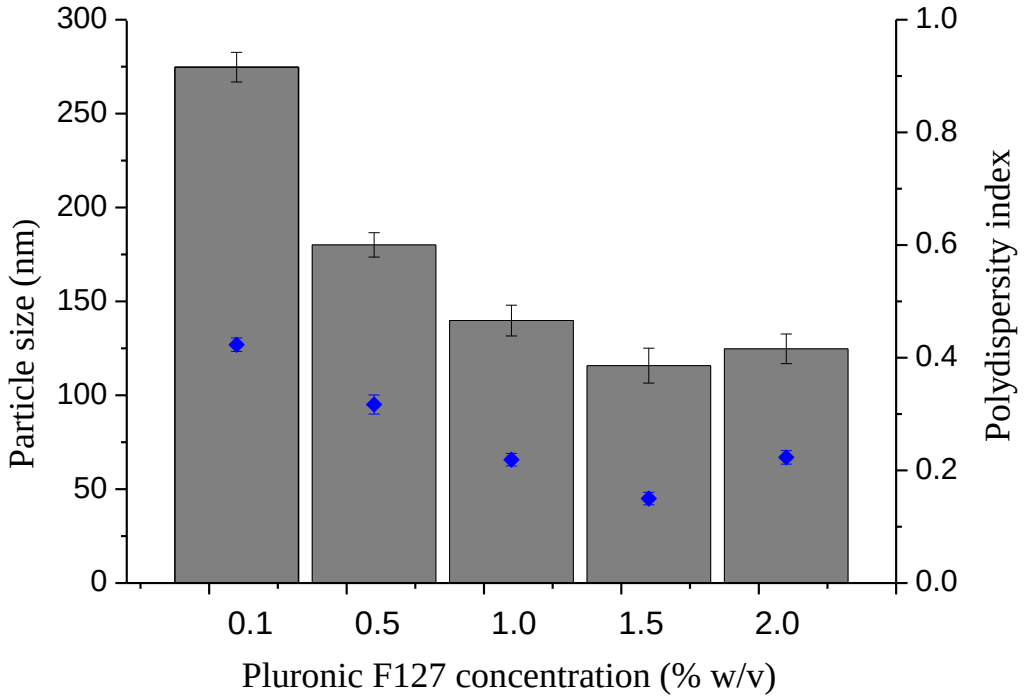

Fig. 2.5: Influence of surfactant concentration on size and PDI (●) of cassava SANPs.

2.3.4.6. Influence of homogenization speed

In order to obtain emulsified systems during the fabrication of NPs by emulsification method, the application of energy is a fundamental step. To verify the influence of this factor on NPs size and PDI, homogenization speed was varied between 6,000 rpm and 22,000 rpm at constant stabilizer concentration (Pluronic® F127, 1.0% w/w) and homogenization time of 15 min. The results in Fig. 2.6 clearly show that an increase in the homogenization speed from 6,000 rpm to 18,000 rpm leads to a decrease in particle size of SANPs (from 537.35 nm to 127.59 nm) and PDI (from 0.383 to 0.141). With further increase in rpm (22,000), there

was no significant reduction in particle size (p = 0.052) and PDI (p = 0.213). Hence, homogenization results in smaller sized droplet formation during emulsification and thus smaller particles after solvent diffusion.

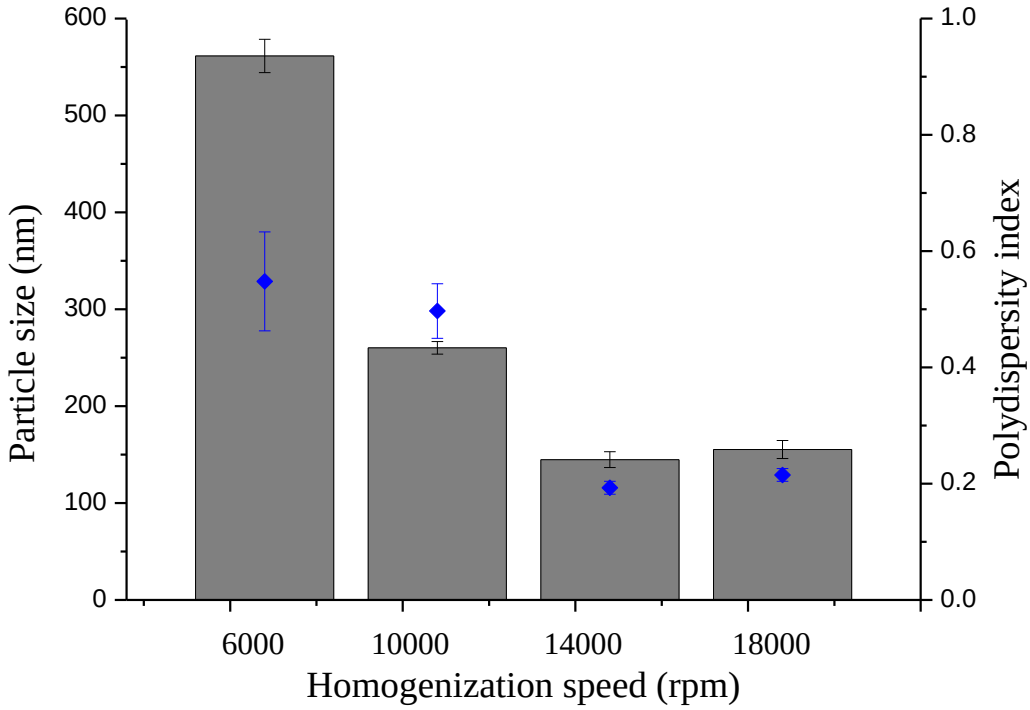

Fig. 2.6: Influence of homogenization speed on size (▭) and PDI (●) of cassava SANPs.

2.3.4.7. Influence of homogenization time

The effect of homogenization time on particle size and PDI of cassava SANPs is presented in Fig. 2.7. In all cases, increase in homogenization time resulted in NPs having smaller mean diameter and lower PDI. With longer homogenization time (15 - 20 min), higher energy is released leading to a dispersion of polymeric organic phase with small size nano-droplets and monomodal distribution profile resulting in the formation of smaller NPs. This phenomenon has been described by Shi *et al.*, 2011.

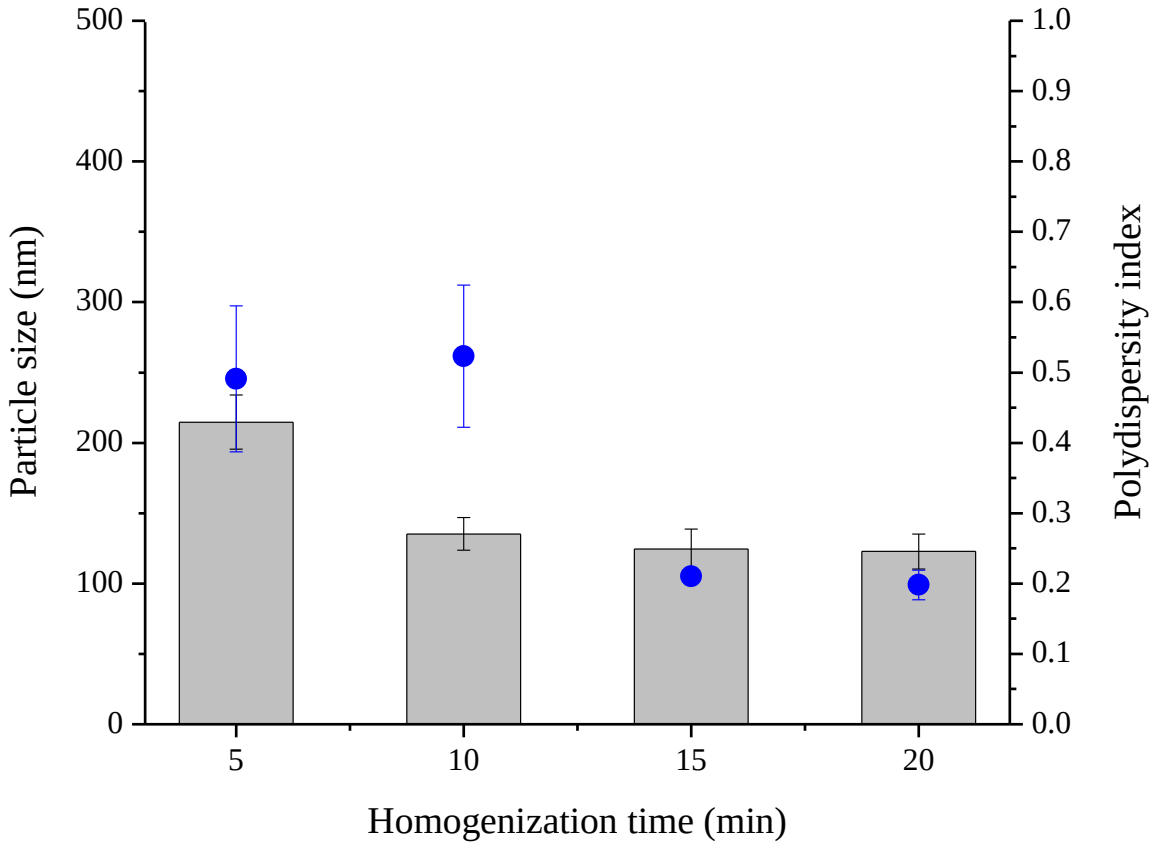

Fig. 2.7: Influence of homogenization time on size (▭) and PDI (●) of cassava SANPs.

2.3.5. Optimization

RSM combined with CCD model offers the possibility of investigating a number of variables at different levels with only a limited number of experiments. As mentioned earlier, surfactant concentration, homogenization speed and homogenization time were identified as critical independent variables and their effects on particle size and PDI were further studied and optimized using RSM. To obtain a good estimate of the quadratic regression model coefficients, each independent variable must be studied at least at three distinct levels and consequently CCD was used in the optimization study as it considers five distinct levels. Pluronic® F127 was used in the optimization study as it provided the desired particle size and low PDI.

Table 2.4 shows the experimental results concerning the tested variables on mean particle size and PDI. For each response, the model which generated a higher F value was identified as the best fitted model. Each obtained model was validated by ANOVA. Three dimensional response surface plots were drawn for the optimization of starch NP formulation.

Table 2.4: Summary of experimental responses (size and PDI of SANPs) for cassava starch

Run	Factors			Responses	
	X_1	X_2	X_3	Y_1	Y_2
1.	1.30	12000.00	15.00	119.67	0.119
2.	2.00	6000.00	20.00	219.17	0.209
3.	1.30	12000.00	15.00	124.84	0.106
4.	2.48	12000.00	15.00	188.52	0.148
5.	1.30	12000.00	15.00	117.32	0.123
6.	2.00	18000.00	20.00	99.25	0.102
7.	1.30	1909.24	15.00	304.31	0.312
8.	2.00	18000.00	10.00	161.14	0.138
9.	0.12	12000.00	15.00	305.84	0.235
10.	0.60	6000.00	20.00	232.12	0.217
11.	1.30	12000.00	23.41	187.44	0.161
12.	0.60	18000.00	10.00	181.14	0.167
13.	1.30	12000.00	06.59	239.11	0.216
14.	2.00	6000.00	10.00	275.31	0.248
15.	0.60	18000.00	20.00	202.83	0.201
16.	1.30	22090.76	15.00	102.53	0.121
17.	1.30	12000.00	15.00	123.74	0.116
18.	0.60	6000.00	10.00	276.51	0.201
19.	1.30	12000.00	15.00	122.54	0.115
20.	1.30	12000.00	15.00	123.21	0.105

X_1= Pluronic® F127 concentration (%w/v) Y_1= Particle size

X_2= Homogenization speed (rpm) Y_2= PDI

X_3= Homogenization time (min)

2.3.5.1. Response model selection

In order to select the best fit model for the dependent variables, particle size and PDI, the model summary statistics was used. As shown in Table 2.5, quadratic polynomial model is suggested as a best fit for the responses because the p-value is less than 0.05 whereas the lack of fit p-value is greater than 0.05. Furthermore, adjusted R-square and predicted R-square values of particle sizes (0.9171 and 0.8609) and PDI (0.9609 and 0.9007) were in a reasonable agreement i.e., within 0.2 of each other (Table 2.5). ANOVA results also revealed that the three independent variables, i.e., surfactant concentration ($p < 0.05$), homogenization speed ($p < 0.05$) and homogenization time ($p < 0.05$), were found to be significant and can be considered in the quadratic model equations (Aziz *et al*., 2008; Kusic *et al.,* 2010).

From the foregoing, it is apparent that the models proposed are adequate for their respective responses and there is no reason to suspect any violation of the independence or constant variance assumption. Since both of the response models were significant, the adjusted and predicted R- square of both response models were in good agreements, the adequate precision were over 4 and the residuals were well-behaved. It is, therefore, reasonable to conclude that the selected models were fairly accurate and could be used for further analysis.

Table 2. 5: Fit summary statistics for size and PDI of cassava SANPs

Response	**Source**	**R^2**	**Adjusted R^2**	**Predicted R^2**	**p-value**	**Lack of fit p-value**	**Remark**
	Linear	0.5259	0.4370	0.3233	< 0.0001	< 0.0001	
Particle	2FI	0.5600	0.3569	0.0677	0.0001	< 0.0001	
size	Quadratic	0.9564	0.9171	0.8609	< 0.0001	0.05111	Suggested
	Cubic	0.9834	0.9476	-2.5514	0.1563	0.0001	Aliased
	Linear	0.4605	0.3593	0.2041	0.0001	0.0001	
PDI	2FI	0.5430	0.3321	0.0122	< 0.0001	< 0.0001	
	Quadratic	0.9811	0.9691	0.9007	0.0002	0.391	Suggested
	Cubic	0.9795	0.9351	-2.6634	0.0817	0.0058	Aliased

The normal probability plots of the residuals for particle size and PDI and the plots of the residuals versus the predicted response for particle size and PDI are shown in Appendix A. The important information on the model performance is summarized in residuals (i.e. difference between observed and predicted values) providing a clear view for any

discrepancy fit to the model. Hence, two plots related to residual, the normal probability plot of residuals and the plot of internally studentized residuals versus predicted values are considered as additional tests of model adequacy checking tools (see detail in appendix A) (Kusic *et al*., 2010).

2.3.5.2. Response Surface Analysis

The effect of the formulation variables on a response was assessed by studying the three-dimensional response surface plots. These plots were used to describe the interaction and quadratic effects of two independent variables on the response at one time, while keeping the third variable constant.

Influence of formulation and process variables on particle size: In order to fabricate NPs of the desired size, the relationship between independent variables and responses was further evaluated using the quadratic polynomial equation and surface response plot. The following second order reduced quadratic model equations were derived for cassava SANPs by best fit method to describe the relationship between the response: particle size (Y_1), and the independent variables: surfactant concentration (X_1), homogenization speed (X_2) and homogenization time (X_3). Polynomial equations for the SANPs in terms of coded coefficients of the formulation parameters are given below:

$$\text{Particle size } (Y_1) = +122.58 - 24.53X_1 - 51.12X_2 - 16.67X_3 - 13.68X_1X_2 - 11.92X_1X_3 + 7.54X_2X_3 + 39.78X^2_1 + 24.31X^2_2 + 27.80X^2_3 \quad \text{.....Eq. 2.4}$$

The magnitude of a coefficient in the polynomial equations implies the relative effect of the independent variable on the response whereas the sign indicates either positive effect (+) or negative effect (-) of independent variables on the response. Looking at Eq. 2.4, it is evident that the particle size (Y_1) of starch NPs is affected negatively by all the three independent variables. However, the effect of homogenization speed (X_2) is stronger than the other two variables, as it has larger coefficient (–51.12) as compared to the coefficients associated with percentage of surfactant concentration (–24.53) and homogenization time (–16.63).

The effect of the independent variables on the particle size is also demonstrated with 2D and 3D surface plots. The 2D and 3D response surface plots are the graphical representations of the fitted regression models. These plots, presented on the basis of the model equations,

display the interaction between the independent variables and assist in determining the optimum values of the variables within the ranges considered (Sampaio *et al*., 2006). The contour plots shown in Fig. 2.8 indicate the combined effect of percentage of surfactant concentrations, homogenization speed and homogenization time on the particle size.

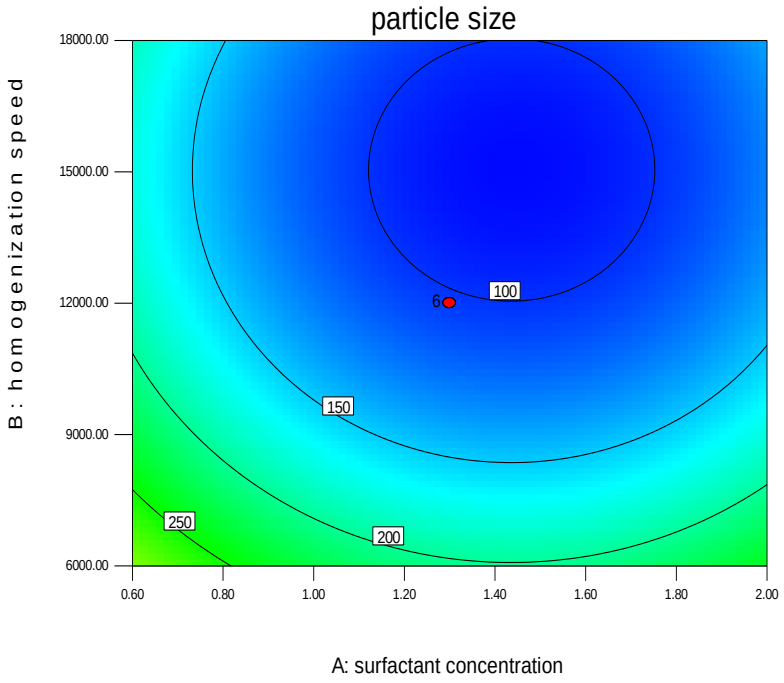

Fig. 2.8: Contour plot of percentage of surfactant concentration and homogenization speed on the particle size of cassava SANPs

The 3D plots for the interaction between Pluronic® F127 concentrations, homogenization speed and time as well as their interactive effects on particle size of SANPs are presented in Fig. 2.9 (a, b, and c). Analysis of surface response for the interaction of Pluronic® F127 concentration and homogenization speed indicates a decrease in the mean particle size of SANPs with increased concentration of surfactant at all homogenization speed levels (Fig. 2.9 a & b). This decrease, however, eventually ceases i.e., beyond a certain concentration of Pluronic® F127, no further decrease in particle size of the NPs is observed. As reported elsewhere, this may be due to the attainment of the best possible packing concentration and the smallest globule size. The excess non-adsorbed surfactant in the continuous aqueous phase might not play a considerable role in emulsification or protection of coalescence as proposed by Chin, *et al.*, 2014.

Further analysis of the response surface for the interaction of homogenization speed and time at constant Pluronic® F127 concentration indicates that initially, with increased

homogenization speed, particle size decreases but further increase in speed shows no significant effect (Fig. 2.9 c). The particle size reduction at increased homogenization speed may be related to a high shear force generated in the homogenization process which causes a reduction in emulsion droplet size and consequently a decrease in particle size as reported elsewhere (Gardouh *et al.*, 2012).

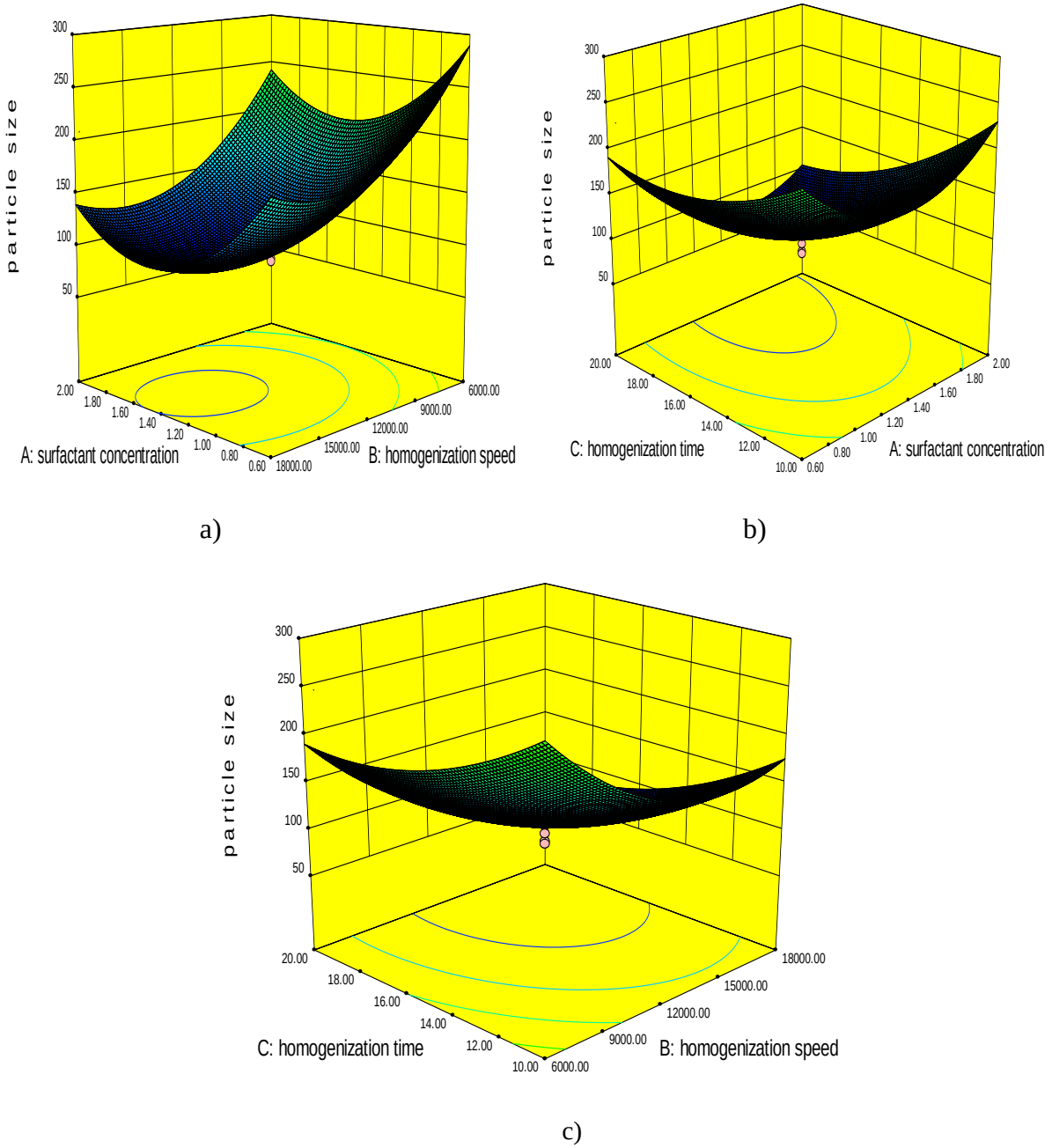

Fig. 2.9: Three dimensional response surface plots of the effect of independent variables on particle sizes of cassava SANPs; a) effect of Pluronic® F127 concentration and homogenization speed, b) effect of Pluronic® F127 conc. and homogenization time, and c) effect of homogenization time and speed.

Influence of formulation and process variables on PDI

The other critical response is PDI which is used to describe variation of particle size in a sample of particles. It is a dimensionless number extrapolated from autocorrelation function and ranges from 0 to 1. When this index is close to 0, the particle size range becomes low.

The polynomial equations relating PDI (Y_2) and the independent variables of cassava SANPs are given in the following Equations.

$$Y_2 = +0.13 - 0.060X_1 - 0.073X_2 - 0.016X_3 - 0.023X_1X_2 + 0.019X_1X_3 \\ -0.017X_2X_3 + 0.056X_1^2 + 0.073X_2^2 + 0.023X_3^2 \quad \text{.....Eq. 2.5}$$

As shown in Eq. 2.5, the PDI of SANPs is also affected negatively by all the three independent variables (Pluronic® F127 concentration, homogenization speed and homogenization time). In all cases the homogenization speed was more predominant factor on PDI as indicated by its larger coefficient as compared with the other two variables.

The contour plots for PDI as a function of preparation factors are constructed by fixing one of the variables (Fig. 2.10). This gives a diagrammatic representation of relationship between the experimental responses and input variables. As shown in Fig. 2.10, the patterns of contour lines reflect the quadratic interaction between the independent variables of PDI.

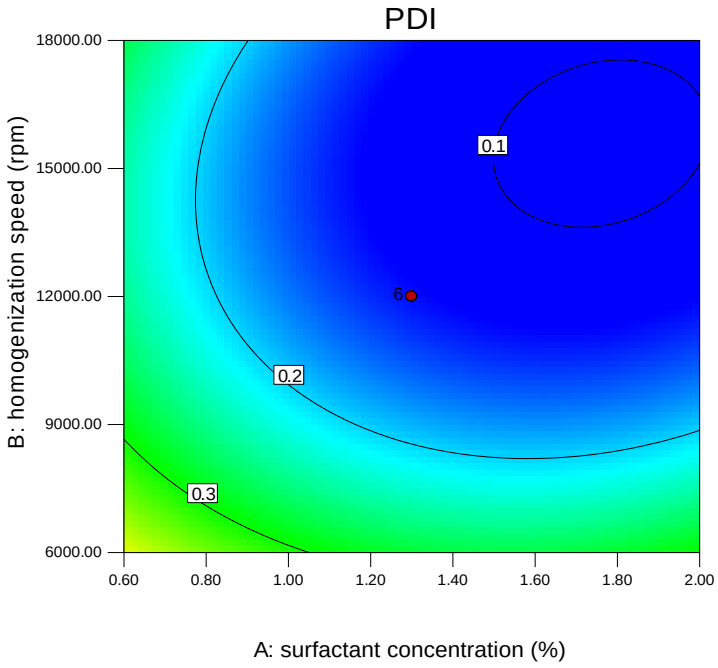

Fig. 2.10: Contour plot of percentage of surfactant concentration, homogenization speed and homogenization time on the PDI of cassava SANPs

The effect of these independent variables on PDI is also seen in 3D surface plots. The 3D surface responses of PDI keeping homogenization time, homogenization speed and Pluronic® F127 concentration constant are shown in Fig.2.11. As shown in these Figures, PDI decreases as Pluronic® F127 concentration, homogenization speed and homogenization time increase.

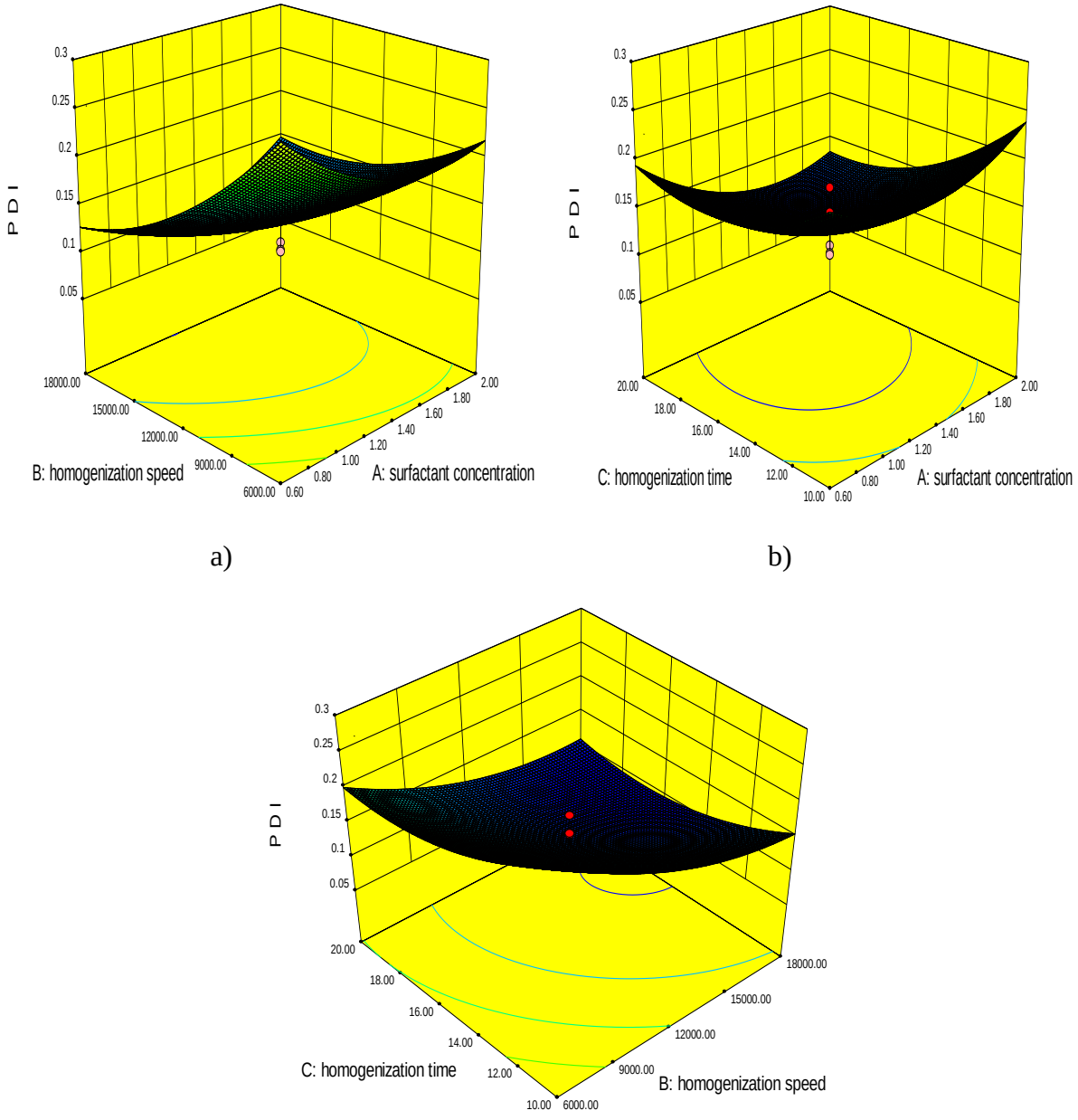

a) b)

c)

Fig. 2.11: Three dimensional response surface plots of the effect of independent variables on PDI of cassava SANPs a) effect of Pluronic® F127 conc. and homogenization speed, b) effect of Pluronic® F127 conc. and homogenization time, and c) effect of homogenization time and speed.

2.3.5.3. Simultaneous optimization of particle size and PDI

After generating the model polynomial equations to relate the dependent and independent variables, the SANP formulations were optimized for the two responses simultaneously. The final optimal experimental parameteres were obtained using both numerical and graphical optimization techniqies of Design-Expert 8.0.7.1 software, which allows compromise among various responses and searches for a combination of factor levels that jointly optimize a set of responses by satisfying the requirements for each response in the set. Table 2.6 presents constraints assigned for factors and responses during numerical and graphical optimizations.

Table 2.6: Constraints assigned for factors and responses in numerical and graphical optimization

	Factor constraints	
Factors	**Low**	**High**
Surfactant concentration (%)	0.6	2.0
Homogenization speed (rpm)	6000.0	18000.0
Homogenization time (min)	10.0	20.0

	Response constraints		
Response	**Goal**	**Lower limit**	**Upper limit**
Particle size (nm)	Minimize	10.0	200.0
PDI	Minimize	0	0.2

Numeric optmization

The particle size and PDI were simultaneously optimized for cassava SANPs using numerical optimization technique (Design Expert 8.0.7.1 software), which provided the specific point of independent variables that yields the desired responses. From the software, the predicted optimum responses (particle size of 94.48 nm and PDI of 0.107) and the corresponding levels of independent variables (Pluronic® F127: 1.51%, homogenization speed: 15,382.80 rpm, homogenization time: 15.97 min) were obtained for cassava starches according to the set goals (Fig. 2.12).

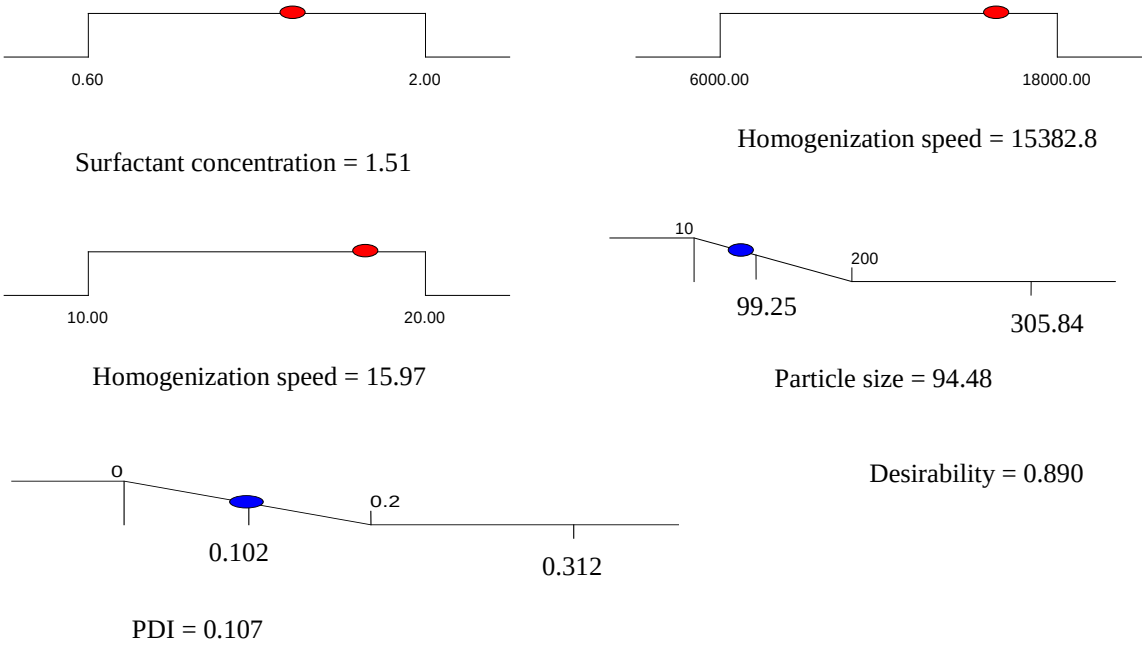

Fig. 2.12: Numerical optimization results of predicted optimum values and the corresponding levels of parameters for cassava SANPs.

In the numerical optimization of this study, the desired goals for each response was chosen and different importance were assigned to each goal to adjust the shape of its particular desirability functions. To find the global (overall) diesirability function, the software performs thousands of interactions and calculations and finally it comes up with the maximum desirability score and the conditions on which it was arrived. In multiple response optimization using desirability approach, individual desirability functions d_i indicate measures of how well the goals for each response are satisfied, whereas overall desirability function is a measure of how well the combined goals for all responses are satisfied. Desirability function ranges from 0 and 1, with value closer to one indicating a higher satisfaction of response goal(s). In this study, the value of overall desirability function of cassava SANPs was obtained from the Design Expert solver to be 0.89 (Fig. 2.13). This was calculated from the optimal point obtained from $Y_1 = 94.48$ and $Y_2 = 0.107$.

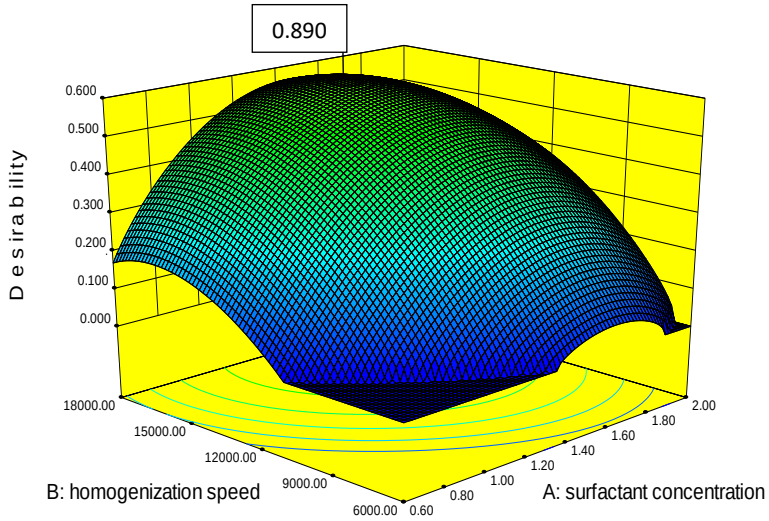

Fig. 2.13: 3D overall desirability function of cassava SANPs

Graphical optimization

With the aim to definitively pointing out the optimal conditions of the particle size and PDI, a graphical optimization was conducted using the Design Expert 8.0.7.1 software. The methodology essentially consists of overlaying the curves of the two models obtaied from the CCD according to the specific criteria imposed in Table 2.6. Fig. 2.12 show the overlay plot in which the plain areas represent the areas satisfying the imposed criteria. The point identified by the flag was chosen in the graph as representative of the optimized area corresponding to percentage surfactant concentration, homogenization speed and homogenization time. Under these conditions the model predicts the particle size of 94.48 nm and PDI 0.107 for cassava SANPs.

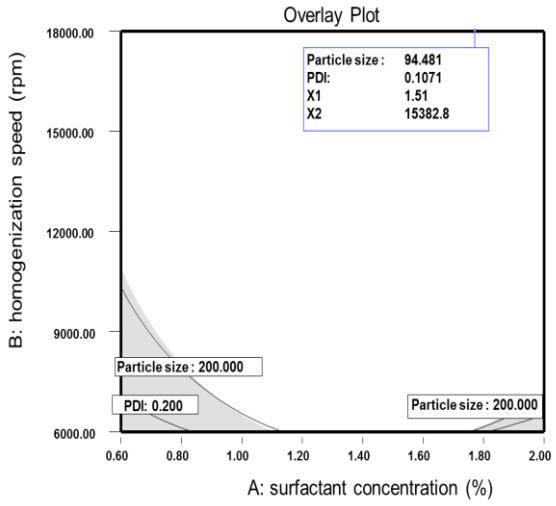

Fig. 2.14: Overlaying plot of particle size and PDI of SANPs as function of percentage surfactant concentration, homogenization speed and time

2.3.5.4. Confirmation test

Verification experiments were carried out at the predicted optimal fabrication conditions to confirm the adequacy of the model for predicting the responses, particle size and PDI. In this confirmation experiment, the particle size and PDI of cassava SANPs were found to be 96.37 and 0.113, respectively. According to the design expert software, experimentally observed result of particle size is in a reasonable agreement with the predicted value (percentage error < 5%) whereas the observed value of PDI is slightly higher than 5%. Although PDI is not in the ± 5% range, the observed value is with in the acceptable range, PDI < 0.2. The agreement between the observed value and the predicted value of particle size by the equation confirms the statistical significance of the model and its adequate precision in predicting the optimum condition in the domain of levels chosen for the independent variables.

Conclusion

DS of cassava SA increased with longer reaction times. In optimizing the fabrication of cassava SANPs by spontaneous emulsification and solvent evaporation technique, the type and amount of surfactants, homogenization speed and homogenization time were found to be critical factors in obtaining the desired particle size and PDI of the NPs. The predicted response of particle size of SANPs was found to be in a reasonable agreement with experimentally determined response whereas the observed value of PDI is slightly higher than 5%. In conclusion, judicious selection of solvent system and surfactant as well as optimizing formulation and process variables is crucial in order to fabricate the desired NP size below 200 nm with PDI less than 0.2.

CHAPTER 3: EFFECT OF STARCH ORIGIN ON FABRICATION OF SANPS

3.1. Introduction

A great deal of attention has been devoted to starch and its derivatives mainly in the context of its applications in nanotechnology in which starch NPs can be used as drug carriers (Sodhi and Singh, 2005; Babić *et al.,* 2009; Freire *et al.,* 2009; Bello-Perez *et al.,* 2010). Starches, in general, are used in the fabrication of NPs mainly in their modified form particularly by chemical modification. Acetylation is one of the most widely used chemical modifications. It makes starch hydrophobic and prevents the formation of hydrogen bonding between hydroxyl groups and water molecules. Hydrophobically modified starches are used in the fabrication of starch nanostructures which could be used as carriers of different drugs (Besheer *et al*. 2007; Namazi *et al.* 2011). In acetylation, hydrophilic hydroxyl groups are substituted with hydrophobic acetyl groups. The acetyl groups react with free hydroxyl groups present in the starch polymers to produce specific ester (Singha *et al*., 2007; Sweedman *et al.,* 2013; Wurzbugr, 1964).

Starch granules are synthesized in a broad array of plant tissues and within many plant species (Zobel *et al.,* 1988). The chemical composition and the physical characteristics are essentially typical to the biological origin of the starch, i.e. they are unique to each type of starch. Therefore, what has been studied about the structural features, drug delivery application of one type of starch does not necessarily apply to other types of starch (Swinkels, 1985; Schwartz and Whistler, 2009). Hence, the current study investigates the effect of starch origin on the fabrication of starch based NPs and the attributes of the latter, namely, particle size and PDI.

3.2. Materials and methods

3.2.1. Materials

Fresh cassava and dioscorea tubers were collected from Saula, south west Ethiopia. Enset *boulla* was purchased from Wolaita, south west Ethiopia. Maize starch (Sigma Aldrich Chemie GmbH, Steinheim, Germany); Pluronic® F127 [Poloxamer 407- poly ethylene oxide/poly propylene oxide block copolymer, BASF, Mannheim, Germany]; Ethyl acetate (Sigma Aldrich Chemie GmbH, Taufkirchen, Germany) were used as received.

3.2.2. Methods

3.2.2.1. Isolation, synthesis and characterization of SA

Isolation of cassava, dioscorea and enset starch: Enset starch was extracted from boulla following the method described elsewhere (Gebre-Mariam and Schmidt 1996). Starches from cassava and dioscorea tubers were extracted according to the methods described in section 2.2.2.1.

Acetylation of cassava, dioscorea, enset and maize starches: Starch acetates (SAs) were prepared following the method described in section 2.2.2.2.

Determination of the degree of substitution (DS): The DS of SAs were determined by saponification titration method, as described in section 2.2.2.3.

Determination of Fourier Transform Raman Spectra: Raman spectra of native and SAs were recorded with Bruker FT-Raman spectrometer RFS 100/S (Bruker Optics, Germany) using a diode pumped Nd:YAG laser at an operating wavelength of 1064 nm. The measurements were performed using the 180^0 angle scattering geometry with 400 scans and laser power of 250 mW at the sample location. The interferograms were apodized with the Blackman–Harris 4-term function and Fourier-transformed to obtain spectra with a resolution of 4 cm^{-1} (Fechner e*t al.*, 2005; Phillips *et al.*, 1999).

Morphological characterization: Electron micrographs of acetylated starch were obtained using an environmental scanning electron microscope (ESEM E3, Electro Scan, Wilmington, MA, USA) with an LaB6 cathode and an acceleration voltage of 10 to 20 kV. Through water cooled Peltier stage, the specimen was held at a constant temperature of 6 ^oC. During evacuation, the specimen was kept wet by using an additional water reservoir (Fechner *et al.*, 2003).

3.2.2.2. Preparation of SANPs

NPs were prepared either by emulsification-solvent evaporation method or nanoprecipitation method.

Emulsification and solvent evaporation method: The fabrication of SANPs was based on emulsification-solvent diffusion and evaporation method described in section 2.2.2.4.

Nanoprecipitation method: Preparation of SANPs was based on nanoprecipitation method described by Han *et al*. (2013). In brief, 120 mg of acetylated starch was dissolved in 100 mL of organic solvent (ethyl acetate) separately. An aliquot of SA solution (2 ml) was added drop-wise (1ml/min) into a fixed quantity of aqueous solution (8 ml) containing Pluronic® F127 (1.0 % w/v) while stirring on a magnetic stirrer at a constant stirring rate (1200 rpm). The ultimate NPs were stirred slowly at room temperature for 5 h until ethyl acetate was completely evaporated from the suspension. All the experiments were done in triplicate.

3.2.2.3. Particle size and PDI analysis

Particle size and PDI analysis of the NPs were determined according to the method described in section 2.2.2.5.

3.2.2.4. Short-term stability studies

Stability studies were carried out on optimized SANPs according to International Conference on Harmonization (ICH) guideline (ICH Guideline 2003). The initial particle size and PDI analysis of the NP dispersions were determined using the 90Plus Particle Size Analyzer as described earlier. The NP suspensions were then divided into three sample sets and the first set was stored at 5 °C ± 3 °C, the second at 25 °C ± 2 °C/60% ± 5% RH and the third stored at 40 °C ± 2 °C/75% ± 5% RH. Samples were withdrawn at 0, 30, 60, and 90 days and subjected to particle size and PDI measurements.

3.2.2.5. Statistical analysis

All the data were subjected to statistical analysis by making use of software package called IBM SPSS Statistics for Windows, Version 21.0 (IBM Corporation, Armonk, NY, USA). Origin®, version 8.5 (OriginLab Corporation, MA, USA) and MS Excel 2010 (Microsoft Corporation, USA) were used for plotting graphs. The differences among the starches were determined using analysis of variance (ANOVA) followed by Tukey-HSD post hoc test for multiple comparisons. Results with p-values of less than 0.05 were considered to be statistically significant.

3.3. Results and discussion

3.3.1. Characterization of SA

3.3.1.1. Degree of acetylation

The mean value of acetyl contents and DSs of cassava, dioscorea, enset and maize SAs are presented in Table 3.1. The acetyl content of the four starches varied from 17.70 to 42.56 % and the DS from 0.84 to 2.74. Although the acetyl contents and DSs vary slightly from starch to starch, these variations are not statistically significant ($p > 0.05$) and not directly related with the starch granule sizes (Table 3.1). It has been reported that slight differences in acetyl contents and DS among starches can be attributed to the botanical origin and characteristics of starch granules (Wilkins *et al*., 2003). Since similar experimental conditions were maintained during acetylation of the four starches, the differences in acetyl contents and DS in cassava, dioscorea, enset and maize starches might be due to the origin of starch, granule composition, degree and type of crystallinity and amylose content (Gebre-Mariam and Schmidt 1988; Paulos *et al.*, 2009; Sandhu and Singh 2007).

Table 3.1: Acetyl contents and DSs of acetylated cassava, dioscorea, enset and maize starches obtained under similar reaction conditions, n = 3

Starch type	Time (h)	Acetyl content (% A)	DS	Mean granule Size (μm)
Cassava	1	20.32 (1.29)	0.91	
	3	29.87 (0.63)	1.50	
	6	36.65 (0.64)	2.15	12[*]
	9	42.56 (0.25)	2.74	
Dioscorea	1	17.70 (1.72)	0.84	
	3	30.66 (0.46)	1.62	
	6	36.48 (1.02)	2.10	29[**]
	9	42.10 (0.17)	2.69	
Enset	1	20.42 (0.20)	0.96	
	3	31.41(0.52)	1.71	46[#]
	6	34.62 (0.19)	1.97	
	9	41.51 (0.33)	2.63	
Maize	1	19.78 (0.22)	0.92	
	3	34.54 (0.83)	1.82	5[#]
	6	36.55 (0.14)	2.14	
	9	42.49 (0.20)	2.73	

The values in the parentheses indicate standard deviations, [*]Paulos *et al*., 2009, [**]Gebre-Mariam and Schmidt, 1996, [#]Gebre-Mariam and Schmidt, 1998

3.3.1.2. Fourier Transform Raman Spectra

Raman vibrational band has sufficient intensity to verify the changes in chemical structures of starch molecules resulting from acetylation (Fechner *et al.*, 2005; Phillips *et al.*, 1999). The FT Raman spectra of acetylated cassava (DS 0.91, 1.50, 2.15), dioscorea (DS 0.84, 1.62 and 2.10), enset (DS 0.96, 1.71 and 1.97) and maize (DS 0.92, 1.82 and 2.14) starch samples revealed the changes in the functional groups that took place due to acetylation (Figs. 3.1, 3.2, 3.3 and 3.4). Upon acetylation of the native starch, the 2940 cm^{-1} C-H stretch peak increased in intensity and new Raman peaks appeared at 656 cm^{-1} and 1739 cm^{-1}. Unlike native starches, acetylated starches have a strong carbonyl (C-O) stretch peak in the Raman spectra around 1739 cm^{-1}. Thus, the 1739 cm^{-1} peak serves as a marker to confirm the acetylated products. The 941 cm^{-1} peak due to C-C stretch vibrations remains unchanged after acetylation and it is convenient to measure the growth of the 1739 cm^{-1} peak relative to the 941 cm^{-1} peak (Kizil *et al.*, 2002). For instance, the Raman peak intensities for acetylated dioscorea starches (DS 0.84, 1.62 and 2.10) were found to be 0.07596, 0.09647 and 0.11338, respectively. Apparently, the relationship between the DS and the Raman peak intensity at 1739 cm^{-1} is linear.

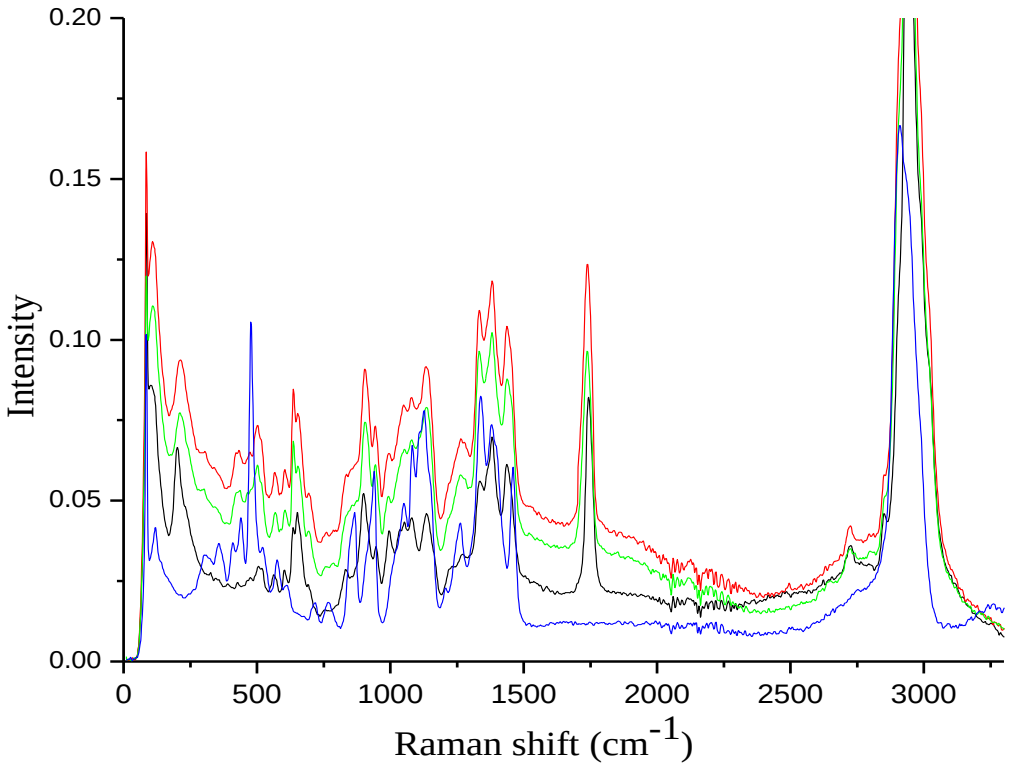

Fig. 3.1: FT Raman spectra of native (——) and acetylated cassava starch with 0.91 (——), 1.50 (——), and 2.15 (——) DSs.

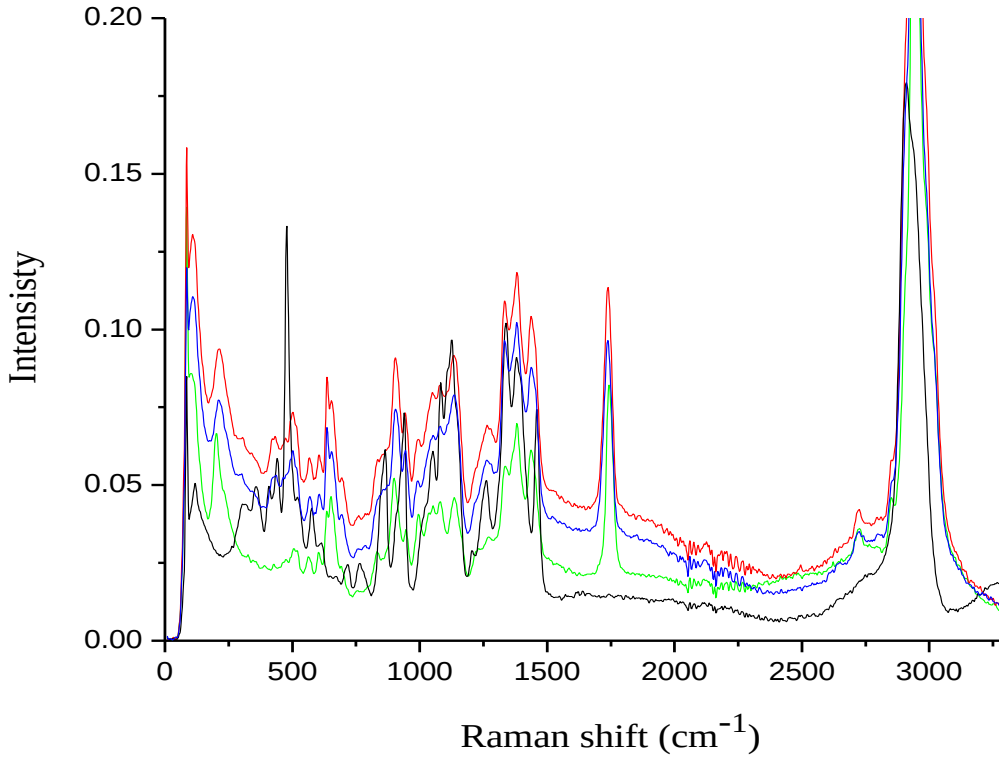

Fig. 3.2: FT Raman spectra of native (——) and acetylated dioscorea starch with 0.84 (——), 1.62 (——) and 2.10 (——) DSs.

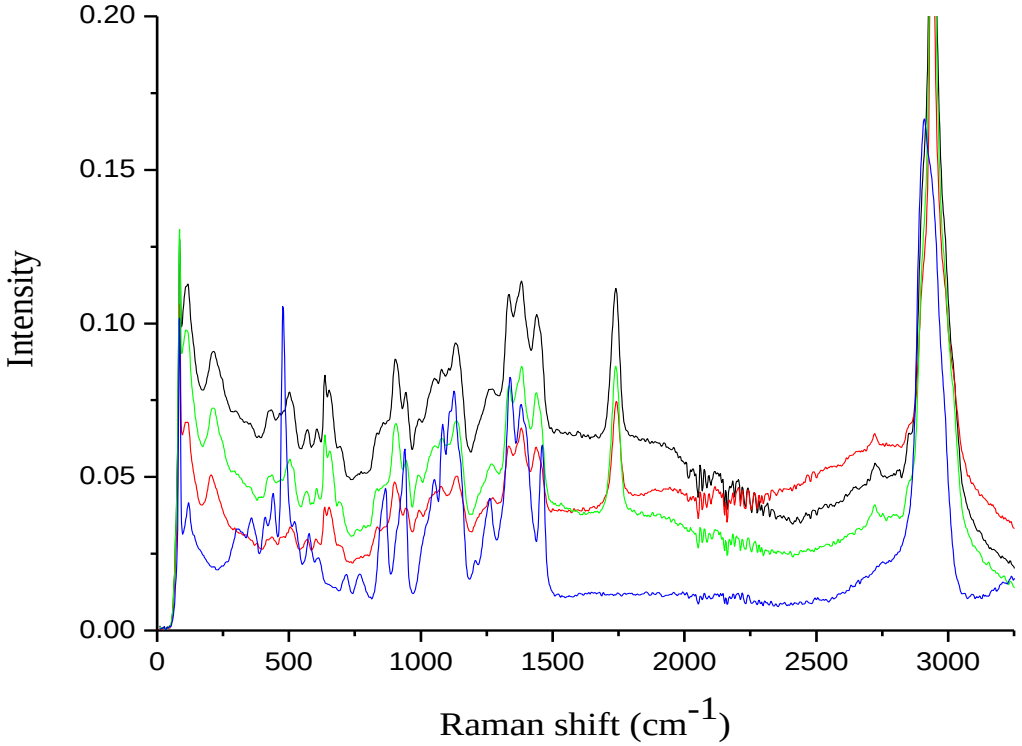

Fig. 3.3: FT Raman spectra of native (——) and acetylated enset starch with 0.96 (——), 1.71(——) and 1.97 (——) DSs.

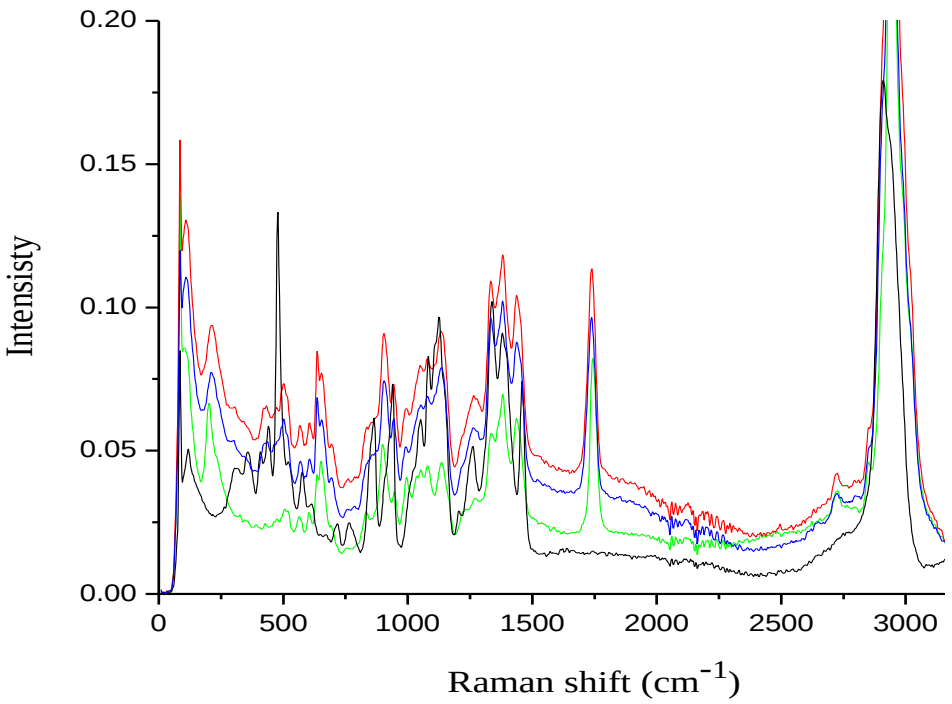

Fig. 3.4: FT Raman spectra of native (——) and acetylated maize starch with 0.92 (——), 1.82 (——) and 2.14 (——) DSs.

3.3.1.3. Starch granule morphology and size

The photomicrographs of native cassava, dioscorea, enset and maize starches are depicted in Fig. 3.5 a, b, c and d, respectively. Native cassava starch granules exhibited essentially spherical shape with a flat and relatively rough surface on one side of the granules whereas dioscorea starch granules display oval shape with smooth surface. Enset and maize starches were found to be elliptical and polyhedral in shape, respectively.

Fig. 3.6, 3.7, 3.8 and 3.9 show the microphotographs of acetylated starches of cassava, dioscorea, enset and maize starches with various DSs. The morphologies of the granules show obvious external structural distinction as compared to the native ones. Moreover, the starch granules show sign of rupture and exhibit different sizes of cavities on their surfaces due to esterification. The eroded appearances are apparently less smooth than those of the native starches i.e., all starch granules lose their smooth surface texture and shape and exhibit a beehive-like structure with uniform porosity. It can also be seen that there are no intact granules and the interior part of starch is also susceptible to the esterification. In addition, ESEM pictures of acetylated starches clearly reveal that the surfaces are fused (demonstrating that esterification alters the structure of starch granules). As indicated by Olayinka *et al*., 2013 starch granule fusion might be the result of surface gelatinization upon the addition of

NaOH to maintain alkaline condition during AA addition. The overall changes observed on acetylated starches show that the external as well as internal parts of the starch granules are influenced by the esterification. Evidently, the introduction of acetyl groups not only modifies surface morphology but also induces significant changes in the shapes and the sizes of the starch granules as pointed out by Kalita *et al.*, 2014.

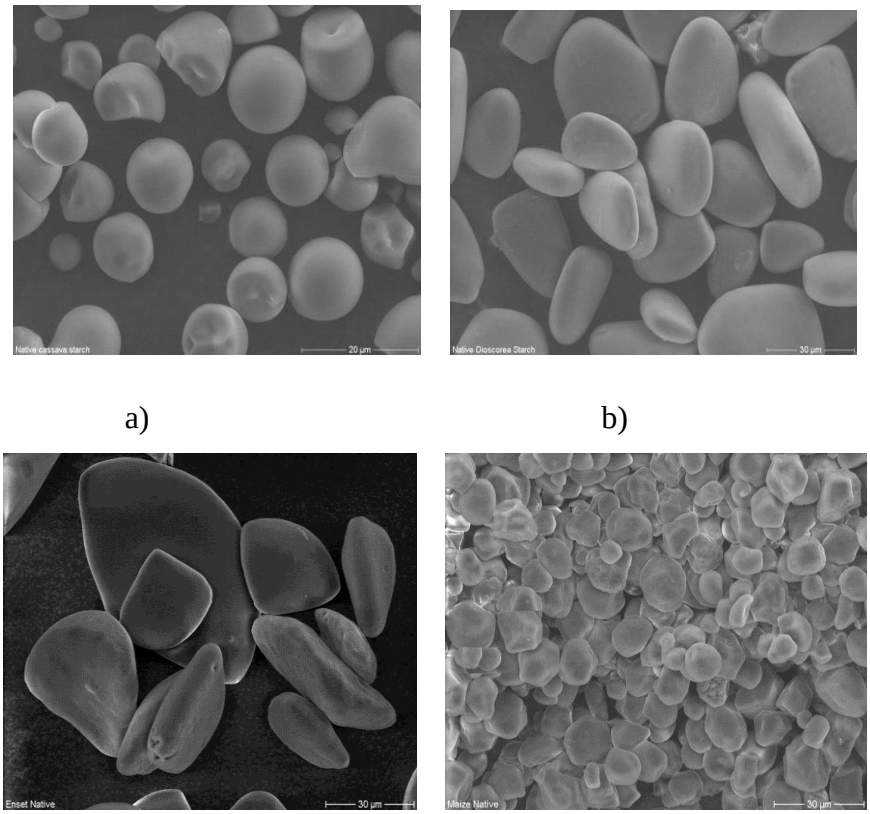

a) b)

c) d)

Fig. 3.5: Environmental scanning electron micrographs of native starches with magnification of 2000X; a) cassava, b) dioscorea, c) enset, d) maize

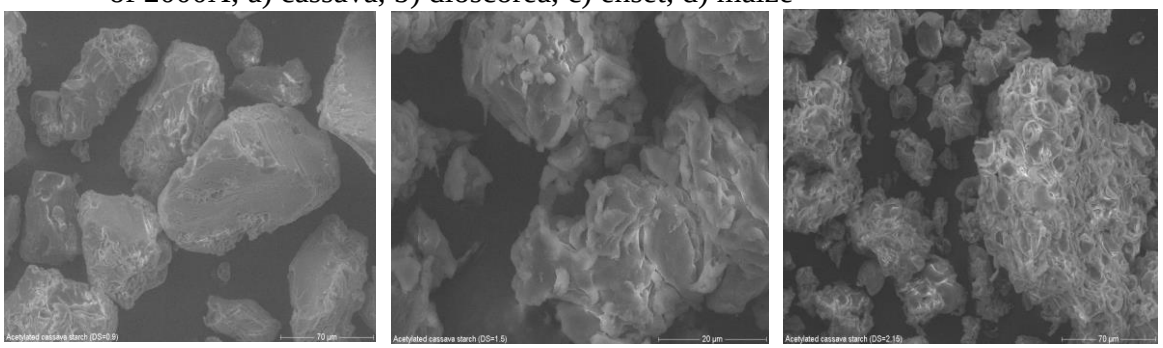

a) b) c)

Fig. 3.6: Environmental scanning electron micrographs of cassava SA with magnification of 2000X; (a) DS 0.91; (b) DS 1.5 (c) DS 2.15

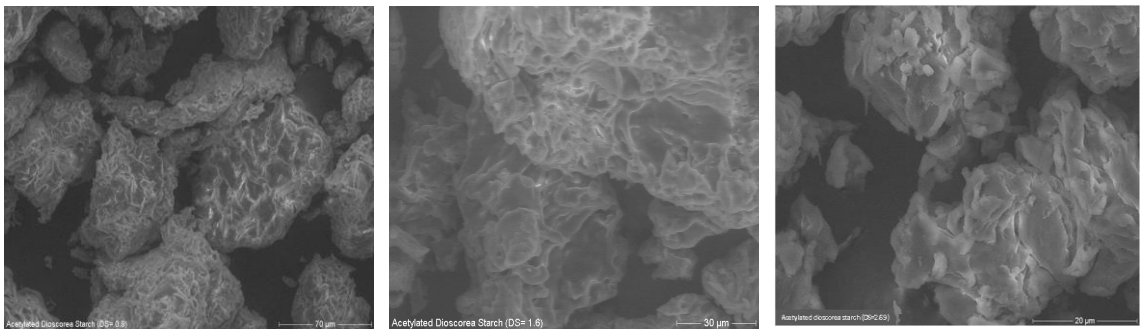

a) b) c)

Fig. 3.7: Environmental scanning electron micrographs of dioscorea SA with magnification of 2000X; a) DS 0.84, b) DS 1.62, and c) 2.10

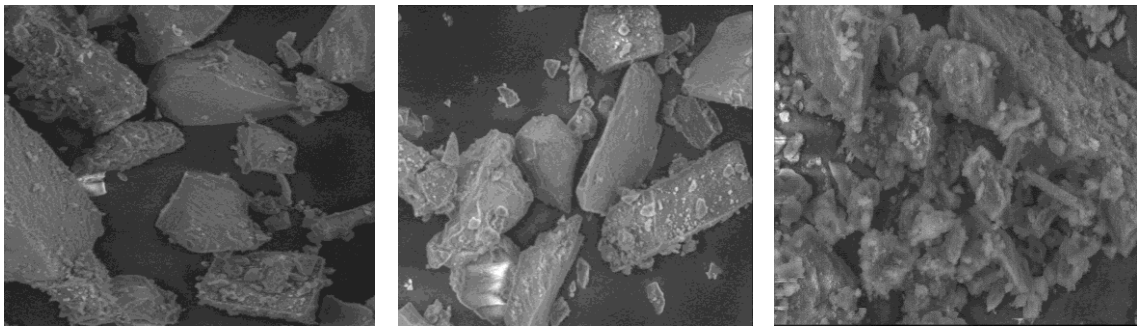

a) b) c)

Fig. 3.8: Environmental scanning electron micrographs of enset SA with magnification of 2000X; a) DS 0.96, b) DS 1.71, and c) 1.97

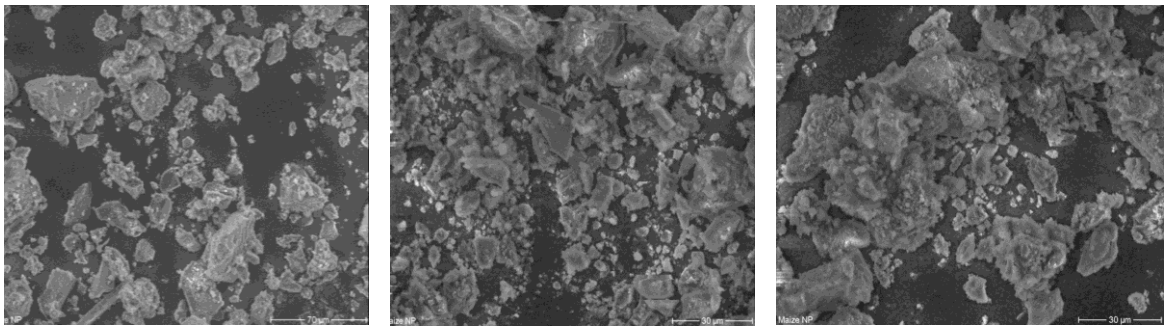

a) b) c)

Fig. 3.9: Environmental scanning electron micrographs of maize SA with magnification of 2000X; a) DS 0.92, b) DS 1.82, and c) 2.14

3.3.2. Effect of DS on fabrication of SANPs

To investigate the effects of DS on mean particle size and PDI of NPs, SAs having low, medium and high DS were used. As depicted in Fig. 3.10, the size of the SANPs of cassava, dioscorea, enset and maize starches ranged from 77.88 to 95.74 nm and PDI from 0.039 to

0.252. The comparison of these results using Tukey HSD test indicated that the DS has significant effect on the particle size and polydispersity index of SANPs ($p < 0.05$). For all SAs studied, an increase in DS was found to increase the mean particle size and PDI of NPs ($p < 0.05$) (Table 3.2). This might be due to increase in molecular weight of amylose and amylopectin owing to hydrophobic addition to starch granules. Moreover, these differences between DSs might also be associated with the hydrophobic interaction between SA molecules during NP formation. That is, probably loosely packed hydrophobic core was formed due to decrease in hydrogen bonding between hydrophobic starch molecules. In a different study, Wei and co-workers, (2015) have reported that the molecular weight and DS of hydrophobic groups are important parameters that influence physicochemical, biological and pharmaceutical properties of NPs.

Table 3.2: Multiple comparisons of effect of DS on particle size and PDI of NPs of acetylated cassava, dioscorea, enset and maize starches

Comparison		**Particle size**		**PDI**	
DS	DS	Mean Difference	Sig.	Mean Difference	Sig.
Low	Medium	- 5.047*	0.000	0.077*	0.000
	High	- 8.685*	0.000	0.137*	0.000
Medium	Low	5.047*	0.000	- 0.077*	0.000
	High	- 3.637*	0.011	0.060*	0.000
High	Low	8.685*	0.000	- 0.137*	0.000
	Medium	3.637*	0.011	- 0.060*	0.000

*The mean difference is significant at the 0.05 level.

3.3.3. Effect of starch origin on size and PDI of NPs

Table 3.3 presents the post hoc comparative analysis of size and PDI of SANPs of cassava, dioscorea, enset and maize starches. The analysis using Tukey test indicated that the sizes and PDI of dioscorea SANPs were significantly different from those NPs obtained from cassava, enset and maize SAs ($p < 0.05$). Similarly, differences were also observed between the NPs of cassava and maize, enset and maize SAs. The differences in size and PDI among SANPs might be attributed to the difference in the molecular weight of SA polymers, their granule

composition and crystallinity. LeCorre *et al.*, 2011 suggested that starches with different crystalline types and amylose content could render different NPs size and morphology.

As shown earlier (Table 3.1), the mean granule size of cassava, dioscorea, enset and maize starches are 12, 29, 46 and 5 µm; whereas the corresponding size of NPs obtained from these starches were found to be 94.48, 90.27, 98.74, 104.61 nm, respectively (Fig. 3.10). Thus it appears that there is no relationship between granule size of starch and the size of NPs.

Table 3.3: Post hoc comparisons using Tukey HSD test of the effect starch origin on mean particle sizes of SANPs of cassava, dioscorea, enset and maize starches

Starch type	Starch type	Mean Difference	Sig.	95% Confidence Interval	
				Lower Bound	Upper Bound
Cassava	Dioscorea	6.553*	0.004	1.651	11.454
	Enset	-2.843	0.027	-7.745	2.057
	Maize	-8.057*	0.000	-12.959	-3.156
Dioscorea	Cassava	-6.553*	0.004	-11.454	-1.651
	Enset	-9.397*	0.000	-14.298	-4.495
	Maize	-14.611*	0.000	-19.512	-9.709
Enset	Cassava	2.843	0.027	-2.057	7.745
	Dioscorea	9.397*	0.000	4.495	14.298
	Maize	-5.213*	0.033	-10.115	-0.312
Maize	Cassava	8.057*	0.000	3.156	12.959
	Dioscorea	14.611*	0.000	9.709	19.512
	Enset	5.213*	0.033	0.312	10.115

*The mean difference is significant at the 0.05 level.

3.3.4. Effect of method of fabrication of SANPs on size and PDI

Fig. 3.10 and 3.11 depict the size and PDI of the SANPs of cassava, dioscorea, enset and maize starches fabricated by emulsification solvent evaporation and nanoprecipitation methods, respectively. As shown in Table 3.4, there is significant difference between these methods ($p < 0.05$). The size of the NPs fabricated by emulsification solvent evaporation method ranged from 77.88 to 95.74 nm and PDI ranged from 0.039 to 0.252. Under similar fabrication conditions, nanoprecipitation method provided NPs with larger size (ranging from

184.85 nm to 216.69 nm) and higher PDI (in the range of 0.277 and 0.334) than the emulsification solvent evaporation method (Fig. 4.2). Similar findings were obtained by Han *et al.* (2013) who reported SANPs fabricated with similar conditions resulted in size ranging between 204 nm to 287 nm.

In general, emulsification solvent evaporation method is more preferred to fabricate SANPs with size below 200 nm than nanoprecipitation method. It has been reported that emulsification solvent diffusion and evaporation method produces small sized particles with narrow size distribution over a wide range of processing parameters (Santander-Ortega *et al.*, 2010). This is because emulsification solvent diffusion and evaporation method requires a source of external energy (high speed homogenization) to break coarse droplets to the desired size. The droplets are eventually converted into particles through solvent diffusion and evaporation. Hence, spontaneous emulsification and solvent evaporation method was used for the fabrication of SANPs in the subsequent comparative studies.

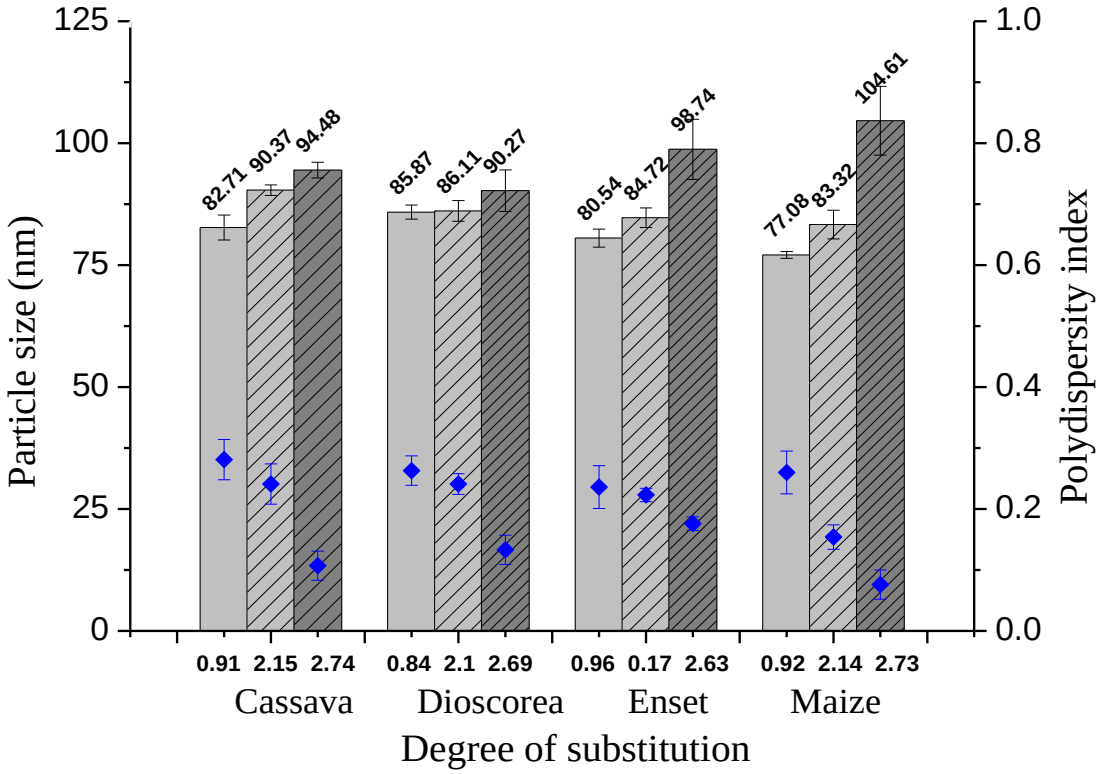

Fig. 3.10: Effect of starch granule type and DS on size (▭) and PDI (●) of SANPs fabricated by emulsification solvent evaporation method

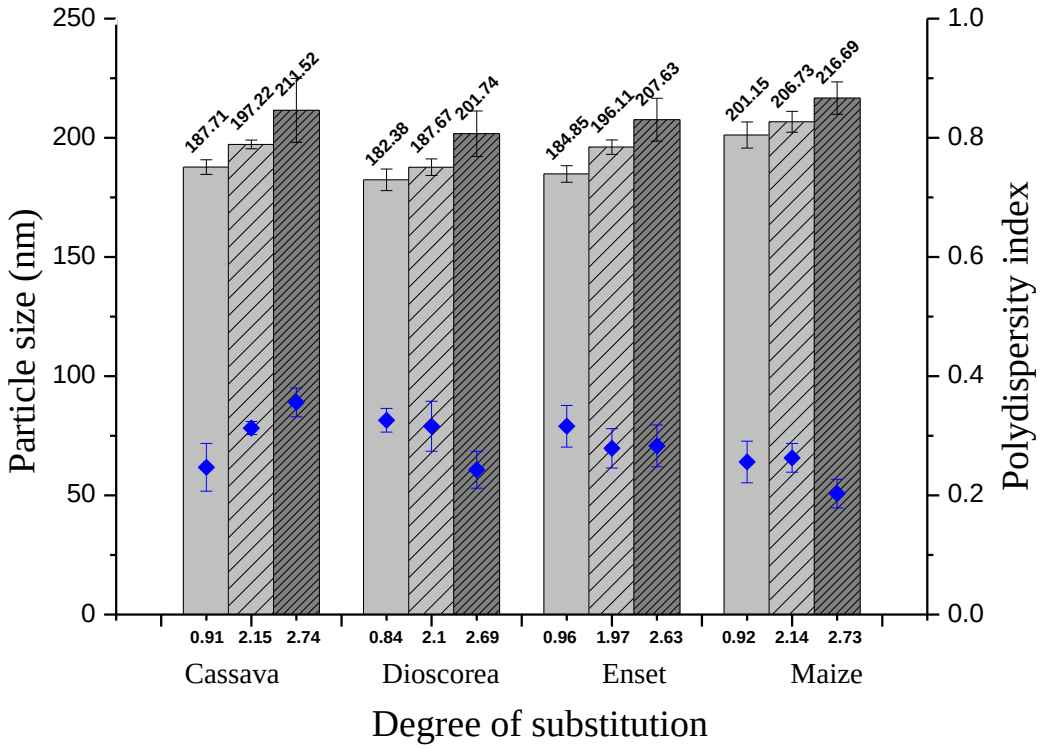

Fig. 3.11: Effect of starch granule type and DS on size (▭) and PDI (●) of SANPs fabricated by nanoprecipitation method

Table 3. 4: Tests of between subjects effects of SANPs fabricated by emulsification and nanoprecipitation methods

Variables	Particle size			PDI		
	Type III sum of square	Mean Square	Sig.	Type III sum of square	Mean Square	Sig.
DSs	1826.554	913.277	0.000	0.455	0.227	0.000
Starch types	624.660	208.220	0.001	1.053	1.053	0.000
Methods	1011005.113	1011005.113	0.000	0.014	0.005	0.001

3.3.5. Surface morphology of SANPs

The surface morphologies of cassava, dioscorea, enset and maize SANPs fabricated by emulsification solvent evaporation are depicted in Fig. 3.12. The photomicrographs of the NPs were obtained after drying following centrifugation. The average size and the shape of the NPs (Fig. 3.12) are completely different from the native starches (Fig. 3.5) and acetylated starches (Fig. 3.6, 3.7, 3.8 and 3.9).

In the process of NP fabrication by emulsification solvent evaporation method, changes in surface morphologies become distinctive as native starches are acetylated and as SANPs are subsequently formed (Fig. 3.12). The rupture of the starch granules engendered by the esterification is transformed into the spherically shaped particles due to the emulsification leading to interfacial deposition of polymers following displacement of a semipolar solvent (ethyl acetate) miscible with water from a lipophilic internal phase. The rapid NP formation is controlled by the rapid diffusion of solvent into aqueous phase. Although there are some differences in the morphology of starch NPs, it is obvious that the starch NPs tend to self-aggregate forming microscale agglomerates. The aggregation behaviour of starch NPs can be explained by the presence of a large number of hydroxyl groups on the surface of starch NPs which readily participate in the formation of hydrogen bonding or van der Waals attraction between NPs.

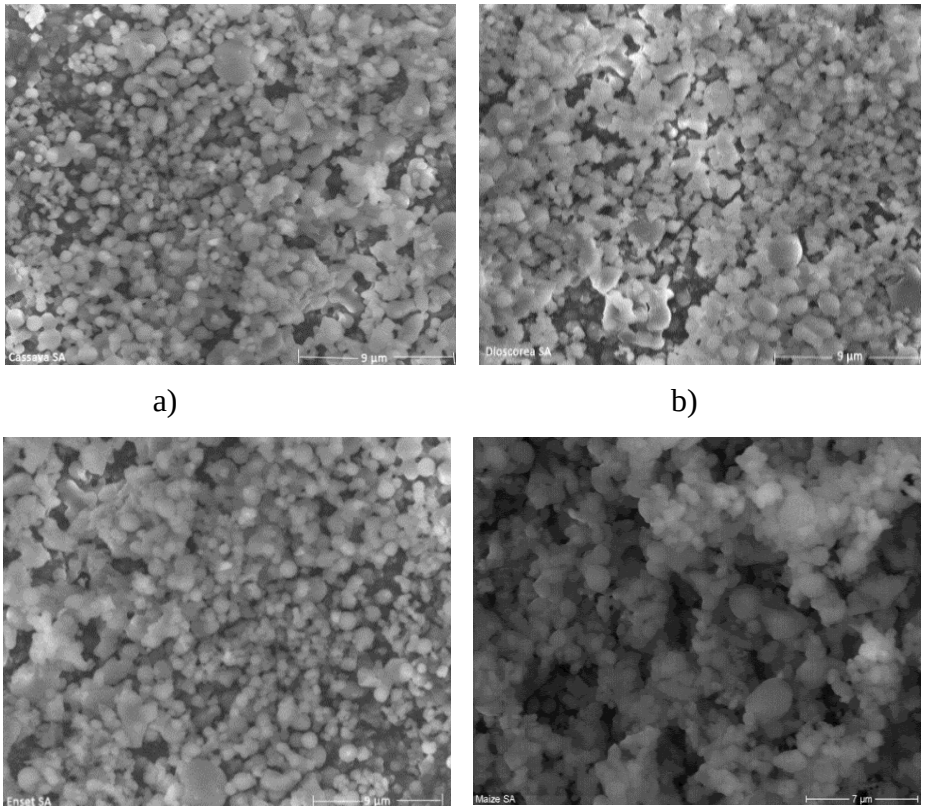

a) b)

c) d)

Fig. 3.12: Environmental scanning photomicrographs of SANPs with magnification of 20000X; a) Cassava, b) Dioscorea, c) Enset, d) Maize

3.3.6. Short term stability profile of SANPs

Fig. 3.13 depicts the particle size and PDI of NPs fabricated by emulsification solvent evaporation method and stored at different temperatures for up to 3 months. The SANPs showed negligible increase in particle size and PDI, ($p > 0.05$). Although none of the SANPs dispersions indicated any sign of agglomeration or colour change during the storage period, those NPs stored at 40 °C ± 2 °C/75% ± 5% RH showed slight but not significant increase in particles size as compared to those stored at 4 ^{o}C and 25 ^{o}C ($p = 0.321$). The NPs stored at all temperature for up to 3 months retained their particle size and PDI. The study, therefore, suggests that cassava, dioscorea, enset and maize SANPs fabricated by emulsification and solvent evaporation method were stable at all storage conditions during the study period.

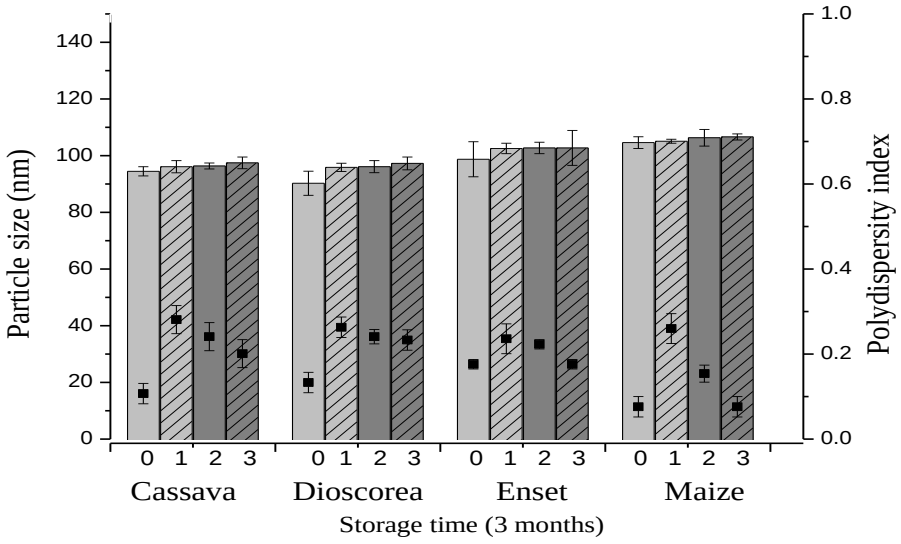

a)

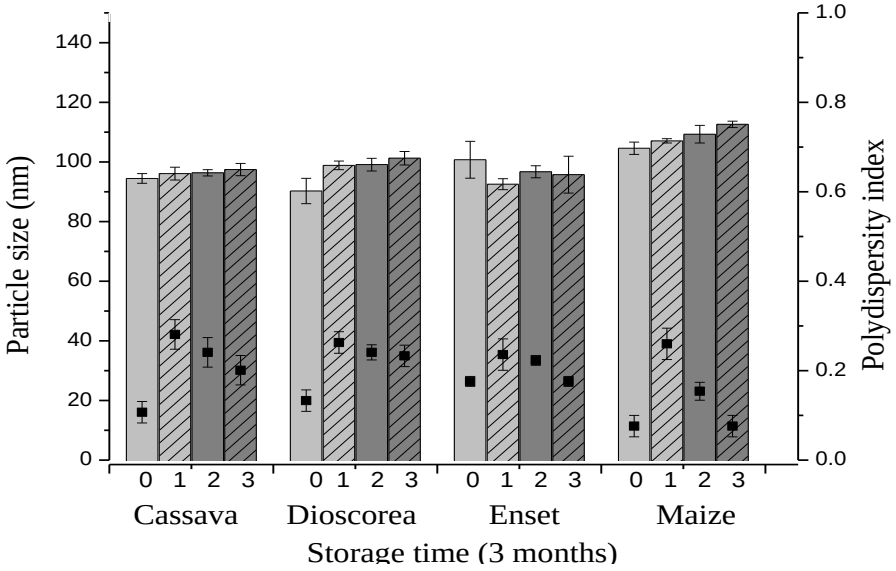

b)

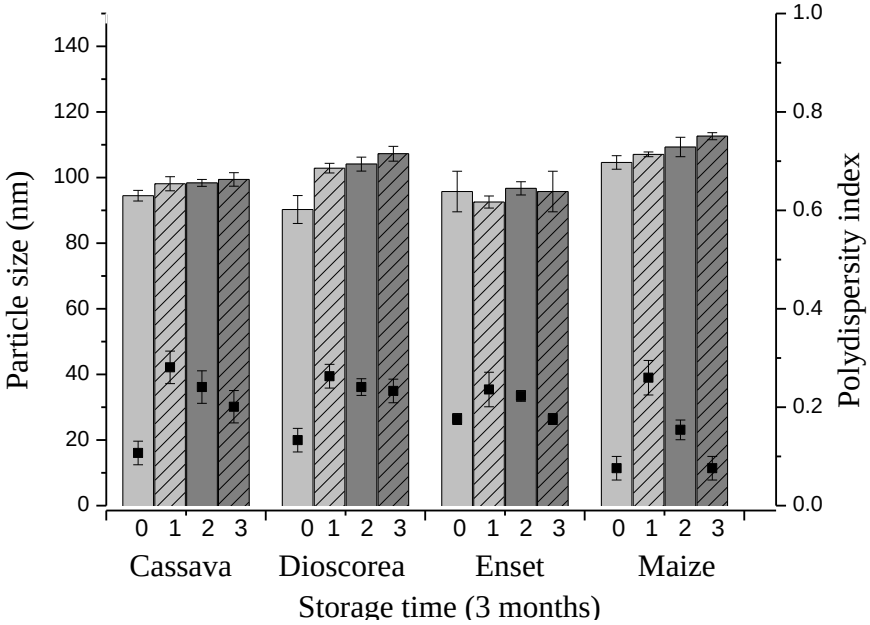

c)

Fig. 3.13: Stability profiles of SANPs prepared by emulsification solvent evaporation in terms of particle size and PDI; stored at a) 4 ^{o}C b) 25 ^{o}C and c) 40 ^{o}C for 3 months.

Conclusion

Starch acetate nanoparticles have been fabricated from acetylated cassava, dioscorea, enset and maize starches. FT Raman spectra verified the change in the chemical structure of the native starch molecules due to acetylation. Morphological studies with ESEM showed the changes that occurred due to esterification i.e., the granular structure of the starches was completely destroyed which resulted in amorphous particles of clumped starches. In comparison, the sizes and PDIs of SANPs of cassava, dioscorea, enset and maize starches differed significantly from one another; indicating, the origin of starch has significant influence on fabrication of SANPs. Stability studies showed that all SANPs were stable over the study period of three months.

CHAPTER 4: ASSESSMENT OF SANPs AS NANO DRUG CARRIERS

4.1. Introduction

Starch, as one of the most abundant biopolymers in nature, has been considered as a suitable material for pharmaceutical applications (Liu *et al.*, 2008). Nowadays there is a growing interest in starch as a precursor material for fabricating starch-based NPs for drug delivery (Chin *et al.*, 2014; Le Corre *et al.*, 2010). The importance of starch as nano-drug delivery component is increasing in line with the considerable current interest in material sustainability. This polymer, however, cannot fit into such drug delivery system in its native form (Tuovinen *et al.*, 2004). Therefore, to prepare starch nanostructure which could serve as a carrier for different drugs, its backbone structure is modified with hydrophobic molecules resulting in hydrophobized starch copolymer (Besheer *et al.*, 2007; Freiberg and Zhu, 2004; Namazi *et al.*, 2011). When these copolymers are exposed to aqueous environment, they spontaneously form micelles or self-associate to form colloidally stable NPs with inner hydrophobic core (Myrick *et al*. 2014). This hydrophobic core can easily encapsulate hydrophobic drugs (Gonçalves and Gama 2008). The starches investigated in the current study were acetylated (Reddy and Yang 2009; Tuovinen *et al.*, 2003).

Ibuprofen, NSAID, is generally used as analgesic and antipyretic for a variety of inflammatory pathologies (Kayrak *et al.*, 2003). IBU can be used as short duration therapy (e.g. headache) or as chronic therapy, such as in osteoarthritis and rheumatoid arthritis. Although IBU has poor water solubility, when given orally it is well absorbed (Kumar *et al.*, 2003; Zhu *et al.*, 2005). However, it is rapidly eliminated from systemic circulation displaying a relatively short half-life (1.7-2 h), and therefore, requiring high dosage for an effective and prolonged pharmacological activity. Prolonged use may cause NSAID-related gastric toxicity, including gastric irritation and bleeding, abdominal pain and ulcers (Moore, 2007). Hence, to achieve effective and prolonged drug levels for an extended period of time without having related gastric effects, IBU is a potential candidate for a new drug delivery systems based on controlled and sustained release. The development of oral controlled and sustained release offers a potential benefit for NSAIDs. The rationale behind it is allowing the release of the drug at a desired rate, providing sustained levels (fewer doses required) and reducing the contact with gastric mucosa (reduced gastric damage). To this end, nanoparticles have raised increased attention due to their properties and benefits for drug performance.

They are capable of releasing optimum amounts of drug, while avoiding premature release (Reis *et al.*, 2006b).

Ceramides (CERs) have been identified in human SC, which play a major role in the water-retaining properties of the epidermis and are claimed to dramatically increase skin's hydration level, repair the cutaneous barrier, prevent vital moisture loss, and contribute to reducing dry flaky skin and aged appearance (Motta *et al.*, 1993; Rogers *et al.*, 1996). They can also be used against some skin diseases such as atopic dermatitis (Imokawa *et al.*, 1991; Di Nardo *et al.*, 1998) and psoriasis (Motta *et al.*, 1994). Hence, CERs and their derivatives have drawn attention as active components in both pharmaceutical and cosmetic industries. However, the effectiveness of these compounds is limited due to their inherent hydrophobicity and potential precipitation as fine lipid micellar suspensions when administered in hydrophilic formulations. Moreover, from conventional dosage forms, they cannot penetrate the SC to reach the site where they exert their biological activity (Guterres *et al.*, 2007; Sahle *et al.*, 2015). Therefore, to realise the therapeutic benefits of these lipids, an appropriate drug delivery system that can enhance their solubility and SC permeability should be developed. Hence, the potential application of SANPs as TDDS (transdermal drug delivery system) was investigated by studying its influence on the *in vitro* release and penetration of oat ceramides (CERs), plant CERs. In plants, CERs are mainly found as constituents of glucosylceramides (GlcCERs) and glycosyl-phosphoryl inositol CERs; the most abundant being GlcCERs (Markham *et al.*, 2013).

The aim of this work was, therefore, to study the potential application of SA based NPs of as drug carriers (SANPs).

4.2. Materials and methods

4.2.1. Materials

Oat grain was obtained from Addis Ababa, Ethiopia. Acetic anhydride (May and Baker Ltd, Dagenham, UK); Mowiol 4-88-Poly vinyl alcohol (Kuraray Specialties Europe GmbH, Frankfurt/M., Germany); Pluronic® F68 (BASF, Mannheim, Germany); Pluronic® F127 (BASF, Mannheim, Germany); Hydrogen chloride solution (4.0 M in dioxane) and 1, 4-dioxane anhydrous (99.8%) (Sigma-Aldrich Chemie GmbH, Steinheim, Germany); n-hexane (Grüssing GmbH, Filsum, Germany); Ethanol (Brüggemann GmbH & Co. KG, Heilbronn,

Germany); Euxyl® PE 9010 (2-phenoxethanol (90%) and 3[(2-etylhexyl)oxy] 1,2 Propandiol (10), Schülke & Mayr GmbH, Norderstedt, Germany); Carbopol®980 Polymer (crosslinked polyacrylic acid, Lubrizol Advanced Materials Europe BVBA (Brussels, Belgium); Tris (hydroxymethyl)-aminomethane (Merck KGaA (Darmstadt, Germany); Ibuprofen (Sigma Aldrich Chemie GmbH, Taufkirchen, Germany); Tween® 80 (Carl Roth GmbH, Karlsruhe, Germany); Chloroform (Fisher Scientific UK LTD, Loughborough, UK); Dichloromethane (BDH Lab Supplies, Poole, England), and ethyl acetate (Sigma Aldrich Chemie GmbH, Taufkirchen, Germany), were used as received.

4.2.2. Methods

4.2.2.1. Isolation of GlcCERs and Preparation of CERs

Glucosylceramides (GlcCERs) were isolated from the lipid extract of Ethiopian oat grain (*Avena abyssinica*) following the method described in Tessema *et al.*, (2017). The glycosidic linkage of the GlcCERs was then cleaved by acid treatment and the predominant CERs species were isolated using column chromatography. The oat GlcCERs enriched fraction was dissolved in anhydrous 1, 4-dioxane (30 mg/mL) at room temp. and the solution was mixed with 4.0M HCl in dioxane (1:1) in a round bottom flask. The reaction mixture was stirred on a magnetic stirrer at 500 rpm for 18 h at room temperature. The content of the mixture was kept in an ice water bath and neutralized with saturated $NaHCO_3$ solution. The reaction mixture was exhaustively extracted with $CHCl_3$ (three times) on a separatory funnel to separate the CERs from the hydrophilic components of reaction mixture (including the sugar moiety). The $CHCl_3$ phase was washed with saturated NaCl solution (brine) and dried under nitrogen stream. Oat CERs enriched fraction was purified by column chromatography with a gradient elution: first elution with $CHCl_3$ followed by a second elution with $CHCl_3$/MeOH (9:1, v/v). The oat CERs (CER I and CER II) enriched fraction was used for the preparation of the formulations. The two predominant CER I and CER II were found to contain Sphingoid base with chain length of 11 and 15 carbon, respectively.

4.2.2.2. Preparation of ibuprofen and Oat CER loaded NPs

The preparation of ibuprofen and oat CER loaded SANPs was based on emulsification-solvent diffusion and evaporation method described by Desgouilles *et al.,* 2003 and Santander-Ortega *et al.,* 2010. In brief, 120 mg of SA of cassava, dioscorea, enset and maize (low, medium and high DS) and 30 mg of drugs were dissolved in 100 mL of organic solvent

(ethyl acetate) separately. The organic solution (2 mL) was emulsified in aqueous phase (8 mL) containing Pluronic® F127 as surfactant resulting in oil in water (O/W) emulsion. Emulsification of this biphasic system was enhanced by using a high speed homogenizer (Pro Scientific Inc, Oxford, USA). After the formation of stable emulsion, the organic solvent was evaporated under magnetic stirring for 5 h at room temperature to transform the nanoemulsion into NP suspension. All experiments were done in triplicates.

4.2.2.3. Particle size and PDI of ibuprofen and Oat CER loaded NPs

The Particle size and PDI of ibuprofen and Oat CER loaded NPs were measured following the methods described in section 3.2.2.3.

4.2.2.4. Preparation of oat CER-based formulations

Preparation of MEs and ME gel: Oat CER MEs were prepared by mixing all the components of the MEs (oil, hydrophilic phase and surfactant) in vials and sonicating the mixtures for 30 min at 40 °C. Carbopol®980 gel (1%) was used as a thickening agent for the preparation of ME gel. Lecithin based MEs (LBME) and Carbopol®980 gel (1%) were mixed (in 1:2 ratio) and the pH was adjusted with 7.5% of Tris for the gel formation.

Preparation of Starch-based NP gel: The NP gel was prepared by incorporating one part of the SANPs suspension (SANP-DS 2.74) into two parts of Carbopol®980 gel (1%). The aqueous system was neutralized by 7.5% of Tris to get the gel formulation. Euxyl® PE 9010 (1%) was used as a preservative. A pure gel containing equal portion of distilled water instead of NPs suspension was prepared for comparison purpose.

Preparation of oat CER-based amphiphilic cream*:* Oat CERs enriched fraction (10 mg) were incorporated into 1 g of an amphiphilic cream (Basiscreme, Deutscher Arzneimittel Codex (DAC), Caesar & Loretz GmbH, Hilden, Germany). The cream is composed of white soft paraffin (25.5%), glycerol monostearate (4%), cetyl alcohol (6%), polyoxyethylene glycerol monostearate (7%), medium-chain triglycerides (7.5%), propylene glycol (10%) and distilled water (40%) (Tessema *et al.*, 2018).

4.2.2.5. UV calibration curve of ibuprofen

Stock solution containing 100 µg/ml of ibuprofen (IBU) in phosphate buffer solution (PBS), pH 7.4 was prepared. From this stock solution, seven different concentrations (4, 6, 7, 8, 9, 10, 12 µg/ml) were prepared using PBS pH 7.4 as solvent. The UV absorbance readings of these solutions were measured at 221 nm using UV/Visible spectrophotometer (SPEKOL® 1500, Jena, Germany). PBS (pH 7.4) was used as a blank (Vutpala and Sailaja 2014). As seen in appendix B, the absorbance versus concentration of solutions was plotted and a calibration curve with a linear regression equation of: Y= 0.057X + 0.0173 (where, Y is the absorbance and X is the concentration in µg/ml) and correlation coefficient of 0.9984 was obtained.

4.2.2.6. Drug loading (DL) capacity and encapsulation efficiency (EE)

DL and the EE of SANPs were determined after loading the NPs with IBU as a model drug (Jiang *et al*., 2005; Reis *et al.*, 2014). The NPs were freed from the non-encapsulated drug by centrifugation at 20,000 rpm for 30 min. Subsequently, the content of unencapsulated drug in the supernatant was quantified spectrophotometrically after sufficient dilution with phosphate buffer solution (PBS, pH 7.4).

The DL and EE were determined from the following equations, respectively.

$$\%DL = \frac{\text{Weight of drug in NPs}}{\text{Weight of NPs}} \times 100 \quad (4.1)$$

$$\%EE = \frac{[\mathrm{M_{intial\ drug} - M_{free\ drug}}]}{\mathrm{M_{intial\ drug}}} \times 100 \quad (4.2)$$

Where: $M_{initial\ drug}$ is the amount of initial drug used for the formulation and $M_{free\ drug}$ is the amount of free drug detected in the supernatant after centrifugation.

4.2.2.7. In vitro drug release from SANPs

In vitro drug release profiles from physical mixture of IBU and SAs, and IBU-loaded acetylated starch NPs were determined according to the methods described by Vutpala and Sailaja (2014). In this, 50 mg of each of physical mixture and NPs loaded with IBU were dispersed in a dialysis tube (molecular weight cut off: 1200 Da, Sigma Aldrich Chemie GmbH, Munich, Germany) containing 10 ml PBS, pH 7.4. The dialysis tube was then placed in a dissolution medium (900 ml) containing the same buffer solution (PBS, pH 7.4) at 37 ^{o}C. Aliquots of dissolution medium were removed at given time intervals, and replaced with the same amount of fresh dissolution medium. The amount of IBU released was determined from

UV absorption at 221 nm (UV-Vis spectrophotometer, SPEKOL® 1500, Jena, Germany). The cumulative drug release was calculated as follows:

$$\text{Cummulative drug release } (\%) = \frac{Volume\ of\ sample\ withdrawn\ (ml)}{\text{Bath volume (ml)}} \times P(t-1) + Pt \qquad (4.3)$$

Where Pt is percentage release at time t and P (t – 1) is percentage release previous to 't'.

4.2.2.8. Mechanism of drug release

The dissolution data were fitted into the following drug release models to evaluate the in vitro drug release kinetics from the hydrophobic SANPs: cumulative percent drug release versus time (zero order kinetic model); log cumulative of percent drug released versus time (first order kinetic model); cumulative percent drug release versus square root of time (Higuchi model); cube root of drug percent remaining in matrix versus time (Hixson-Crowell cube root model); log cumulative percentage drug release versus log time (Korsmeyer-Peppas model) (Ranjan *et al*., 2012).

4.2.2.9. In vitro penetration studies of oat CERs

A multilayer membrane system was used to investigate the *in vitro* penetration of oat CERs from various formulations. The model comprises circular 40 mm penetration cells arranged one over the other in a penetration cell stand. Each cell consists of a covering plate, a stencil, four layers of membrane films and a base plate. The formulation (an amount equivalent to 50 µg of oat CERs) was uniformly spread through the stencil (with a square opening of 4 cm2 at the centre) which was kept above the upper membrane and the whole cell was covered by the covering plate. A nitrocellulose film was placed between the lower membrane and the base plate to prevent any possible adhesion. The cells were kept at 32 °C in a thermostatic chamber for predetermined time intervals (15, 30 and 60 min) allowing release and penetration of oat CERs. The cells were taken out, the unabsorbed formulation over the surface of the top membrane was removed by a cotton swab, the membranes were separated and the oat CERs in each layer as well as remained unabsorbed were extracted with 1 mL (3 mL for the cotton swab) of n-hexane/ethanol (2:1, v/v) (with sonication at 40 °C for 30 min) in test tubes. The extracts were dried under nitrogen stream at 40 °C and the dried residues were re-dissolved in CHCl3/MeOH (1:1, v/v) (4 mL was used for cotton swab and the top layer and 2 mL for the three bottom layers). The samples were filtered through 0.45 µm

syringeless filters (Whatman Mini-UniPrepTM, Dassel, Germany) and the amount of oat CERs was quantified by an LC-MS method (Tessema *et al.*, 2018).

4.2.2.10. LC-MS

The amounts of oat CERs released and penetrated across the artificial multilayer membrane and excised human skin were quantified by the LC-MS method (Tessema *et al.*, 2018). An LC-MS/MS system consisting of UHPLC coupled on-line to a triple quadrupole MS (QqQ-MS, TSQ Quantum Ultra, Thermo Fisher Scientific, Bremen, Germany) equipped with HESI source with an atmospheric pressure chemical ionization (APCI) probe was used. The oat-derived CERs were separated on a YMC-Pack ODS-AQ column (150×2.0mm I.D., S-3 μm, 200 Å pore size, YMC Europe GmbH, Dinslaken, Germany) under the following chromatographic conditions: mobile phase comprised eluent A (aqueous + 0.1% v/v formic acid) and eluent B (MeOH + 0.1% v/v formic acid in), flow rate was set to 0.3 mL/min, column temperature was 40 °C, injection volume was 10 μL and total run duration was 40 min. The separation relied on a multi-step gradient elution accomplished as follows: 5 min isocratically at 90% eluent B, followed by sequential linear gradients to 95% and 100% eluent B in 5 and 20 min, respectively. The post-run equilibration time was 10 min. The MS was operated in the positive ion mode using selected ion monitoring (SIM, m/z 554 and m/z 610) and the following APCI settings: source vaporizer temperature of 450 °C, capillary temperature of 275 °C, source (discharge) current of 6 μA, sheath gas pressure of 55 psi and ion sweep gas pressure of 30 psi. The method’ s limit of detection (LOD) and quantification (LOQ) were estimated to be around 10 and 30 ng/mL for each oat CER, respectively.

4.2.2.11. Statistical analysis

One-way ANOVA ($p < 0.05$) followed by Tukey’s test as post hoc analysis was used to indicate the existence of significant differences between sets of data. The results are presented as the mean ± SD of at least three experiments.

4.3. Results and discussion

4.3.1. Ibuprofen loaded SANPs

4.3.1.1. Particle size and PDI

Fig. 4.1 depicts the size and PDI of ibuprofen loaded SANPs of cassava, dioscorea, enset and maize starches fabricated by emulsification solvent evaporation method. As shown in the Figure the size of the NPs ranged from 94.64 to 107.8 nm and PDI ranged from 0.076 to 0.243. In all cases, ibuprofen loaded SANPs were fabricated with size below 200 nm with PDI less than 0.2.

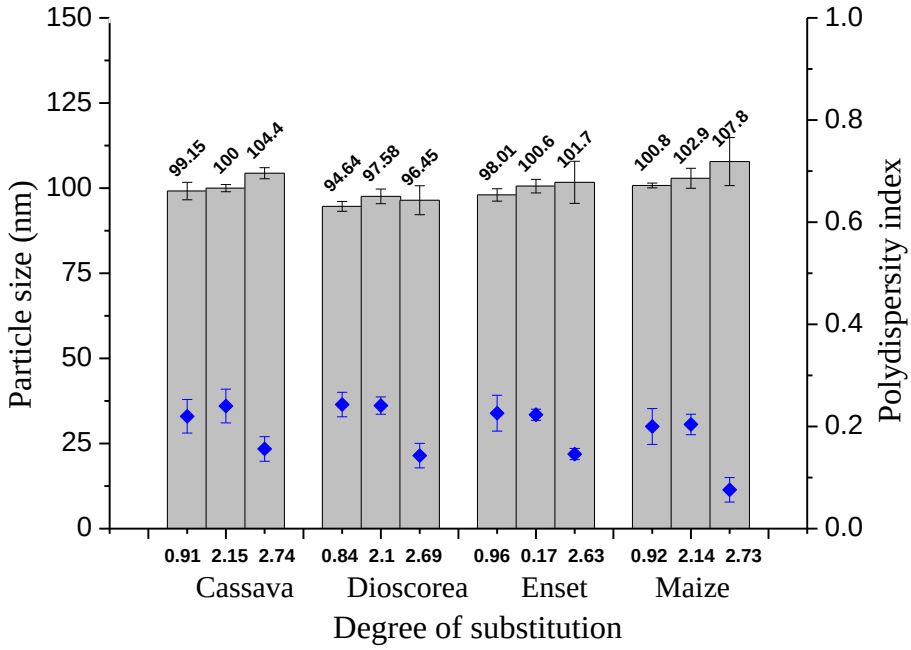

Fig. 4.1: Size (▭) and PDI (●) of IBU-loaded SANPs fabricated by emulsification solvent evaporation method

4.3.1.2. Drug loading (DL) capacity and encapsulation efficiency (EE)

DL and EE are very important parameters in drug delivery systems; they are indices used to evaluate the usability of nanocarriers, revealing the amount of drug actually incorporated into NPs. In this study, DL and EE were determined for optimized cassava, dioscorea, enset and maize SANPs (with high DSs) containing lower and higher ratio of IBU to SA 1:1 and 1:4, respectively. As shown in Fig. 4.4, the 1:1 ratio- produced the average DL of NPs ranged from 17.66 to 19.52 % while EE ranged from 46.20 to 53.30 %. Similarly, the 1:4 ratio yielded the average DL of NPs ranged from 28.22 to 31.09 % while EE ranged from 70.41 to 75.14% (Fig. 4.2a and b). The NPs of the four SAs resulted with significantly different DL

and EE both at l:1 and 1:4 ratios ($p < 0.05$). These differences might be due to their differences in granule size, amylose content and molecular weight of amylose and amylopectin.

In this study, the higher IBU/SA ratio (1:4) produced higher loading and EE compared to IBU/SA ratio (1:1). This might be due to the presence of sufficient SA polymer that completely entraps the IBU during the NPs formation. On the other hand, the lower concentration of SA (a ratio of 1:1) is assumed to provide decreased layer thickness of the NPs and this apparently might contribute to the leakage of the drug resulting in lower EE as reported elsewhere (Carneiro *et al.*, 2013; Sharma *et al.*, 2016).

The DL and EE of SANPs were also studied using SAs with low, medium and high DSs. The DL and EE of ibuprofen loaded SANPs increases consistently with increase in DS of SA. The average DL and EE of ibuprofen loaded SANPs increased from 9.3 to 26.6% and 44.7 to 78.3 %, respectively as DS of SAs increased from low to high. The increase in DL and EE of ibuprofen loaded SANPs with DS could be associated with increase in hydrophobic nature of SAs.

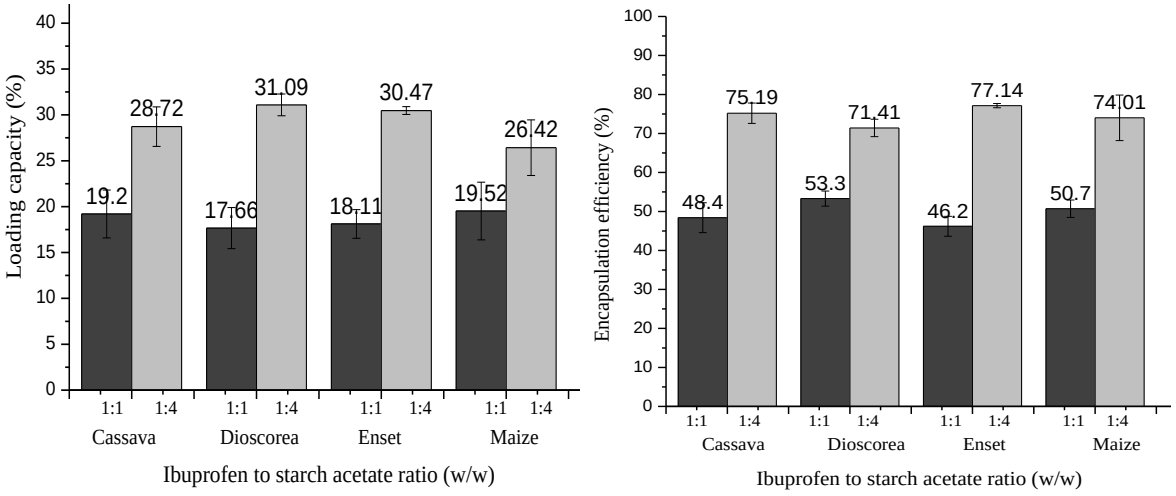

a) b)

Fig. 4.2: DL (a) and EE (b) of IBU-loaded SANPs of cassava, dioscorea, enset and maize SAs

4.3.1.3. In vitro release

Fig. 4.3 depicts the release profile of IBU as a function of time for NP formulations of cassava, dioscorea, enset and maize SAs. In all the four formulations, the drug release was

sustained over the study period of 8 h. The amount of drug release from the NPs over the study period ranged from 55.10% to 61.94%.

As depicted in Fig. 4.3, the drug release was sustained for the whole study period, 8 h and the release profiles were almost similar in all the four formulations, independent of the starch type ($p > 0.05$). The release profiles of the IBU from SA formulations are measurably different from those formulations containing the physical mixture of IBU powder and SA. The formulation containing the physical mixture of IBU and SA released almost all of its drug content in the first 1 h, while formulations of SANPs released far less than a quarter of their contents during the first hour. The observed slow release in the latter is attributed to the limited access of water into the NPs. The SA matrix retains the drug in the internal structure of NPs for a longer period. Similar results were reported by Han *et al*. (2013). The prolonged release time is associated with the enhanced hydrophobic interactions between the drug and the SA resulting in the entrapment of the drug within the polymer matrix for a longer period of time.

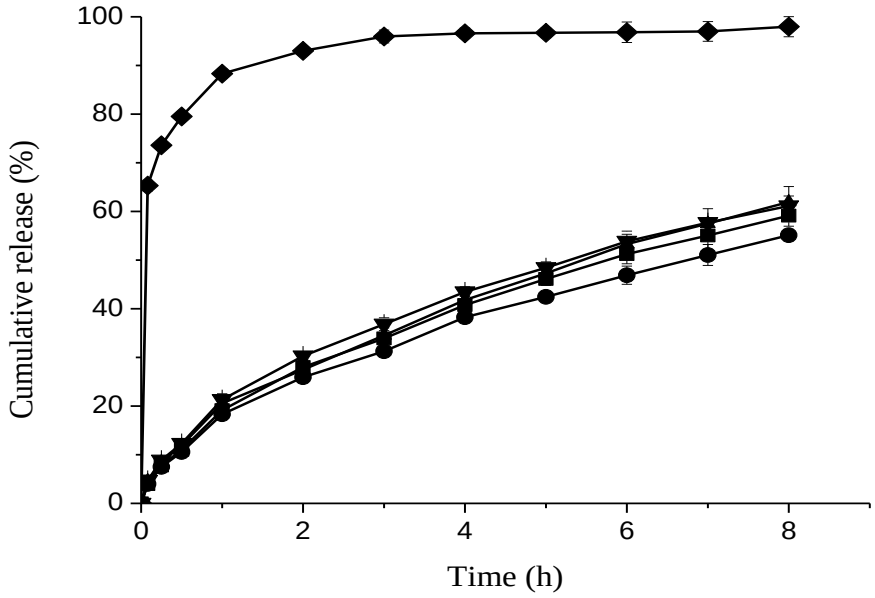

Fig. 4.3: *In vitro* release profiles of IBU from IBU-loaded SANP of cassava SA (■), dioscorea SA (●), enset SA (▲), maize SA (▼) and free drug (◆)

Further, drug release mechanism was evaluated by fitting release data to various models, namely, zero order, first order, Higuchi, Hixson-Crowell and Korsmeyer-Peppas equations (see the detail in appendix C). On the basis of the correlation coefficients, the best curve fitting was obtained with Higuchi model; indicating diffusion as the major mechanism of

drug release from SANPs. The correlation coefficients of the various models are given in Table 4.1.

Table 4.1: Kinetic modelling of drug release data of IBU-loaded SANPs

NP formulations	**Model types**				
	Zero-order (R^2)	First order (R^2)	Higuchi (R^2)	Hixson-Crowell (R^2)	Korsmeyer-Peppas (R^2)
Cassava	0.9537	0.6532	0.9976	0.6795	0.9929
Dioscorea	0.9534	0.6532	0.9978	0.6729	0.9969
Enset	0.9605	0.6471	0.9965	0.6786	0.9943
Maize	0.9433	0.6282	0.9985	0.6601	0.9975

4.3.2. Phyto CERs loaded SANPs for skin delivery

4.3.2.1. Size, PDI and EE

The particle size, PDI and EE of the NPs containing oat CERs are presented in Table 4.2. As can be seen, the oat CER EE of SA increased drastically with an increase in the DS. The NPs prepared from SA with high DS also exhibited lower PDI compared to the NPs prepared from SAs with medium DS (1.74). Therefore, SA with high DS was used for the preparation of NP gel.

Table 4.2: Particle size, PDI and oat CERs EE of SANPs (n = 3)

SANPs	**Particle size (nm)**	**PDI**	**EE (%w/w)**
Low DS	159.4 (0.829)	0.262 (0.010)	2.2 (0.8)
Medium DS	175.3 (1.799)	0.204 (0.017)	23.1 (4.9)
High DS	161.8 (2.854)	0.171 (0.004)	85.2 (1.9)

The values in the parentheses indicate standard deviations

4.3.2.2. In vitro release and penetration of oat CERs

Different formulation approaches including colloidal carriers such as NPs have been designed to overcome the protective barrier of the SC and deliver the CERs into the skin (Neubert *et al.*, 2016, Sahle *et al.*, 2014). The formulations are intended to enhance the permeation of CERs into the SC. At the same time, the formulations should also control the penetration of CERs into the deeper layers of the epidermis and dermis. In this study, the total oat CERs

release and penetration profile from the various formulations is shown in Table 4.3. The release and penetration of oat CERs from the microemulsion (ME) was higher than the amphiphilic cream and the NP/NP gel formulations. As can be seen from Table 4.3, over 90% of oat CERs incorporated in ME were released and penetrated into the four-layer membrane system after 60 min. When the ME was incorporated into gel, the amount of oat CERs released and penetrated in 60 min was reduced to ca. 79%. On the other hand, only 59-63% oat CERs in the NPs were released and penetrated in 60 min, which was drastically reduced to 34% in the NP gel system. Thus, Compared to ME and cream, the release from the NP was slower which can be attributed to the controlled release characteristics of the NPs. Furthermore, minute quantities of oat CERs incorporated in the NP gel formulation penetrated into the lower layers of the multilayer membranes than NP suspension. This could be explained by the high viscosity of the NP gel.

Table 4.3: Total oat CERs released and penetrated (%) into the four-layer membrane system at three different incubation periods (15, 30 and 60 min) (n = 3)

Formulations	**Total CERs Released and penetrated (%)**					
	15 min		30 min		60 min	
	CER I	CER II	CER I	CER II	CER I	CER II
NP	31.6 (16.6)	30.7 (15.6)	51.8 (15.1)	51.2 (11.0)	59.4(11.3)	62.8(15.0)
NP gel	25.0 (8.1)	23.3 (4.0)	29.5 (2.3)	30.4 (5.3)	34.8 (0.3)	34.0 (0.5)
ME	78.7 (3.7)	80.6 (5.2)	88.3 (7.3)	83.7 (5.2)	93.2 (1.9)	92.3 (2.7)
ME gel	65.1 (1.2)	62.9 (1.6)	66.7 (10.0)	65.8 (9.8)	79.0 (3.3)	78.6 (3.2)
cream	58.3 (0.2)	56.6 (2.2)	63.1 (3.5)	62.6 (3.9)	69.7 (9.3)	69.1 (9.8)

The values in the parentheses indicate standard deviations

Conclusion

The DL and EE of SANPs increased with an increase in the DS. Thus, by controlling the DS of SA and hence hydrophobicity it is possible to improve DL and EE of SANPs. *In vitro* drug release of SANPs was sustained over 8 h of study period. Drug release profile of SANPs followed Higuchi Model. The skin penetration of oat CER from SANPs was lower as compared to MEs and creams. SANPs retarded the release of oat CERs. In conclusion, this study provided insight into the potential applications of SANPs as sustained release nano drug carrier.

CHAPTER 5: FABRICATION AND EVALUATION OF CASSAVA SANPs LOADED WITH DRUGS OF VARIOUS BCS CLASSES: INFLUENCE OF DRUG SOLUBILITY AND PARTITION COEFFICIENT

5.1. Introduction

As mentioned earlier, as of recently there has been considerable interest in developing biodegradable polymer-based nanoparticles to effectively deliver poorly bioavailable drugs (Galindo-Rodriguez *et al.,* 2004; Guo and Huang, 2004; Hughes, 2005; Lin *et al.,* 2010; Shi *et al.,* 2010). Different kinds of NPs consisting of a wide range of materials such as natural and synthetic polymers, lipids and surfactants have been formulated and characterized (Chawla and Amiji 2002; Feczkó *et al.,* 2011; Nobs *et al.,* 2004; Shi *et al.,* 2011). Predominantly, developing biodegradable polymer-based nanocarriers has attracted considerable interest (Barratt, 2003; Ma *et al.,* 2008; Mahapatro and Singh 2011; Marin *et al.,* 2013).

Natural polymers, especially polysaccharides, are among the most studied polymers as components of various drug delivery systems. Within this group, dextran-, alginate-, and chitosan-based systems have all been well explored (Efthimiadou *et al.,* 2014; Paques *et al.,* 2014; Rampino *et al.,* 2013; Wasiak *et al.,* 2016). Starch has also been investigated for novel drug delivery systems such as nasal and other site-specific applications (Balmayor *et al.,* 2008; Boesel *et al.,* 2004; Brouillet *et al.,* 2008; Ozsoy *et al.,* 2009) as well as nano-sized drug delivery systems (Chin *et al.,* 2014; Dandekar *et al.,* 2012; Jain *et al.,* 2008; Singh and Nath, 2013;Yu *et al.,* 2007). As previously pointed out, starch has received increasing attention due of its outstanding properties such as biocompatibility, biodegradability, non-toxicity, non-immunogenicity, stability and compatibility with most drugs (Bemiller, 1997; Lorenz and Kulp, 1981). These attributes along with its availability from renewable resources and its economic benefits make starch an ideal substrate for the preparation of NPs (Besheer *et al.,* 2007; Liu *et al.,* 2008; Minimol *et al.,* 2013; Winarti *et al.,* 2014). Additionally, its molecular structure allows different chemical modifications enhancing its functionality and expanding its industrial applications.

To serve as a nano carrier for drugs, the preparation of starch nanostructure from native starch mostly requires modification of its backbone structure with hydrophobic molecules (Besheer *et al.*, 2007; Namazi *et al.*, 2011). Upon exposure to aqueous environment, the modified hydrophobic starch molecules spontaneously form micelles or self-associate to form colloidally stable NPs with inner hydrophobic core (Myrick *et al.*, 2014). This hydrophobic core can easily encapsulate hydrophobic substances like insoluble drugs (Gonçalves and Gama, 2008). However, the EE of nanocarriers depends on the physicochemical properties of drug substances.

In this study, therefore, starch isolated from cassava was chemically modified (by acetylation) and SANPs loaded with different model drugs (ibuprofen, acyclovir and furosemide) were prepared and characterized. The effects of DS of SA as well as solubility and partition coefficient of the drugs on the various parameters of NPs (size, PDI, DL, EE and release profile) were investigated.

As fabrication of NPs requires a precise control over the desired particle size and PDI, it was imperative to optimize the process and formulation variables to formulate NPs with desired properties (in terms of stability and drug release). Hence, RSM with CCD was employed to obtain the optimum formulation and process variables.

5.2. Materials and methods

5.2.1. Materials

Fresh cassava tubers were collected from Saula, south west Ethiopia. Mowiol 4-88-Poly vinyl alcohol (Kuraray Specialties Europe GmbH, Frankfurt/M., Germany); Pluronic® F68 (BASF, Mannheim, Germany); Pluronic® F127 (BASF, Mannheim, Germany); Hydrogen chloride solution (4.0M in dioxane) and 1, 4-dioxane anhydrous (99.8%) (Sigma-Aldrich Chemie GmbH, Steinheim, Germany); n-hexane (Grüssing GmbH, Filsum, Germany); Ethanol (Brüggemann GmbH & Co. KG, Heilbronn, Germany); Euxyl® PE 9010 (Schülke & Mayr GmbH (Norderstedt, Germany); Carbopol®980 Polymer (Lubrizol Advanced Materials Europe BVBA (Brussels, Belgium); Tris (hydroxymethyl)-aminomethane (Merck KGaA (Darmstadt, Germany); Ibuprofen (Sigma Aldrich Chemie GmbH, Taufkirchen, Germany); Acyclovir (Zhejiang Zhebei Pharmaceutical Co., Ltd, Xinshi, China) and Furosemide (Ipca Laboratories, Chennai, India); Tween® 80 (Carl Roth GmbH, Karlsruhe, Germany); Chloroform (Fisher Scientific UK LTD, Loughborough, UK); Dichloromethane (BDH Lab

Supplies, Poole, England), and ethyl acetate (Sigma Aldrich Chemie GmbH, Taufkirchen, Germany), were used as received.

5.2.2. Methods

5.2.2.1. Preparation of acyclovir, furosemide and ibuprofen loaded SANPs

The preparation of ibuprofen, acyclovir and furosemide loaded NPs was based on emulsification-solvent diffusion and evaporation method described in section 4.2.2.1.

5.2.2.2. Particle size and PDI of acyclovir, furosemide and ibuprofen loaded NPs

The Particle size and PDI of acyclovir, furosemide, and ibuprofen loaded NPs were measured following the methods described in section 3.2.2.3.

5.2.2.4. UV calibration curve of acyclovir and furosemide

Stock solution containing 100 μg/ml of acyclovir and furosemide in PBS, pH 7.4 were prepared. From this stock solution, six different concentrations for acyclovir (2, 4, 6, 8, 10, 12 μg/ml) and furosemide (3, 5, 7, 9, 11, 13 μg/ml) were prepared. The UV absorbance readings of these solutions were measured at 252 nm and 271 nm, respectively for acyclovir and furosemide using double beam UV/Visible spectrophotometer (SPEKOL® 1500, Jena, Germany). PBS (pH 7.4) was used as a blank (Vutpala and Sailaja 2014). The absorbance versus concentration of solutions was plotted and a calibration curve with a linear regression equation of: $Y= 0.0622X + 0.0131$ and $Y= 0.0666X + 0.0005$ (where, Y is the absorbance and X is the concentration in μg/ml) and correlation coefficient of 0.9983 and 0.9992 were obtained respectively for acyclovir and furosemide (see detail in Appendix B).

5.2.2.5. Determination of solubility of ibuprofen, acyclovir and furosemide

The solubility of each drug, ibuprofen, acyclovir and furosemide was determined in purified water or buffer solution by shake flask method as described by Aragón *et al.,* 2010 and Jouyban, 2009. In this, an excess amount of drug was taken in a 100 ml conical flask in which 50 ml of solvent was added and then stirred. The solid-liquid mixtures were stirred up to 24 hat room temperature. The samples were filtered through 0.45 μm membrane filter. Measured quantities of filtered samples were transferred into another volumetric flask and made further dilutions. The absorbances were measured for ibuprofen at 221 nm, acyclovir at 252 nm and furosemide at 271 nm using UV visible spectrophotometer (UV-Vis spectrophotometer, SPEKOL® 1500, Jena, Germany).

5.2.2.6. Determination of partition coefficient of ibuprofen, acyclovir and furosemide

The partition coefficient of each drug, ibuprofen, acyclovir and furosemide was determined in *n*-octanol-water system according to the method described by (Bannan *et al.,* 2016; Scheytt *et al.,* 2005; Takács-Novák *et al.,* 1994). In this, 50 mg of drug was dissolved in 25 ml of n-octanol saturated with water and was placed in 100 ml separatory funnel. To this system, 25 ml of water saturated with n-octanol was added. The content of the separatory funnel was shaken well for 30 min. The mixture was then left for 24 h at room temperature to achieve thermodynamic equilibrium. The concentration of the drug in aqueous phase before and after the shaking was determined by using double beam UV/Visible spectrophotometer.

5.2.2.7. DL and EE

DL and EE of acyclovir, furosemide and ibuprofen loaded cassava SANPs were determined as described in section 4.2.2.5.

5.2.2.8. In vitro drug release

The *in vitro* drug release profiles of acyclovir, furosemide and ibuprofen loaded SANPs were determined following the method described in section 4.2.2.6.

5.2.2.9. Mechanism of drug release

Data obtained from *in vitro* drug release studies were fitted into different kinetic Models according to the method described in section 4.2.2.7.

5.2.2.10. Optimization of NP formulation

A CCD model was used to statistically optimize the formulation and process variables and evaluate the main effects, interaction effects and quadratic effects of the formulation factors on the particle size (Y_1), size distribution (Y_2), percentage DL (Y_3) and EE (Y_4) of drug loaded SANPs. Details of the design are listed in Table 5.1.

Table 5.1: Relationship between coded and actual values of the variables used for starch NP fabrication

	Coded level of variables				
Factors	-1.68	−1	0	1	+1.68
X_1 = Pluronic® F127 (% *w/v*)	0.12	0.60	1.30	2.00	2.48
X_2 = drug to SA ratio (% *w/w*)	1.25	20.00	47.5	75.00	93.75
X_3 = Homogenization speed (rpm)	1909.24	6000.00	12000.00	18000.00	22090.76
Responses	**Constraints**				
Y_1 = Particle size	Minimize				
Y_2 = PDI	Minimize				
Y_3 = DL	Maximum				
Y_4 = EE	Maximum				

5.2.2.11. Statistical analysis

All the data were subjected to statistical analysis using IBM SPSS Statistics for Windows, Version 21.0 (IBM Corporation, Armonk, NY, USA). Origin®, version 8.5 (OriginLab Corporation, MA, USA), Design Expert (Version 9) (Stat-Ease, Inc, Minneapolis, MN) and MS Excel 2010 (Microsoft Corporation, USA) were used for plotting graphs. One-way ANOVA was applied for comparison of the results. In the optimization process, t-test and lack of fit test were used to determine the significance and validity of the regression model, respectively. P value of less than 0.05 was considered to be significant difference.

5.3. Results and discussion

5.3.1. Effect of DS on size and PDI of drug loaded SANPs

In order to assess the effect of DS on size and PDI of NPs, cassava SANPs containing three different drugs (ibuprofen, acyclovir and furosemide) were fabricated from acetylated starches of low (0.91), medium (2.15) and high (2.74) DS. As depicted in Fig 5.1, the mean particle size and PDI of each drug, ibuprofen, acyclovir and furosemide loaded SANPs were found to increase with increase in DS. Statistical analysis of the results for the three drugs indicated that the sizes of NPs fabricated from SA of low DS were significantly different from those NPs obtained either from medium DS ($p = 0.016$) or high DS ($p = 0.003$).

Similarly, the PDI of NPs obtained from SA of low DS were significantly different from those NPs obtained from medium DS ($p = 0.0085$) and high DS ($p = 0.0076$).

The increase in particle size and PDI might be attributed to increase in molecular weight of the modified starch. Moreover, these differences between DSs might also be associated with the hydrophobic interaction between SA molecules during formation of NP. That is, probably loosely packed hydrophobic core was formed due to decrease in hydrogen bonding between hydrophobic starch molecules. In a different study, Wei and co-workers have also reported that the molecular weight and DS of hydrophobic groups are important parameters that influence physicochemical, biological and pharmaceutical properties of NPs (Wei *et al.*, 2015).

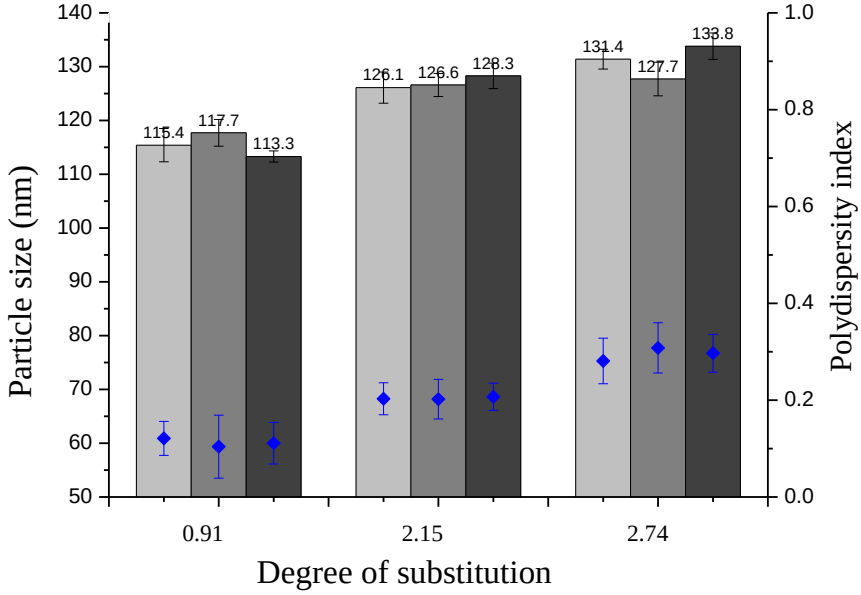

Fig. 5.1: Effect of DS on size and PDI (●) of cassava SANPs formulated with ibuprofen ( ), acyclovir ( ) and furosemide ( ).

5.3.2. Effect of solubility and partition coefficient of the drugs on DL and EE of SANPs

The effect of the solubility and partition coefficient of the drugs on DL and EE of NPs were studied using SAs with low, medium and high DSs. As shown in Fig. 5.2 and Fig. 5.3, for NPs fabricated from SA with high DS (2.15 and 2.74), as solubility of drug decreases the DL and EE increases whereas for NPs fabricated from SA with low DS (0.91), as solubility of drug decreases DL and EE also decrease. The DL and EE of ibuprofen and furosemide loaded SANPs increase consistently with increase in DS of SA. As shown in the figures, average DL of ibuprofen and furosemide loaded NPs increased from 10.7 to 26.6% and 9.9 to 27.9%,

respectively, as DS of SAs increased from low to high. Similarly, EEs of these drugs increased from 44.7 to 77.9% and 39.9 to 80.5%, respectively. On the other hand, acyclovir loaded NPs fabricated from SA with low DS (0.91) exhibited higher DL and EE as compared to those fabricated from SAs with higher DS (2.15 and 2.74). The DL and EE of acyclovir loaded SANPs decreased from 16.5 to 11.1% and 64.5 to 50.9%, respectively, as the DS of SA increased from low (0.91) to high (2.74).

The increase in DL and EE of ibuprofen and furosemide loaded NPs with DS could be associated with increase in hydrophobic nature of SAs. Furosemide having the highest partition coefficient (log P = 2.07) and, thus, being the most lipophilic drug has the highest DL and EE values in SANPs than the less hydrophobic drug, ibuprofen and the hydrophilic drug, acyclovir. Since aqueous solubility is inversely proportional to the partition coefficient (Table 5.2), acyclovir with the highest aqueous solubility has the lowest loading values in SANPs.

Table 5.2: Solubility and partition coefficient of drugs used in the formulation of SANPs

Drugs	Mol. Wt.	Solubility at 25 °C (mg/ml)		Partition coefficient (log p)	
		Purified water	PBS[a]	Octanol/ purified water	Octanol/ PBS
Ibuprofen	206.285	0.024	0.030	1.200	1.270
Acyclovir	225.208	2.120	2.110	0.447	0.490
Furosemide	330.739	0.012	0.011	2.070	2.020

[a]PBS: phosphate buffer pH 7.4

A hydrophilic drug is more likely to stay in aqueous medium (in dissolved state) and also has the tendency to escape to aqueous medium (or the continuous phase) rather than being loaded into NPs. When there is poor interaction between the drug and the polymer, the drug will tend to diffuse from the organic phase to the external aqueous medium during the spontaneous emulsification process of the polymer. Although acyclovir was completely dissolved in the ethyl acetate (0.53 mg/ml at 25 ^{o}C), it might have leaked out during diffusion of the remaining ethyl acetate from the organic phase droplets into the aqueous dispersing medium. On the other hand, furosemide and ibuprofen are less likely to leak from the organic phase and are expected to readily co-precipitate with the SA during emulsification and solvent evaporation process. This might be associated with their easy congruousness with

hydrophobic SAs. As shown in Fig. 5.2, acyclovir is approximately 177 and 88 fold soluble in aqueous medium than furosemide and ibuprofen, respectively.

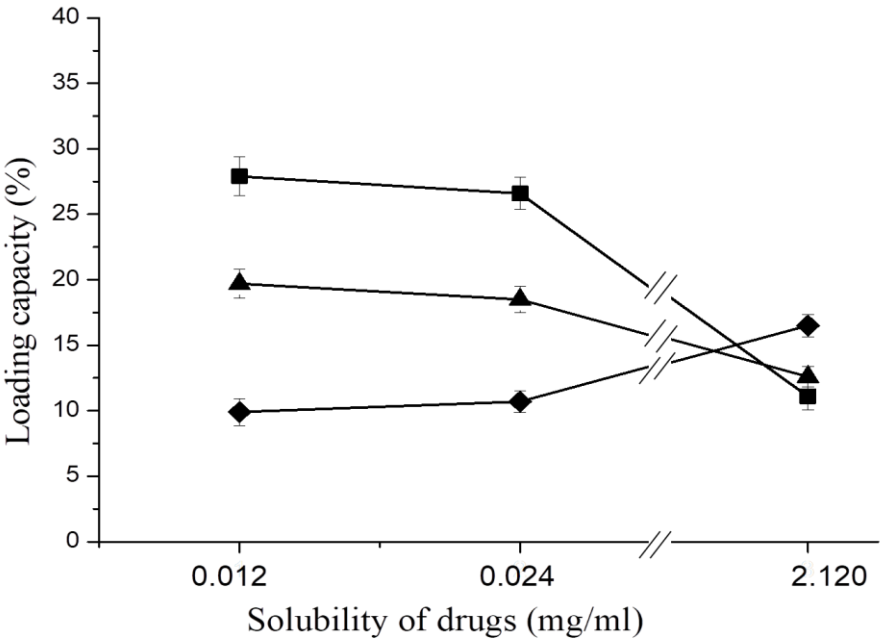

Fig. 5.2: The relationship between solubility of drugs and DL of SANPs fabricated with DS of 0.91(◆), DS of 2.15 (▲) and DS of 2.74 (■). (0.012, 0.024 and 2.120 mg/ml are solubilities of furosemide, ibuprofen and acyclovir, respectively). The symbol "//" indicates the scale breaks on X-axis.

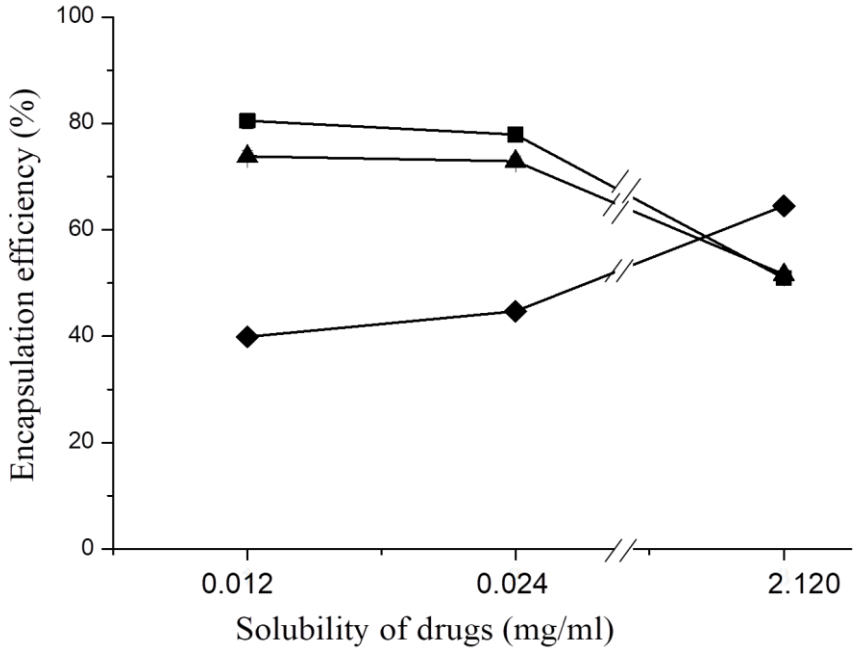

Fig. 5.3: The relationship between solubility drugs and EE of SA NPs fabricated with DS of 0.91(◆), DS of 2.15 (▲) and DS of 2.74 (■). (0.012, 0.024 and 2.120 mg/ml are solubilities of furosemide, ibuprofen and acyclovir, respectively). The symbol "//" indicates the scale breaks on X-axis.

5.3.3. Effect of drug to SA ratio on particle size and PDI

To evaluate the effect of weight ratio of drug to SA on particle size and PDI of the NPs, the drug to SA ratio was varied between 1:1 and 1:5. As shown in Table 5.3, an increase in the proportion of SA results in increase in particle size and PDI of ibuprofen, acyclovir and furosemide loaded SANPs. Though within the desired range, the increments in size and PDI of NPs may be associated with the emulsification solvent diffusion and evaporation method. During formation of NPs, the emulsion system probably incurred higher resultant viscosity of the organic phase which might have resulted in aggregation of NPs upon solvent diffusion. The results are in agreement with those reported by Mainardes and Evangelista, 2005.

Table 5.3: Effect of drug to SA ratio on the mean particle size and PDI of the resulting NPs

Drug to SA ratio	Ibuprofen		Acyclovir		Furosemide	
	Size (nm)	PDI	Size (nm)	PDI	Size (nm)	PDI
1:1	104.71(6.86)	0.102 (0.01)	110.22 (4.91)	0.121 (0.02)	96.62 (5.48)	0.104 (0.02)
1:2	114.56 (4.22)	0.113 (0.01)	119.74 (2.15)	0.201 (0.01)	107.76 (3.44)	0.113 (0.03)
1:3	119.70 (7.12)	0.122 (0.01)	126.33 (5.44)	0.219 (0.02)	114.25 (4.11)	0.182 (0.01)
1:4	123.46 (3.64)	0.149 (0.02)	141.82 (1.39)	0.222 (0.03)	135.54 (2.32)	0.201 (0.01)
1:5	124.72 (5.38)	0.183 (0.03)	139.63 (6.49)	0.341 (0.02)	144.22 (3.41)	0.243 (0.02)

The values in the parentheses indicate standard deviations

5.3.4. Effect of drug to SA ratio on DL and EE

For the various drug to SA ratios, the average DL of NPs ranged between 8.7 and 28.5% while EE ranged between 43.4 and 80.5% (Table 5.4). As shown in the Table, the highest drug to SA ratio (1:5) produced relatively the highest DL and EE. This might be due to the presence of sufficient SA polymer that completely entraps the drug during the formation of the NPs. On the other hand, the lowest amount of SA (a ratio of 1:1) gives rise to a decrease in the layer thickness of the NPs. This apparently might contribute to the leakage of the drug and consequently lower EE as reported elsewhere (Carneiro *et al.,* 2013; Carvalhoa *et al.,* 2013; Sharma *et al.,* 2016).

Table 5.4: DL and EE of SANPs at various drug to SA ratios

Responses	Drugs	Drug to SA ratio				
		1:1	1:2	1:3	1:4	1:5
DL	Ibuprofen	12.4 (1.40)	18.5 (1.48)	23.2(1.46)	26.6 (1.13)	26.9 (1.30)
	Acyclovir	08.7 (1.08)	11.2 (1.16)	13.6 (1.13)	16.1 (1.33)	16.7 (1.44)
	Furosemide	11.8 (1.03)	18.3 (1.30)	24.1 (1.34)	27.9 (1.28)	28.5 (1.39)
EE	Ibuprofen	47.4 (2.41)	59.5 (2.22)	64.7 (2.02)	76.4 (2.11)	77.9 (2.52)
	Acyclovir	43.3 (2.32)	43.7 (1.97)	48.8 (1.55)	52.5 (2.08)	53.7 (2.21)
	Furosemide	46.1 (2.07)	60.3 (2.33)	66.4 (2.04)	77.7 (1.84)	80.5 (2.03)

The values in the parentheses indicate standard deviations

5.3.5. Optimization of drug loaded SANPs

Judicious selection and optimization of critical variables would enable fabrication of the desired NPs. The critical variables for drug loaded SANPs were determined similar to those unloaded SANPs explained in section 3.3.1. In this, Pluronic® F127, drug to SA ratio and homogenization speed were the main factors that affect the particle size, size distribution, DL and EE of the drug loaded SANPs. Pluronic® F127 was selected as surfactant of choice (see section 3.3.1.4).The batches were evaluated for particle size, PDI, DL and EE. The particle sizes of SANPs prepared from Tween 80 and PVA were greater than 200 nm and the DL and EE were < 15% and 58%, respectively. Both Pluronic® F68 and Pluronic® F127 provided particle size less than 200 nm (178 nm and 125 nm, respectively) and comparable DL and EE. Hence, Pluronic® F127 was used for further studies. The operating variable, namely, rpm of the homogenizer was also investigated during the trial studies. The effects of these parameters on mean particle size and drug EE were evaluated. The results showed that appropriate shear force has to be applied to prevent separation of the phases or formation of aggregates. Higher homogenization speed during emulsification stage provides adequate shock to bring down interfacial barrier and facilitate size reduction. Thus, drug-loaded SANPs were produced under optimized conditions of formulation and process variables. The optimization was performed by applying constraints during the factorial study with an objective of achieving maximum entrapment of the drug in the formulation while keeping particle size and PDI low. Therefore, the effect of independent variables Pluronic® F127

(X_1), drug to SA ratio (X_2) and homogenization speed (X_3) on response variables, particle size (Y_1), PDI (Y_2), DL (Y_3) and EE (Y_4) were analyzed.

5.3.5.1. Effect on particle size (Y_1) and PDI (Y_2)

According to the design experiments, the particle size and PDI of drug-loaded SANPs ranged between 93.7 - 379.6 nm and 0.097 - 0.372, respectively. In all cases, the surfactant concentration, drug to polymer ratio and homogenization speed had significant effects on mean particle size and PDI. Particle size and PDI decreased with an increase in the concentration of Pluronic® F127 (0.6 – 2%) and homogenization speed (6000 - 18000 rpm) ($p < 0.05$). On the other hand, drug to SA ratio had a direct correlation with the dependent variables. These relationships are indicated by the magnitudes of the coefficients in the polynomial equation (Table 5.5). Looking at the Table, it is evident that particle size and PDI of the SANPs are affected negatively by all the three independent variables; the effect of drug to SA ratio being predominant.

Table 5.5: Evaluation of effects of Pluronic® F127 (X_1), drug to SA ratio (X_2) and homogenization speed (X_3) and, their interactions on size and PDI of drug loaded SANPs

Term	Coefficient					
	Particle size			PDI		
	Ibuprofen	Acyclovir	Furosemide	Ibuprofen	Acyclovir	Furosemide
Constant	+105.45	+108.37	+100.94	+0.130	+0.11	+0.131
X_1	– 16.91	– 14.24	– 15.93	– 0.019	– 0.012	– 0.013
X_2	– 61.30	– 65.73	– 59.44	– 0.073	– 0.044	– 0.058
X_3	– 22.79	– 27.21	– 28.73	– 0.016	– 0.025	– 0.035
X_1X_2	– 19.77	– 23.85	– 21.84	– 0.023	– 0.005	– 0.023
X_1X_3	– 12.78	– 12.26	– 08.27	– 0.019	– 0.009	– 0.017
X_2X_3	– 04.30	– 05.44	– 02.76	– 0.017	– 0.025	– 0.012
X_1^2	+ 34.54	+ 33.37	+ 29.58	+ 0.056	+ 0.046	+ 0.037
X_2^2	+ 32.03	+ 35.22	+ 31.24	+ 0.073	+ 0.047	+ 0.028
X_3^2	+ 11.47	+ 12.61	+ 11.53	+ 0.023	+ 0.049	+ 0.032

Increase in the mean particle size and PDI is observed with increase in SA concentration for all the concentrations of Pluronic® F127 studied. The contrary relationship observed between particle size and drug to polymer ratio could be attributed to the increase in viscosity with an increase in polymer concentration, thus posing resistance to droplet breakdown, and also, resulting in poor dispersibility of primary emulsion in the aqueous phase. It has been reported elsewhere that with in the concentration investigated (0.6 - 2%), an increase in the amount of Pluronic® F127 in a formulation may lead to decreased particle size due to stabilization of emulsion droplets; with higher number of surfactant molecules covering the surface of droplets and consequently, providing increased protection of the latter against coalescence (Georgieva *et al.,* 2009).

5.3.5.2. Effect on DL (Y_3) and EE (Y_4)

In all the formulations, it was observed that surfactant concentration, drug to SA ratio and homogenization speed had significant effect on entrapment of the drug ($p < 0.0001$). As can be seen from Table 5.6, supplementary material, the ANOVA F-value of the quadratic model indicated that the model p-value is less than 0.05 and considered to be significant while the lack of fit of the model is not significant ($p > 0.05$). This indicates that response variable Y_3 and the set of formulation variables were significantly related. Hence, the second order reduced quadratic model equation was derived for SANPs by best-fit method to describe the relationship between the responses and the independent variables (Table 5.7).

Table 5.6: Fit summary statistics for DL and EE of ibuprofen (IBU), acyclovir (ACY) and furosemide (FRS) and loaded cassava SANPs

Response	Loaded drugs	DL			EE		
		R^2	p-value	Lack of fit p-value	R^2	p-value	Lack of fit p-value
Particle size	IBU	0.9508	0.0020	0.1200	0.9965	0.0053	0.3407
	ACY	0.9976	0.0028	0.1401	0.9957	0.0001	0.0921
	FRS	0.9601	0.0076	0.1020	0.9992	0.0008	0.2180
PDI	IBU	0.9508	0.0020	0.1200	0.9965	0.0053	0.3407
	ACY	0.9976	0.0028	0.1401	0.9957	0.0001	0.0921
	FRS	0.9601	0.0076	0.1020	0.9992	0.0008	0.2180

As can be seen from coefficients in Table 5.7, the effect of variables on the DL and the interaction between them are significant ($p < 0.0001$). In all cases, the DL and EE of SANPs are affected negatively by surfactant concentration, drug to polymer ratio and homogenization speed. Furthermore, the interactions between the variables are also negative (leading to increase in DL and EE). The DL and EE of NPs decreased upon increasing the concentration of Pluronic® F127 and increased with increasing concentration of polymer. The later effect is advantageous not only for transporting the required amount of drug to the target site but also for prolonging the residence time. The high DL and EE of SA can be attributed to several factors. First, the hydrophobic nature of SA molecules makes it relatively easy to entrap hydrophobic drug. Second, due to their hydrophobic nature, ibuprofen and furosemide are not lost to the external aqueous phase during the formulation process. Third, as a polymer, SA in highly concentrated solution precipitates rapidly on the surface of dispersed phase and prevents diffusion of drug across the phase boundary. Finally, the concentrated polymer solution forms a highly viscous solution resulting in delayed diffusion of drug through the polymer droplets.

Table 5.7: Evaluation of effects of Pluronic® F127 (X_1), drug to SA ratio (X_2) and homogenization speed (X_3) and, their interactions on DL and EE of drug loaded SANPs

Term	Coefficient					
	DL			EE		
	Ibuprofen	Acyclovir	Furosemide	Ibuprofen	Acyclovir	Furosemide
Constant	+26.75	+18.74	+30.32	+80.13	+56.32	+84.38
X_1	– 1.33	– 2.17	– 2.07	– 3.14	– 2.44	– 2.17
X_2	– 2.41	– 5.22	– 4.44	– 13.90	– 12.41	– 14.44
X_3	– 2.92	– 1.04	– 2.11	– 1.05	– 2.21	– 1.51
X_1X_2	– 0.94	– 1.46	– 0.34	– 3.44	– 1.75	– 4.82
X_1X_3	– 0.56	– 0.79	– 0.66	– 0.81	– 1.01	– 2.52
X_2X_3	– 2.06	– 0.96	– 2.09	– 0.83	– 2.74	– 1.33
X_1^2	+ 0.50	+ 2.56	+ 3.37	+ 3.33	+ 4.22	+ 5.91
X_2^2	+ 1.18	+ 0.25	+ 1.41	+ 0.82	+ 0.11	+ 2.01
X_3^2	+ 3.16	+ 2.46	+ 3.27	+ 2.94	+ 2.05	+ 2.71

5.3.5.3. Simultaneously optimized formulation of drug-loaded SANPs

After finding the model that best represents each response, optimal conditions for the preparation of drug-loaded SANPs were obtained by solving the equations, analyzing R^2 and improving or maintaining each response within the desired range. For fabrication of ibuprofen-loaded NPs, the optimum concentration of Pluronic® F127, drug to SA ratio, and homogenization speed were found to be 1.2%, 1:4.4 and 13,394 rpm, respectively. Similarly, the optimum condition for acyclovir (1.3% Pluronic® F127, 1:4.6 drug to SA ratio and 13,698 rpm of homogenizer); and for furosemide the corresponding values were-1.3% Pluronic® F127: 1:4.2 drug to SA ratio, and 13,452 rpm of homogenizer). At these levels of independent variables, the predicted mean particle size, PDI, DL and EE were calculated. The experimentally obtained and model predicted values are presented in Table 5.8. The predicted values of the multiple batches prepared under the optimal conditions were very close to the experimental values, with low percentage bias, suggesting that the optimized formulations were reliable and reasonable.

Table 5.8: Predicted and observed values of particle size, PDI, DL and EE of SANPs under optimum fabrication conditions

Responses	Ibuprofen		Acyclovir		Furosemide	
	Predicted response	Observed response	Predicted response	Observed response	Predicted response	Observed response
Size (nm)	104.9	109.1(1.7)	108.1	112.1 (2.2)	106.3	113.4 (1.6)
PDI	0.097	0.109 (0.001)	0.127	0.115 (0.01)	0.102	0.135 (0.002)
DL (%)	30.40	28.13(0.4)	20.02	17.72 (1.1)	31.21	29.87 (0.7)
EE (%)	80.51	78.92 (2.5)	60.33	58.11 (1.8)	82.65	84.17 (3.1)

The values in the parentheses indicate standard deviations

5.3.6. In vitro release of drugs from SANPs

Fig. 5.4a, b and c depict the cumulative release profile of each of the three drugs from SANPs with DS of 0.91, 2.15 and 2.74, respectively. As can be seen in Fig. 5.4a, the SANPs with DS of 0.91 showed a much faster release of the three drugs than those of SANPs with higher DS. The release profiles of all the three drugs from SANPs fabricated from low DS were found to be above 60% during 8 h study period. On the other hand, the SANPs with DS of 2.15 and 2.74 presented different release patterns as a function of the encapsulated drug (Fig. 5.4b and

c). In this case, the three drugs displayed three different release patterns. The release rates followed the following sequence: acyclovir (1.02 µg/min) > ibuprofen (0.33 µg/min) > furosemide (0.27 µg/min); which correspond to their respective characteristic solubility. In all cases, the release of hydrophilic drug acyclovir from SANPs was approximately 75%. There was an initial phase of rapid release of acyclovir followed by a more gradual release over a period of 8 h. The rapid initial release of acyclovir was probably due to the portion of the drug adsorbed on the surface of the NPs and the large surface to volume ratio of the NPs. It may also be attributed to the hydrophilic nature of acyclovir. As shown in Table 5.2, acyclovir is hydrophilic drug (log P of 0.45) while furosemide and ibuprofen are hydrophobic drugs (log P of 2.07 and 1.20, respectively).

In general, the sustained release pattern of furosemide and ibuprofen from SANPs of higher DS (2.15 and 2.74) is associated with the enhanced hydrophobic interactions between the drug and the SA. Drug-SA polymer interaction, which is hydrophobic, could even be more intense for the SANPs with high DS (2.74). This interaction could be associated with enhanced partitioning of the hydrophobic drug molecules into the hydrophobic core-shell structure of NPs and retention thereof. Therefore, along with the SA polymer hydrophobic nature, the release profile also depends on the solubility and partition coefficient of the incorporated molecule.

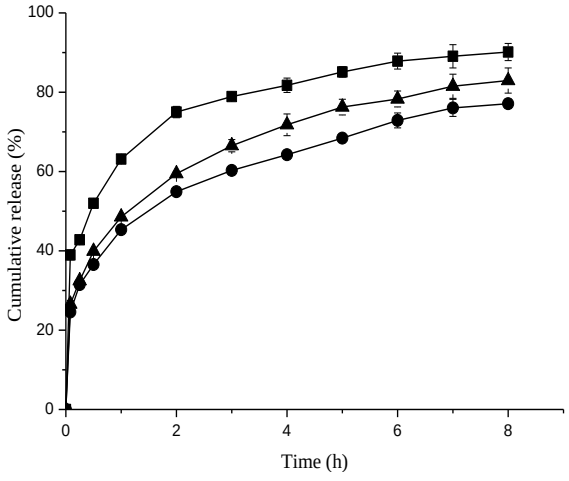

a)

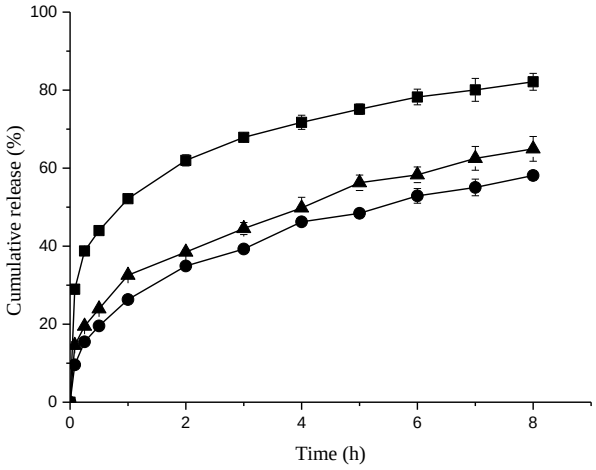

b)

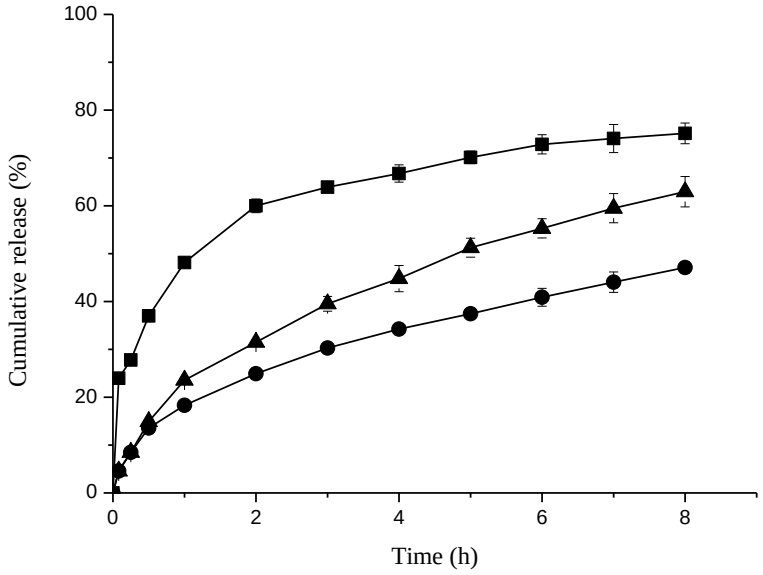

c)

Fig. 5.4: Effect of drug solubility on *in vitro* release profiles from cassava SANPs with DS of 0.9 (a), 2.15 (b) and 2.74 (c) (ibuprofen (▲), acyclovir (■) and furosemide (●)

5.3.7. Drug release mechanism

Drug release date fitted to various models, namely, zero order, first order, Higuchi, Hixson-Crowell and Korsmeyer-Peppas; and the correlation coefficients calculated from linear plots (Fig. 5.5) are shown in Table 5.9. The results indicate that the release of all the three drugs, ibuprofen, acyclovir and furosemide can be reasonably well described by Higuchi and Korsmeyer-Peppas models owing to high R^2 values close to 1. These models yielded nearly similar R^2 values for ibuprofen and furosemide, which can be considered as appropriate kinetic models to describe the release of these drugs from SA matrix. For acyclovir, however, the drug-release mechanism is best described by Korsmeyer–Peppas model, with R^2 = 0.9863.

For each of the three loaded drugs, Korsmeyer-Peppas model showed diffusion exponent (n) < 0.5, indicating diffusion is the major mechanism of drug release from SANPs. Studies have shown that diffusion of drug molecules from polymeric matrix of NPs, the biodegradation of polymeric matrix of NPs, or a combination of the two are the major mechanisms of drug release from NPs (Anderson and Shive, 1997; Barichello *et al.,* 1999; Gardouh *et al.,* 2013). In the present study, SA degradation in neutral medium is very slow, and no degradation of the SA in the buffer medium is expected to occur within the period of the release study. Thus, it may be assumed that the release is mainly mediated through the diffusion (a concentration

gradient process) with very little or no degradation of polymer matrix within the studied period.

Table 5.9: Kinetic modelling of drug release data of ibuprofen, acyclovir and furosemide loaded SANPs

Loaded drug	Models					
	Zero-order (R^2)	First-order (R^2)	Higuchi (R^2)	Hixson-Crowell (R^2)	Korsmeyer-Peppas (R^2)	n-value
Ibuprofen	0.6175	0.5994	0.9950	0.6324	0.9960	0.239
Acyclovir	0.7860	0.3406	0.9352	0.4073	0.9863	0.343
Furosemide	0.6474	0.5885	0.9931	0.6112	0.9961	0.241

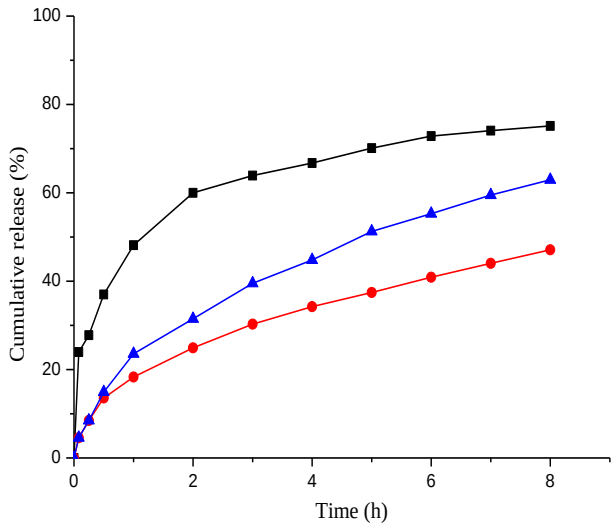

I: O-order release model

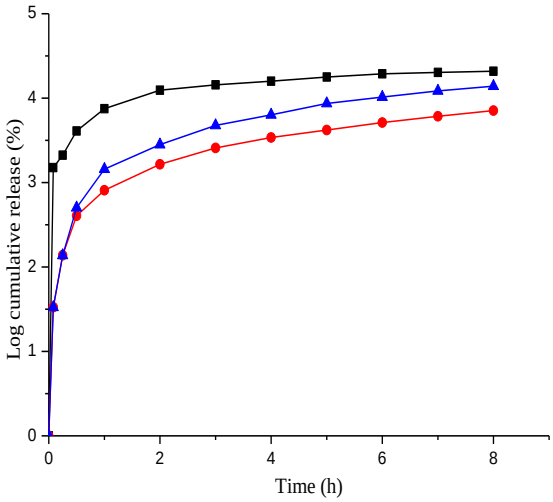

II: 1st order release model

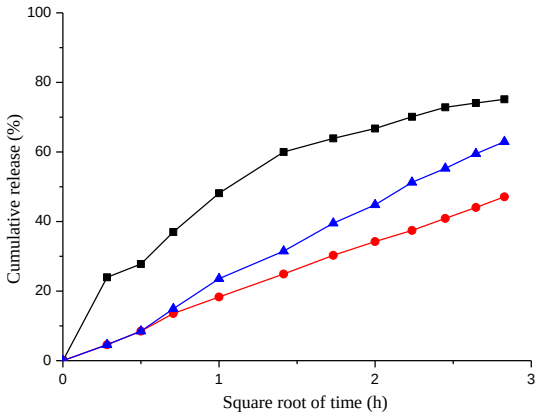

III: Higuchi release Model

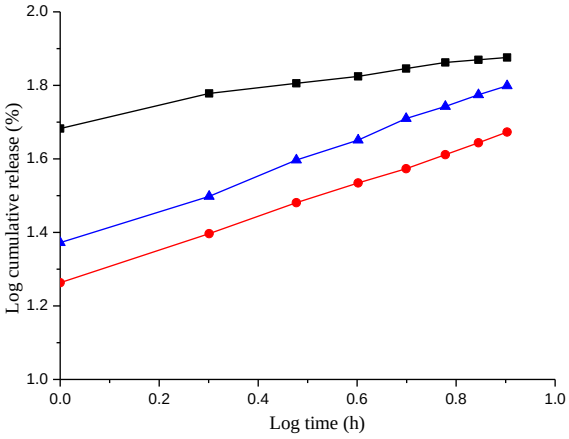

IV: Korsemeyer-Peppas release model

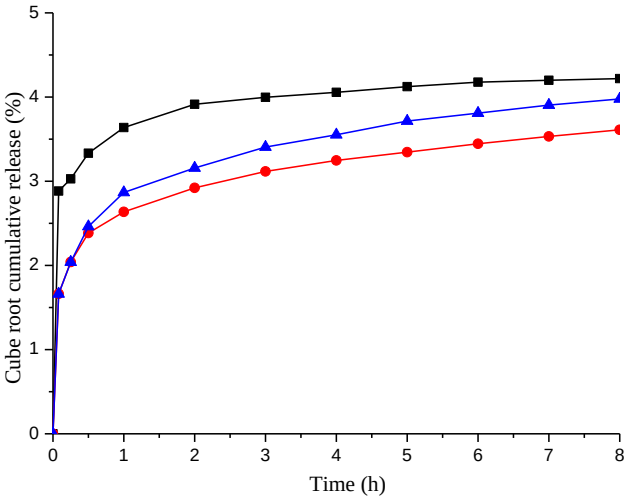

V: Hixson Crowell release

Fig. 5.5: Drug release kinetic models: zero order (I), first order (II), Higuchi (III), Korsemeyer-Peppas (IV) and Hixson-Crowell (V) of ibuprofen (▲), acyclovir (■) and furosemide (●) loaded cassava SANPs.

Conclusion

From the foregoing, it is apparent that hydrophobic drugs are more efficiently loaded and encapsulated into hydrophobic SANPs than hydrophilic drugs. The release profiles depended on the solubility and partition coefficient of drugs. The release rates followed the following sequence: acyclovir > ibuprofen > furosemide which corresponds to their respective characteristic solubility. In conclusion, the findings suggest that solubility and partition coefficient of incorporated drug molecules are key factors to be considered in the fabrication of SA-based NPs for sustained release.

Suggestions for further work

The present study strongly indicates the potential applications of SANPs as nano drug carrier. Therefore, the following are suggested for further work:

- Conducting *in vivo* study and correlating the drug release profile obtained *in vitro* with *in vivo* results to confirm that SANPs control and extend the drug release *in vivo* and to establish predictive *in vitro-in vivo* correlation (IVIVC).
- Conducting cytotoxicity and cellular penetration studies for both unloaded and drug loaded NPs on Caco-2 cell lines.
- Conducting studies on surface modification with the view of enhancing the *in vivo* performance of SANPs.
- Undertaking comparative study of acetylated SANPs and propylated and acid modified starches and see the effect of propylation and acid modification
- Conducting stability studies for SANPs for extended period of time.

List of Publications that emanated from this Dissertation

1. Paulos, G., Mrestani, Y., Heyroth, F., Gebre-Mariam, T., Neubert, R.H.H. (2016). Fabrication of acetylated dioscorea starch nanoparticles: Optimization of formulation and process variables, Journal of Drug Delivery Science and Technology, 31:83-92.

2. Tessema E.N, Gebre-Mariam T., Paulos G., Wohlrab J., Reinhard H.H. Neubert R.H.H. (2018). Delivery of oat-derived phytoceramides into the stratum corneum of the skin using nanocarriers: Formulation, characterization and in vitro and ex-vivo penetration studies, European Journal of Pharmaceutics and Biopharmaceutics 127: 260–269

3. Paulos, G., Neubert, R.H.H., Gebre-Mariam, T., (2019). Fabrication and Evaluation of Cassava Starch Acetate Nanoparticles Loaded with Drugs of Various BCS Classes: Influence of Drug Solubility and Partition Coefficient, Journal of Nanomaterials and Molecular Nanotechnology, 8

4. Paulos G., Neubert R.H.H., Gebre-Mariam T. Effect of starch origin on fabrication of starch acetate nanoparticles. (Manuscript prepared for publication)

References

Amsa, P., Kosalge, A., Tamizharasi, S., Karthikeyan, D., Sivakumar, T., Shinde, V., (2010). Formulation and evaluation of chitosan nanoparticle of Acyclovir. *Res. J. Pharm. Technol.*3: 121–126.

Anderson, J.M., Shive, M.S., (1997). Biodegradation and biocompatibility of PLA and PLGA microspheres. *Adv. Drug Deliv. Rev*. 28:5–24.

Anarjan, N., Jafarizadeh-Malmiri, H., Nehdi, I.A., Sbihi, H.M., Al-Resayes, S.I., Tan, C.P., (2015). Effects of homogenization process parameters on physicochemical properties of astaxanthin nanodispersions prepared using a solvent-diffusion technique. *Int. J. nanomed.* 10:1109–1118.

Aragón, D.M., Rosas, J.E., Martínez, F., (2010). Thermodynamic study of the solubility of ibuprofen in acetone and dichloromethane. *Brazilian J. Pharm. Sci.* 46:227–235.

Arayne, M.S., Sultana, Sabah, N.U., (2007). Fabrication of Solid Nanoparticles for Drug Delivery: Review. *Pak. J. Pharm.* 20**:** 251–259.

Ayucitra, A., (2012). Preparation and characterization of acetylated corn starches. *Int. J. Chem. Eng. Appl.* 3:156–159.

Aziz, H., Kamaruddin, A., Abu-Baker, M., (2008). Process optimization studies on solvent extraction with naphthalene-2-boronic acid ion-pairing with trioctylmethyl ammonium chloride in sugar purification using design of experiments, *Sep. Purif. Technol.* 60: 190–197.

Babić, J., Šubarić, D., Ačkar, Đ., Kopjar, M., Tiban, N.N. (2009). Acetylation and characterisation of corn starch. *J. Food Sci. Technol.* 46: 423–426.

Balmayor, E., Tuzlakoglu, K., Marques, A., Azevedo, H. and Reis, R., (2008). A novel enzymatically-mediated drug delivery carrier for bone tissue engineering applications: combining biodegradable starch-based microparticles and differentiation agents. *J. Mater. Sci. Mater. Med*. 19:1617–1623.

Bannan, C., Calabró, G., Kyu, D.Y., Mobley, D.L., (2016). Calculating partition coefficients of small molecules in octanol/water and cyclohexane/water. *J. Chem. Theory computation* 12:4015–4024.

Barichello, J., Morishita, M., Takayama, K., Nagai, T., (1999). Encapsulation of Hydrophilic and Lipophilic Drugs in PLGA Nanoparticles by the Nanoprecipitation Method. *Drug Dev. Ind. Pharm.* 25: 471–476.

Barratt, G.M., (2000). Therapeutic applications of colloidal drug carriers. *Pharm. Sci. Technol. Today* 3: 163–171.

Barratt, G., (2003). Colloidal drug carriers: achievements and perspectives. *Cell Mol. Life Sci.* 60: 21–37.

Bello-Perez, L.A., Agama-Acevedo, E., Zamudio-Flores, P.B., Mendez-Montealvo, G., Rodriguez-Ambriz, S.L., (2010). Effect of low and high acetylation degree in the morphological, physicochemical and structural characteristics of barley starch. *Food Sci. Technol.* 43: 1434–1440.

Bemiller, J.N., (1997). Starch Modification: Challenges and Prospects. *Starch/Stärke* 49: 127–131.

Besheer, A., Hause, G., Kressler, J., Mäder, K., (2007). Hydrophobically modified hydroxyethyl starch: synthesis, characterization, and aqueous self-assembly into nano-sized polymeric micelles and vesicles. *Biomacromol.* 8:359–367.

Bhowmik, D., Chiranjib, Jayakar R.M., (2009). Role of Nanotechnology in Novel Drug Delivery System. *J. Pharm. Sci. Technol.*1: 20–35.

Bhandari, P.N., Singhal, R.S., (2002). Studies on the optimisation of preparation of succinate derivatives from corn and amaranth starches. *Carbohydr. Polym*. 47: 277–283.

Bianco, A., Kostarelos, K., Prato, M. (2005). Applications of carbon nanotubes in drug delivery. *Curr. Opin. Chem. Biol.* 9: 674–679.

Berski, W., Ptaszek, A., Ptaszek, P., Ziobro, R., Kowalski, G., Grzesik, M., Achremowicz, B. (2011). Pasting and rheological properties of oat starch and its derivatives. *Carbohydr. Polym.* 83: 665–671.

Birrenbach, G., Speiser P.P., (1976). Polymerized Micelles and their use as Adjuvants in Immunology. *J. Pharm. Sci.* 65: 1763–1766.

Blanshard, J.M.V., Bates, D.R., Muhr, A.H., Worcester, D. L., Higgins, J.S., (1984). Small angle neutron scattering studies of starch granule structure. *Carbohydr. Polym*. 4: 427–442.

Boesel, L.F., Mano, J.F., Reis, R.L., (2004). Optimization of the formulation and mechanical properties of starch based partially degradable bone cements. *J. Mater. Sci. Mater. Med.* 15:73–83.

Brouillet, F., Bataille, B. Cartilier, L., (2008). High-amylose sodium carboxymethyl starch matrices for oral, sustained drug-release: Formulation aspects and in vitro drug-release evaluation. *Int. J. Pharm.* 356:52–60.

Carneiro, H.F, Tonon, R.V, Grosso, C.F., Hubinger, M.D., (2013). Encapsulation efficiency and oxidative stability of flaxseed oil microencapsulated by spray drying using different combinations of wall materials. *J. Food Eng.* 115: 443–451.

Carvalhoa S.M., Noronhaa C.M., Floriania C.L., Linoa R.C., Rochaa G. (2013.) Optimization of α-tocopherol loaded solid lipid nanoparticles by central composite design. *Ind. Crops Prod.* 49: 278–285.

Chawla, J.S., Amiji, M.M., (2002). Biodegradable poly (ε-caprolactone) nanoparticles for tumor-targeted delivery of tamoxifen. *Int. J. Pharm.* 249: 127–138.

Chen, Z., Schols, H.A., Voragen, A.G.J. (2004). Differently Sized Granules from Acetylated Potato and Sweet Potato Starches Differ in the Acetyl Substitution Pattern of their Amylose Populations. *Carbohydr. Polym.* 56: 219 – 226.

Cheng, M., Chen, H., Wang, Y., Xu, H., He, B., Han, J., Zhang, Z., (2014). Optimized synthesis of glycyrrhetinic acid-modified chitosan 5-fluorouracil nanoparticles and their characteristics. *Int. J. Nanomed*. 9: 695–710.

Chin, S.F., Pang, S.C., Tay, S.H., (2011). Size controlled synthesis of starch nanoparticles by a simple nanoprecipitation method: a short communication. *Carbohydr. Polym.* 86: 1817–1819.

Chin, S.F., Yazid, S.N., Pang, S.C., (2014). Preparation and Characterization of Starch Nanoparticles for Controlled Release of Curcumin. *Int. J. Polym. Sci.* 1:1–8.

Cho, H.J., Yoon, H.Y, Koo, H., (2011). Self assembled nanoparticles based on hyaluronic acid-ceramide (HA-CE) and Pluronic for tumor-targeted delivery of docetaxel. *Biomater.* 32: 7181–7190.

Chowdary, K.R., Radhaa, G.V., (2011). Synthesis, characterization and evaluation of starch acetate as rate controlling matrix former for controlled release of nifedipine, *Int. J. Chem. Sci.* 9: 449-456.

Chung, H.J., Lim, S.T., (2006). Physical aging of amorphous starches (a review). *Starch-Stärke* 58: 599–610.

Copeland, L., Blazek, J., Salman, H., Tang, M.C. (2009). Form and Functionality of Starch. *Food Hydrocoll.* 23: 1527–1534.

Couillet, I., Hughes, T., Maitland, F., (2005). Synergistic effects in aqueous solutions of mixed wormlike micelles and hydrophobically modified polymers. *Macromol.* 38: 5271–5282.

Dandekar, P., Jain, R., Stauner, T., Loretz, B., Koch, M., Wenz, G, Lehr, C.M. (2012). A hydrophobic starch polymer for nanoparticle-mediated delivery of docetaxel. *Macromol. biosci*. 12:184–194.

Daoud, S., Ringard-Lefebvre, C., Razzouq, N., Rosilio, V., Gillet, B., Couvreur, P., (2007). Spontaneous association of hydrophobized dextran and poly-beta-cyclodextrin into nanoassemblies. Formation and interaction with a hydrophobic drug. *J. Colloid Interface Sci.* 307*:* 83–93.

Derakhshandeh, K., Karimi, M., Azandaryani, A.H., Bahrami, G., Ghanbari, K., (2016). Pharmacokinetic study of furosemide incorporated PLGA microspheres after oral administration to rat. *Iranian J. Basic Medical Sci.* 19:1049–1055.

Desgouilles, S., Vauthier, C., Bazile, D., Vacus, J., Grossiord, J., (2003). The Design of Nanoparticles Obtained by Solvent Evaporation: A Comprehensive Study. *Langmuir* 19: 9504–9510.

Di Nardo, A., Wertz, P., Giannetti, A., Seidenari, S., (1998). Ceramide and cholesterol composition of the skin of patients with atopic dermatitis. *Acta Derm.-Venereol.* 78: 27–30.

D'Mello, S.R., Das, S.K., Das, N.G., (2009). Polymeric Nanoparticles for Small-Molecule Drugs: Biodegradation of Polymers and Fabrication of Nanoparticles. Drug Delivery Nanoparticles Formulation and Characterization: CRC Press pp16-34.

Drexler, K.E. (1987). "Engines of Creation -The Coming Era of Nanotechnology," Anchor, Reprint edition, New York.

Dutta, P.K., Dutta, J., Tripathi, V., (2004). Chitin and chitosan: chemistry, properties and applications. *J. Sci. Indust. Res.* 63: 20–31.

Efthimiadou, E.K., Metaxa A.F, Kordas G., (2014). Modified Polysaccharides as Drug Delivery. Springer International Publishing Swizerland, pp 1–26.

Ellis, R.P., Cochrane, M.P., Dale, M.F., Duþus, C.M., Lynn, A., (1998). Starch Production and Industrial Use. *J. Sci. Food Agri.* 77: 289–311.

Elomaa, M., Asplund, T., Soininen, P., Laatikainen, R., Peltonen, S., Hyvärinen, S., Urtti, A., (2004). Determination of the degree of substitution of acetylated starch by hydrolysis, 1H NMR and TGA/IR. *Carbohydr. Polym.* 57:261–267.

El-Feky, G.S., El-Rafie, M.H., El-Sheikh, M.A., El-Naggar, M.E., Hebeish A. (2015). Utilization of Crosslinked Starch Nanoparticles as a Carrier for Indomethacin and Acyclovir Drugs. *Nanomed. Nanotechnol.* 6:1–8.

Elsadek, B., Kratz, F., (2012). Impact of albumin on drug delivery-new applications on the horizon. *J. Control. Release* 157: 4–28.

Elzoghby, A.O, Samy, W.M., Elgindy, N.A., (2012). Albumin-based nanoparticles as potential controlled release drug delivery systems. *Rev. J. Control. Release* 157: 168–182.

Emmert, D.H., (2000). Treatment of common cutaneous Herpes SimplexVirus Infections. *American Family Physician* 61: 1697–1704.

Fechner, P.M., Wartewig, S., Futing, M., Heilmann, A., Neubert, R.H., Kleinebudde, P., (2003). Properties of microcrystalline cellulose and powder cellulose after extrusion/spheronization as studied by fourier transform Raman spectroscopy and environmental scanning electron microscopy. *AAPS Pharm. Sci.* 5: 77–89.

Fechner, P.M., Wartewig, S., Kleinebudde, P., Neubert, R.H., (2005). Studies of the retrogradation process for various starch gels using Raman spectroscopy. *Carbohydr. Res.* 240: 2563–2568.

Feczkó, T., Tóth, J., Dósa, Gy., Gyenis, J., (2011). Optimization of protein encapsulation in PLGA nanoparticles. *Chem. Eng. Process*. 50: 757–765.

Fessi, H., Puisieux, F., Devissaguet, J.P., Ammoury, N., Benita, S., (1989). Nanocapsule formation by interfacial polymer deposition following solvent displacement. *Int. J. Pharm.* 55: R1–R4.

Freiberg, S., Zhu, X.X., (2004). Polymer microspheres for controlled drug release. *Int. J. Pharm.* 282:1–18.

Freire, A.C., Fertig, C.C., Podczeck, F., Veiga, F., Sousa, J., (2009). Starch-Based Coatings for Colon-Specific Drug Delivery. Part I: The Influence of Heat Treatment on the Physico-chemical Properties of High Amylose Maize Starches. *Eur. J. Pharm. Biopharm.* 72: 574–586.

Galindo-Rodriguez, S., Allemann, E., Fessi, H., Doelker, E., (2004). Physicochemical parameters associated with nanoparticle formation in the salting-out, emulsification-diffusion, and nanoprecipitation methods. *Pharm. Res*. 21:1428–1439.

Gandhi, A., Jana, S., Sen, K., (2014). In-vitro release of acyclovir loaded Eudragit RLPO(®) nanoparticles for sustained drug delivery. *Int. J. Biol. Macromol.* 67:478–482.

Gardouh, A.R., Gad, S., Hassan, M., Ghonaim, H.M., Ghorab, M.M., (2013). Design and Characterization of Glyceryl Monostearate Solid Lipid Nanoparticles Prepared by High Shear Homogenization. *British J. Pharm. Res.* 3: 326–346.

Gardouh, A.R. Ghorab, M.M. Abdel-Rahman, S.G., (2012). Effect of viscosity, method of preparation and homogenization speed on physical characteristics of solid lipid nanoparticles. *ARPN J. Sci. Technol*. 2: 996–1006.

Garga, S., Jana, A.K., (2011). Characterization and evaluation of acylated starch with different acyl groups and degrees of substitution. *Carbohydr. Polym*. 83: 1623–1630.

Gaumet, M., Vargas, A., Gurny, R., Delie, F., (2008). NPs for drug delivery: the need for precision in reporting particle size parameters. *Eur. J. Pharm. Biopharm.* 69: 1–9.

Gazori, T., Khoshayand, M.R, Azizi E, (2009). Evaluation of Alginate/Chitosan nanoparticles as antisense delivery vector: ormulation, optimization and in vitro characterization. *Carbohydr. Polym.* 77: 599–606.

Gebre-Mariam, T., Abeba, A., Schmidt, P., (1996). Isolation and physico-chemical properties of enset starch. *Starch-Stärke* 48:208–214.

Gebre-Mariam, T., Schmidt, P (1998). Some physico-chemical properties of dioscorea starch from Ethiopia. *Starch-Stärke* 50:241–246.

Georgieva, D., Schmitt, V., Leal-Calderon, F., Langevin, D., (2009). On the Possible Role of Surface Elasticity in Emulsion Stability. *Langmuir* 25: 5565–5573.

Gonçalves, C., Gama, F.M., (2008). Characterization of the self-assembly process of hydrophobically modified dextrin. *Euro. Polym. J.* 44: 3529-3534.

Govender, T., Riley, T., Ehtezazi, T., Garnett, M.C., Stolnik, S., Illum, L., Davis, S.S. (2000). Defining the drug incorporation properties of PLA-PEG nanoparticles. *Int. J. Pharm.* 199: 95–110.

Guo, S, Huang, L., (2004). Nanoparticles Containing Insoluble Drug for Cancer Therapy. *Biotechnol. Adv.* 32: 778–788.

Guterres, S.S., Alves, M.P., Pohlmann, A.R., (2007). Polymeric nanoparticles, nanospheres and nanocapsules, for cutaneous applications. *Drug Target Insights* 2: 147–157.

Guzmán, K.A., Taylor, M.R., Banfield, J.F., (2006). Environmental Risks of Nanotechology: National Nanotechnology Initiative Funding, *Environ. Sci. Technol.* 40: 1401–1407.

Han, F., Gao, C., Liu, M. (2013). Fabrication and characterization of size-controlled starch-based nanoparticles as hydrophobic drug carriers. *J. Nanosci. Nanotechnol.* 13:6996–-7007.

Hermawan, E., Rosyanti, L., Megasari, L., Sugih, K., Muljana, H. (2015). Transesterification of Sago Starch Using Various Fatty Acid Methyl Esters in Densified CO2. *Int. J. Chem. Eng. Appl.* 6:152–155.

Hizukuri, S., Takeda, Y., Yasuda, M., and Suzuki, A. (1981). Multi-branched nature of amylose and the action of debranching enzymes. *Carbohydr. Res*. 94:205–213.

Hizukuri, S., (1986). Polymodal distribution of the chain lengths of amylopectins, and its significance. *Carbohydr. Res.* 147:342–347.

Huang, M., Khor, E., Lim, L-Y., (2004). Uptake and cytotoxicity of chitosan molecules and nanoparticles: effects of molecular weight and degree of deacetylation. *Pharm. Res.* 21: 344–353.

Hughes, G.A., (2005). Nanostructure-mediated drug delivery- Review Article. *J. Nanomed.: Nanotech. Biol. Med.* 1: 22–30.

ICH Guideline, (2003). Stability testing of new drug substances and products Q1A (R2), current step 4. https://www.fda.gov/downloads/drugs/guidances/ucm073369.pdf accessed on 03 April 2016.

Imokawa G., Abe A., Jin K., Higaki Y., Kawashima M., Hidano A., (1991). Decreased Level of ceramides in stratum-corneum of atopic-dermatitis – an etiologic factor in atopic dry skin. *J. Invest. Dermatol*. 96: 523–526.

Jagur-Grodzinski, J., (1999). Biomedical application of functional polymers. *React. Funct. Polym.* 39: 99–138.

Jane, J., Chen, Y.Y., Lee, L.F., McPherson, A.E., Wong, K.S., Kasemsuwan, T., (1999). Effects of Amylopectin Branch Chain Length and Amylose Content on the Gelatinization and Pasting Properties of Starch. *Cereal Chem. J.* 76: 629–637.

Jain, A.K., Khar, R.K., Ahmed, F.J., Diwan, P.V., (2008). Effective insulin delivery using starch nanoparticles as a potential trans-nasal mucoadhesive carrier. *Euro. J. Pharm. Biopharm.* 69:426-435.

Jain, R., Dandekar, P., Loretz, B., Melero, A., Stauner, T., Wenz, G., Koch, M., Lehr, C., (2011). Enhanced cellular delivery of idarubicin by surface modification of propyl starch nanoparticles employing pteroic acid conjugated polyvinyl alcohol: Pharmaceutical Nanotechnology. *Int. J. Pharm.* 420: 147–155.

Jiang, S., Dai L., Qin, Y., Xiong, L., Sun, Q., (2016). Preparation and Characterization of octenyl succinic anhydride modified Taro starch nanoparticles. *PLOS ONE* 11:1–11.

Jiang, B., Hu, L., Gao, C., Shen, J., (2005). Ibuprofen-loaded nanoparticles prepared by a co-precipitation method and their release properties. *Int. J. Pharm.* 304: 220–230.

Jin, Y-J., Ubonvan, T., Kim, D-D., (2010). Hyaluronic acid in drug delivery systems. *J. Pharm. Invest.* 40: 33–43.

Jong, W.H. Borm, P., (2008). Drug delivery and nanoparticles: applications and hazards. *Int. J. Nanomed.* 3: 133–149.

Jouyban A., (2009). Handbook of Solubility Data for Pharmaceuticals. - CRC Press, Boca Raton, Florida, USA. pp 1–35.

Ju B., Yan, D., Zhang S. (2012). Micelles Self-Assembled from Thermoresponsive 2-hydroxy 3- Butoxypropyl Starches for Drug Delivery. *Carbohydr. Polym.* 87: 1404–1409.

Jyothi, A.N., Moorthy, S.N., Rajasekharan, K.N. (2006). Effect of Cross-linking with Epichlorohydrin on the Properties of Cassava (*Manihot esculenta* Crantz) Starch. *Starch/Stärke* 58: 292–299.

Kalita, D., Kaushik, N., Mahanta, C.L., (2014). Physicochemical, morphological, thermal and IR spectral changes in the properties of waxy rice starch modified with vinyl acetate. *J. Food Sci. Technol.* 51:2790–2796.

Kayrak, D., Akman, U., Hortacsu, O., (2003). Micronization of Ibuprofen by RESS. *J. Supercrit. Fluids* 26: 17–31.

Kim, D., Duhamel, J., Amos, R., Gauthier, M., (2017). Characterization of Hydrophobic Modification of Starch NanoParticle by Pyrene Fluorescence. Accessed on 10/06/2017https://uwspace.uwaterloo.ca/bitstream/handle/10012/11276/Kim_Damin.pdf?sequence=5

Kizil, R., Irudayaraj, J., Seetharaman, K., (2002). Characterization of irradiated starches by using FT-Raman and FTIR Spectroscopy, *J. Agric. Food Chem*. 50:3912–3918.

Koo, O.M., Rubinstein, R., Onyuksel, H., (2005). Role of nanotechnology in targeted drug delivery and imaging: a concise review. *J. Nanomed.: Nanotechnol. Biol. Med.* 1: 193– 212.

Kshirsagar, A.C., Singhal, R.S., (2007). Optimization of starch oleate derivatives from native corn and hydrolyzed corn starch by response surface methodology. *Carbohydr. Polym.* 69:455–461.

Kumar, S., Rajikumar S., Ruckmani, K., (2003). Formulation and evaluation of ibuprofen loaded nanoparticles for improved anti-inflammatory activity. *Acta Pharm. Turcica* 45: 125–130.

Kusic, H., Jovic, M., Kos, N., Koprivanac, N., Marin, V., (2010). The comparison of photooxidation processes for the minimization of organic load of coloured waste water applying the response surface methodology, *J. Hazard Mater.* 183: 189–202.

Lam, C.W., James, J.T., McCluskey, R., Hunter, R.L., (2004). Pulmonary Toxicity of Single-Wall Carbon Nanotubes in Mice 7 and 90 Days after Intratracheal Instillation. *Toxicol. Sci.* 77: 126–134.

Lansky, S., Kooi, M., Schoch, T.J. (1949). Properties of the fractions and linear sub-fractions from various starches. *J. Am. Chem. Soc.* 71:4066–4075.

LeCorre, D., Bras, J., Dufresne, A., (2010). Starch nanoparticles: a review. *Biomacromol.* 11:1139–1153.

LeCorre, D., Bras, J., Dufresne, A., (2011). Influence of botanic origin and amylose content on the morphology of starch nanocrystals. *J. Nanopart. Res.* 13: 7193–7208.

Li, Y., Tan, Y., Ning, Z., Sun, S., Gao, Y., Wang, P. (2011). Design and fabrication of fluorescein-labeled starch-based nanospheres. *Carbohydr. Polym*. 86:291–295.

Lin, L., Liu, Q., Song, L., Liu, F., Sha, J., (2010). Recent advances in nanotechnology based drug delivery to the brain. Cytotechnol 62:377–380.

Liu, H., Ramsden, L., Corke, H., (1999). Physical properties of cross-linked and acetylated normal and waxy rice starch. *Starch/Stärke* 51: 249–252.

Liu, Z., Jiao, Y., Wang, Y., Zhou, C., Zhang, Z., (2008). Polysaccharides-based nanoparticles as drug delivery systems. *Adv. Drug Deliv. Rev.* 60:1650–1662.

Lorenz, K., Kulp, K. (1981). Heat moisture treatment of starches. II Functional properties and backing potential. *Cereal Chem.* 58: 49–52.

Lövestam, G., Rauscher, H., Roebben, G., Klüttgen, B.S., Gibson, N., Putaud, J., Stamm, H. (2010). Considerations on a Definition of Nanomaterial for Regulatory Purposes, Luxembourg: Publications Office of the European Union, pp 13-20.

Ma, X., Jian, R., Chang, P., Yu, J., (2008). Fabrication and characterization of citric acid-modified starch NPs/plasticized-starch composites. *Biomacromol.* 9:3314–3320.

Mahapatro, A. Singh, D.K., (2011). Biodegradable nanoparticles are excellent vehicle for site directed *in-vivo* delivery of drugs and vaccines. *J. Nanobiotechnol.* 9: 1–11.

Mainardes, R.M., Evangelista, R.C., (2005). PLGA nanoparticles containing praziquantel: effect of formulation variables on size distribution, *Int. J. Pharm.* 290:137–144.

Marin, E., Briceño, M.I., Caballero-George, C., (2013). Critical evaluation of biodegradable polymers used in nanodrugs. *Int. J. Nanomed.* 8: 3071–3091.

Markham, J.E., Lynch, D.V., Napier, J.A., Dunn, T.M., Cahoon, E.B., (2013). Plant sphingolipids: function follows form. *Curr. Opin. Plant Biol.* 16: 350–357.

Mathematica, Design Expert Software Version 8.0.7.1 http://www.statease.com/soft-ftp, (accessed on 02.09.16).

Minimol, P.F., Paul, W., Sharma, C.P., (2013). PEGylated starch acetate nanoparticles and its potential use for oral insulin delivery. *Carbohydr. Polym.* 95:1–8.

Mohanraj, V.J., Chen, Y. (2006). Nanoparticles – A Review. *Tropical J. Pharma. Res.* 5 (1): 561–573.

Moore, N., (2007). Ibuprofen: A journey from prescription to over-the-counter use. *J .Roy Soc. Med.* 100: 2–6.

Mora-Huertas, C.E., Fessi, H., Elaissari, A., (2010). Polymer-based nanocapsules for drug delivery. *Int. J. Pharm.* 385: 113–142.

Morris, G.A., Keok, S.M., Harding, S.E., (2010). Polysaccharide drug delivery systems based on pectin and chitosan. *Biotechnol. Gen. Eng. Rev*. 27: 257–284.

Motta, S., Monti, M., Sesana, S., Caputo, R., Carelli, S., Ghidoni, R., (1993). Ceramide composition of the psoriatic scale. *Biochim. Biophys. Acta* 1182: 147–151.

Motta, S., Monti, M., Sesana, S., Mellesi, L., Ghidoni, R., Caputo, R., (1994). Abnormality of water barrier function in psoriasis – role of ceramide fractions. *Arch. Dermatol*. 130: 452–456.

Mulhbacher, J., Ispas-Szabo, P., Lenaerts, V., Mateescu, M.A (2001). Crosslinked high amylose starch derivatives as matrices for controlled release of high drug loadings. *J. Control. Release* 76: 51-58.

Myrick, J.M., Vendra, V.K., Krishnan, S., (2014). Self-assembled polysaccharide nanostructures for controlled-release applications. *Nanotechnol. Rev*. 3:319-346.

Nakagawa, Y., Wakuri, S., Sakamoto, K., Tanaka, N., (1997). The Photogenotoxicity of Titanium Dioxide Particles. *Mutat. Res.* 394: 125–132.

Namazi, H., Fathi, F., Dadkhah, A., (2011). Hydrophobically modified starch using long-chain fatty acids for preparation of nanosized starch particles. *Scientia Iranica* 18:439–445.

Neubert, R.H.H., Sonnenberger, S., Dobner, B., Gray, C.W., Barger, K.N., Sevi-Maxwell, K., Sommer, E., Wohlrab, J. (2016). Controlled penetration of a novel dimeric ceramide into and across the stratum corneum using microemulsions and various types of semisolid formulations. *Skin Pharmacol. Phys.* 29: 130–134.

Nobs, L., Buchegger, F., Gurny, R., Allémann, E., (2004). Poly(lactic acid) nanoparticles labeled with biologically active Neutravidin™ for active targeting. *Eur. J. Pharm. Biopharm*. 58: 483–490.

Ochekpe, N., Olorunfemi, P., Ngwuluka, N., (2009). Nanotechnology and Drug Delivery Part 2: Nanostructures for Drug Delivery; a review. *Tropical J. Pharm. Res.* 8: 275–287.

Ofokansi, K., Winter, G., Fricker, G., Coester, C., (2010). Matrix-loaded biodegradable gelatin nanoparticles as new approach to improve drug loading and delivery. *Eur. J. Pharm. Biopharm.* 76: 1–9.

Olayinka, O., Adebowale, K., Olu-Owolabi, I., (2013). Physicochemical properties, morphological and X-ray pattern of chemically modified white sorghum starch. (*J. Food Sci. Technol.* 50: 70–77.

Onofre, F., Wang, Y., Mauromoustakos, A., (2009). Effects of structure and modification on sustained release properties of starches. *Carbohydr. Polym.* 76: 541–547.

Ozean, S., Jackson, D.S., (2005). Functionality behavior of raw and extruded corn starch mixtures. *Cereal Cherm.* 82(2): 223–227.

Ozsoy, Y., Gungor, S., Cevher, E., (2009). Nasal Delivery of High Molecular Weight Drugs: review. *Molecules* 14: 3754–3779.

Parveen, S., Misra, R., Sahoo, S.K., (2012). Nanoparticles: a boon to drug delivery, therapeutics, diagnostics and imaging: Review Article. *J. Nanomed.: Nanotechnol. Biol. Med.* 8: 147–166.

Paques J.P., van der Linden E., van Rijn C.J., Sagis L.M., (2014). Preparation methods of alginate nanoparticles. *Adv. Colloid Interface Sci.* 209:163–171.

Paulos, G., Endale, A., Bultosa, G., Gebre-Mariam, T., (2009). Isolation and physicochemical characterization of cassava starches obtained from different regions of Ethiopia. *Ethiopian Pharm. J.* 27: 42–54.

Paulos, G., Mrestani, Y., Heyroth, F., Gebre-Mariam, T., Neubert, R.H.H., (2016). Fabrication of acetylated dioscorea starch nanoparticles: Optimization of formulation and process variables. *J. Drug Deliv. Sci. Technol.* 31: 83–92.

Payne, G., Yi, H., Wu, L.Q. Bentley, W.E., Ghodssi, R., Rubloff, G.W., Culver, J.N., Payne, G.F., (2005). Biofabrication with chitosan, *Biomacromol.* 6:2881-2894.

Pérez, S., Baldwin, P.M., Gallant, D.J., (2009). Chapter 5 - Structural Features of Starch Granules I. In: Starch (Third Edition). Academic Press, San Diego, pp. 149–192.

Phillips, D.L., Liu, H., Pan, D., Corke, H. (1999). General application of Raman spectroscopy for the determination of level of acetylation in modified starches. *Cereal Chem.* 76: 439-443.

Pons, M., García, M.L, Vall, O., (1991). Influence of stabilizers on particle size and polydispersity of polybutyl- and polyisobutil-cyanoacrylate nanoparticles. *Colloid Polym. Sci.* 269: 855–858.

Raj, V., Prabha, G., (2015). Synthesis, characterization and in vitro drug release of cisplatin loaded Cassava starch acetate–PEG/gelatin nanocomposites. *J. Assoc. Arab Univ. Basic Appl. Sci.* 21:10–16.

Ranjan, A.P., Mukerjee, A., Helson, L., Vishwanatha, J.K. (2012). Scale up, optimization and stability analysis of Curcumin C3 complex-loaded nanoparticles for cancer therapy. *J.Nanobiotechnol*. 10:1–18.

Rao, J.P., and Geckeler, K.E. (2011). Polymer nanoparticles: Preparation techniques and size-control parameters. *Prog. Polym. Sci.* 36: 887–913.

Rampino, A., Borgogna, M., Blasi, P., Bellich, B., Cesàro, A. (2013). Chitosan nanoparticles: preparation, size evolution and stability. *Int. J. Pharm*. 455:219–228.

Reddy, I, Seib, P.A. (2000). Modified waxy wheat starch compared to modified waxy corn starch. *J. Cereal Sci*. 31: 25–39.

Reddy, N., Yang, Y. (2009). Preparation and properties of starch acetate fibers for potential tissue engineering applications. *Biotechnol. bioeng.* 103:1016-–1022.

Reis, C.P., Ferreira, J.P., Candeias, S., Fernandes, C., Martiniho, N., Aniceto, N., Cabrita, A.S., Figueiredo, I.V. (2014). Ibuprofen Nanoparticles for Oral Delivery: Proof of Concept. *J. Nanomed. Biotherapeutic Discov.* 4: 1–5.

Reis, C.P., Neufeld, R.J., Ribeiro, A.J., Veiga F., (2006)a. Nanoencapsulation I. Methods for preparation of drug-loaded polymeric nanoparticles. Nanomedicine: *Nanotechnol. Biol. Med.* 2: 8–21.

Reis, C.P., Neufeld R.J., Ribeiro A.J., Veiga F. (2006)b. Nanoencapsulation II. Biomedical applications and current status of peptide and protein nanoparticulate delivery systems. *Nanomed. Nanotech. Biol. Med.* 2: 53–65.

Rieux, A., Fievez, V., Garinot, M., Schneider, Y., Préat, V. (2006). Nanoparticles as potential oral delivery systems of proteins and vaccines: A mechanistic approach. *J. Control. Release* 116: 1–27.

Rodrigues, A., Emeje, M. (2012). Recent applications of starch derivatives in nanodrug delivery: Review. *J. Carbohydr. Polym.* 87: 987– 994.

Rogers J., Harding C., Mayo A., Banks J., Rawlings A. (1996). Stratum corneum lipids: the effect of ageing and the seasons. *Arch. Dermatol. Res.* 288: 765–770.

Roper , H. (1996). Applications of starch and its derivatives. *Carbohyd. Eur.* 15:4–21.

Sahle, F.F., Dobner, B., Wohlrab, J., Neubert, R.H.H., (2014). Controlled penetration of ceramides into and across the stratum corneum using various types of microemulsions and formulation associated toxicity studies, *Eur. J. Pharm. Biopharm.* 86: 244–250.

Sahle, F.F., Gebre-Mariam, T., Dobner, B., Wohlrab, J., Neubert, R.H.H., (2015). Skin diseases associated with the depletion of stratum corneum lipids and stratum corneum lipid substitution therapy, *Skin Pharmacol. Phys.* 28: 42–55.

Salar, R.K., Gahlawat, S.K., Siwach, P., Duhan, J.S., (2013). Biotechnology: Prospects and Applications. Springer India New Delhi, pp 39–52.

Sampaio, F., Gaveri, D., Mantovani, H., Passos, F., Perego, P., Converti, A., (2006). Use of response surface methodology for optimization of of xylitol production by the new yeast strain. *J. Food Eng.* 76: 376–386.

Sandhu, K.S, Singh, N., (2007). Some properties of corn starches II: Physicochemical, gelatinization, retrogradation, pasting and gel textural properties. *Food Chem.* 101:1499–1507.

Santander-Ortega, M.J., Stauner, T., Loretz, B., Vinuesa, J.L., González, D.B, Wenz, G., Schaefer, U.F., Lehr C.M., (2010). Nanoparticles made from novel starch derivatives for transdermal drug delivery. *J. Controlled Release* 141: 85–92.

Sarei, F., Dounighi, N.M, Zolfagharian, H., Khaki, P., Bidhendi, S.M. ,(2013). Alginate nanoparticles as a promising adjuvant and vaccine delivery system. *Indian J. Pharm. Sci.* 75(4):442-449.

Scheytt, T., Mersmann, P., Lindst R., Heberer, T., (2005). 1-octanol/water partition coefficients of 5 pharmaceuticals from human medical care: carbamazepine, clofibric acid, diclofenac, ibuprofen, and propyphenazone. *Water, Air, Soil Pollution* 165: 3–11.

Schwartz D, Whistler R (2009). History and future of starch. In BeMiller J, Whistler R "Starch: Chemistry and Technology" 3rd Ed., *Elsevier Inc*. pp. 1-10.

Shia, A., Li, D., Wang, L., Li, B., Adhikaric, B., (2011). Preparation of starch-based nanoparticles through high-pressure homogenization and miniemulsion crosslinking: influence of various process parameters on particle size and stability, *Carbohydr. Polym.* 83: 1604-1610.

Shao, C., Dowling, T.C., Haidar, S., Yu, L.X., Polli, J.E., Kane, M.A (2012). Quantification of Acyclovir in Human Plasma by Ultra-High-Performance Liquid Chromatography - Heated Electrospray Ionization - Tandem Mass Spectrometryfor Bioequivalence Evaluation. *J. Anal. Bioanal. Techniques* 3:1-6.

Sharma, N., Madan, P., Lin, S. (2016). Effect of process and formulation variables on the preparation of parenteral paclitaxel-loaded biodegradable polymeric nanoparticles: A co-surfactant study. *Asian J. Pharm. Sci.* 11:404-416.

Shi, A.m., Li, D., Wang, L.J., Li, B. Z., Adhikari, B. (2011). Preparation of starch-based nanoparticles through high-pressure homogenization and miniemulsion cross-linking: Influence of various process parameters on particle size and stability. *Carbohydr. Polym.* 83:1604-1610.

Shi, J, Votruba, A.R., Farokhzad, O.C., Langer, R., (2010) Nanotechnology in Drug Delivery and Tissue Engineering: From Discovery to Applications. *Nano Lett* 10: 3223–3230.

Shogren, R.L., Biswas, A., (2010). Acetylation of starch with vinyl acetate in imidazolium ionic liquids and characterization of acetate distribution. *Carbohydr. Polym.* 81:149-151.

Simi, C., Abraham, T., (2007). Hydrophobic grafted and cross-linked starch nanoparticles for drug delivery. *Bioprocess Biosyst. Eng.* 30:173–180.

Singh, A., Garg, G., Sharma, P.K. (2010). Nanospheres: a novel approach for targeted drug delivery system. *Int. J. Pharm. Sci. Rev. Res.* 5: 84-88.

Singh, A.V., Nath, L.K., (2013). Evaluation of chemically modified hydrophobic sago starch as a carrier for controlled drug delivery. *Saudi Pharm. J.* 21:193-200.

Singh, J., Kaur, L., McCarthy, O.J. (2007). Factors influencing the physico-chemical, morphological, thermal and rheological properties of some chemically modified starches for food applications-A review. *Food Hydrocol.* 21:1-22.

Singh, R., Lillard, J.W. (2009). Nanoparticle-based targeted drug delivery; review. *J. Exp. Mol. Path.* 86: 215–223.

Singha, J., Kaurb, L., McCarthy, O.J., (2007). Factors influencing the physico-chemical, morphological, thermal and rheological properties of some chemically modified starches for food applications-A review. *Food Hydrocol.* 21: 1-22.

Sodhi, N.S., Singh, N. (2005). Characteristics of acetylated starches prepared using starches separated from different rice cultivars. *J. Food Eng.* 70: 117–127.

Song, K.C. Lee, H.S. Choung, Y. Cho, K. Ahn, Y. Choi, E.J. (2006).The effect of type of organic phase solvents on the particle size of poly(d,l-lactide-co-glycolide) nanoparticles, Colloids Surfaces, *Physicochem. Eng. Aspects* 276: 162-167.

Soppimath, K., Aminabhavi, T., Kulkarni A., Rudzinski W. (2001). Biodegradable polymeric nanoparticles as drug delivery devices: Review. *J. Control. Release* 70: 1-20.

Subedi, R.K., Kang, K.W., Choi, H., (2009). Preparation and characterization of solid lipid nanoparticles loaded with doxorubicin. *Eur. J. Pharm. Sci.* 37: 508–513.

Suyao, X., Chunyi, T., Xuanming, L., Danmi, Y., Qiaoling, L., Changgang, X., Dongyin, T., Lijian, Z., (2006). Preparation of folate- conjugated starch nanoparticles and its application to tumor-targeted drug delivery vector. *Chin. Sci. Bull.* 51: 1693–1697.

Sweedman, M.C., Tizzotti, M.J., Schäferb, C., and Gilbert, R.G. (2013). Structure and physicochemical properties of octenyl succinic anhydride modified starches: A review. *Carbohydr. Polym*. 92: 905–920.

Swinkels J.J.M., (1985). Composition and properties of commercial native starches. *Starch/Stärke*, 37: 1-5.

Takács-Novák K, Avdeef A, Box KJ, Podányi B, Szász G (1994) Determination of protonation macro- and microconstants and octanol/water partition coefficient of the antiinflammatory drug niflumic acid. *J. Pharm. Biomed. Anal.* 12:1369–1377.

Tan, Y., Xu, K., Li, L., Liu, C., Song, C., Wang, P. (2009). Fabrication of size-controlled starch-based nanospheres by nanoprecipitation. *ACS Appl. Mater. Interfaces* 1: 956-959.

Tarvainen, M., Sutinen, R., Peltonen, S., Tiihonen, P., Paroneni, P. (2002). Starch Acetate: A Novel Film-Forming Polymer for Pharmaceutical Coatings. *J. Pharm. Sci*. 91: 282 – 289.

Tarvainen, M., Peltonen, S., Mikkonen, H., Elovaara, M., Tuunainen, M., Paronena, P., Ketolainen, J., Sutinen R. (2004). Aqueous Starch Acetate Dispersion as a Novel Coating Material for Controlled Release Products.*J. Control. Release* 96: 179 – 191.

Tessema, E.N., Gebre-Mariam, T., Lange, S., Dobner, B., Neubert, R.H.H., (2017). Potential application of oat-derived ceramides in improving skin barrier function: Part 1. Isolation and structural characterization. *J. Chromatogr. B Anal. Technol. Biomed. Life Sci.* 1066: 87–95.

Tessema, E.N, Gebre-Mariam, T., Paulos, G., Wohlrab, J., Reinhard, H.H. Neubert, R.H.H., (2018). Delivery of oat-derived phytoceramides into the stratum corneum of the skin using nanocarriers: Formulation, characterization and in vitro and ex-vivo penetration studies. *Eur. J. Pharm. Biopharm.* 127: 260–269

Tuovinen, L., Peltonen, S., Järvinen, K. (2003). Drug release from starch-acetate films *J. Control. Release* 91:345–354.

Tuovinen, L, Peltonen, S., Liikola, M., Hotakainen, M., Lahtela-Kakkonen, M., Poso, A, Järvinen, K. (2004). Drug release from starch-acetate microparticles and films with and without incorporated α-amylase. *Biomaterials* 25:4355–4362.

Valodkar, M, Thakore, S. (2011). Organically modified nanosized starch derivatives as excellent reinforcing agents for bionanocomposites. *Carbohydr. Polym.* 86:1244–1251.

Varnamkhasti BS, Hosseinzadeh H, Azhdarzadeh M, (2015). Protein corona hampers targeting potential of MUC1 aptamer functionalized SN-38 core–shell nanoparticles. *Int. J. Pharm.* 494: 430–444.

Vutpala S., Sailaja A.K. (2014). Preparation and characterisation of ibuprofen loaded polymeric nanoparticles by solvent evaporation technique. *Int. J. Pharm. Pharm. Sci.* 6: 416–421.

Wang, C., He, X., Fu, X., Luo, F., (2015). High-speed shear effect on properties and octenylsuccinic anhydride modification of corn starch. *Food Hydrocoll*. 44: 32–39.

Wasiak, I., Kulikowska, A., Janczewska, M., Michalak, M., Cymerman, I.A., (2016). Dextran Nanoparticle Synthesis and Properties. *PLoS ONE* 11:1-17.

Wattanachanta, S, Muhammad, K, Hashim, D.M, Rahman, R.A (2003). Effect of cross-linking reagents and hydroxypropylation levels on dual-modified sago starch properties. *Food Chem*., 80: 463-471.

Wei, W.H., Dong, X.M., Liu, C.G., (2015). In Vitro Investigation of Self-Assembled Nanoparticles Based on Hyaluronic Acid-Deoxycholic Acid Conjugates for Controlled Release Doxorubicin: Effect of Degree of Substitution of Deoxycholic Acid. *Int. J. Mol. Sci.* 16: 7195–7209.

Wilkins, M., Wang, P., Xu, L., Niu, Y., (2003) Variability in starch acetylation efficiency from commercial waxy corn hybrids. *Cereal Chem.* 80:68-71.

Winarti, C., Sunarti, T. C., Mangunwidjaja, D. and Richana, N., (2014). Preparation of arrowroot starch nanoparticles by butanol-complex precipitation, and its application as bioactive encapsulation matrix. *Int. Food res. J.* 21:2207-2213.

Wu, C.Y., Benet L.Z., (2005). Predicting drug disposition via application of BCS: transport/ absorption/ elimination interplay and development of a biopharmaceutics drug disposition classification system. *Pharm. Res.* 22:11-23.

Wurzbugr, O.B. (1964). Esters: acetylation. In: Whistler R ed, Methods in carbohydrate chemistry, 4th edn, Academic Press, New York, pp 286-288.

Xu, Y., Ding, W., Liu, J., Li, Y., Kennedy, J.F., Gu, Q., Shao, S. (2010). Preparation and characterization of organic-soluble acetylated starch nanocrystals. *Carbohydr. Polym.* 80:1078-1084.

Xu, Y., Miladinov, V., Hanna, M.A. (2004). Synthesis and characterization of starch acetates with high substitution. *Cereal Chem.* 81:735-740.

Xu, Z.P., Zeng, Q.H, Lu, G.Q., Yu, A.B. (2006). Inorganic nanoparticles as carriers for efficient cellular delivery. *Chem Eng Sci.* 61:1027–1040.

Yu, D., Xiao, S., Tong, C., Chen, L., Liu, X. (2007). Dialdehyde starch nanoparticles: preparation and application in drug carrier, *Chin. Sci. Bull.* 52:2913-2918.

Zhang, C., Gu, C., Peng, F., Liu, W. Wan, J., Xu, H., Lam, C.W. Yang, X. (2013). Preparation and optimization of triptolide-loaded solid lipid nanoparticles for oral delivery with reduced gastric irritation. *Molecules* 18:13340-13356.

Zhang, J.F., Sun, X. Z. (2004). Mechanical properties of PLA/starch composites compatibilized by maleic anhydride. *Biomacromolecules* 5: 1446–1451.

Zhang, Y., Chen, T., Yuan, P., (2015). Encapsulation of honokiol into self-assembled pectin nanoparticles for drug delivery to HepG2 cells. *Carbohydr. Polym.* 133: 31–38.

Zhang, Z., Gao, F., Bu, H., Xiao, J., Li, Y., (2011). Solid lipid nanoparticles loading Candesartan cilexetil enhance oral bioavailability: in vitro characteristics and absorption mechanism in rats. http://dx.doi.org/10.1016/j.nano.2011.08.016 (accessed on 24/03/2012)

Zhu K.J., Li Y., Jiang H.L., Yasuda H., Ichimaru A. (2005). Preparation, characterization and in vitro release properties of ibuprofen-loaded microspheres based on polylactide, poly(ε-caprolactone) and their copolymers. *J. Microencapsulation* 22: 25-36.

Zobel, H., Young, S., Rocca, L. (1988). Starch gelatinization: An X-ray diffraction study. *Cereal Chem.* 65:443-446.

Appendices

Appendix A

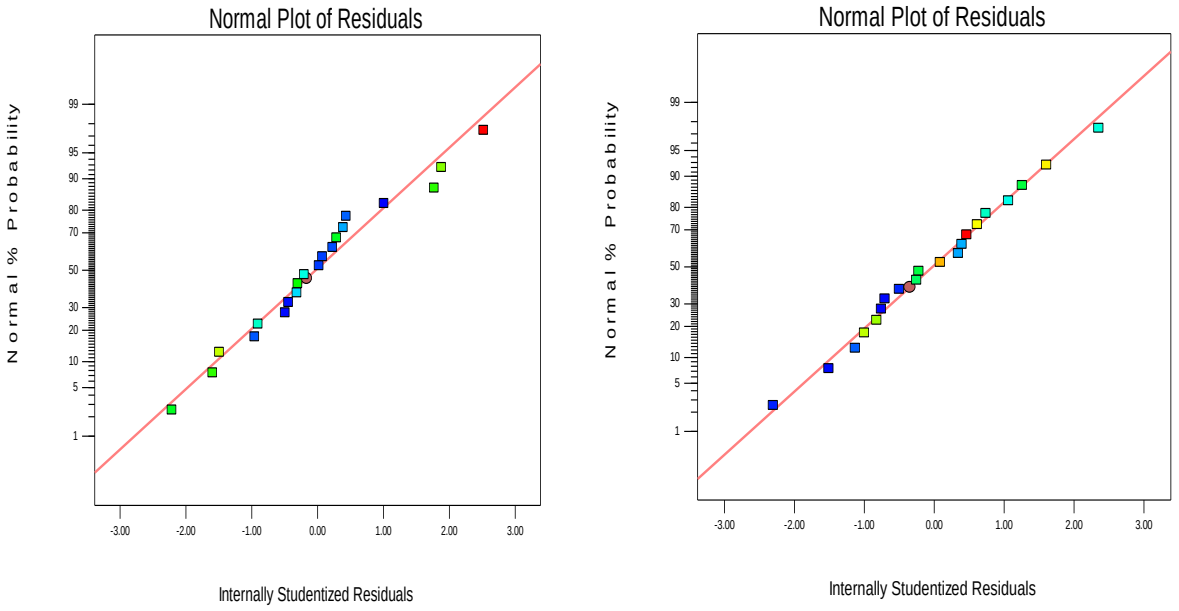

a b

Fig. 1: Normal probability plot of residuals for cassava SANPs a) particle size b) PDI

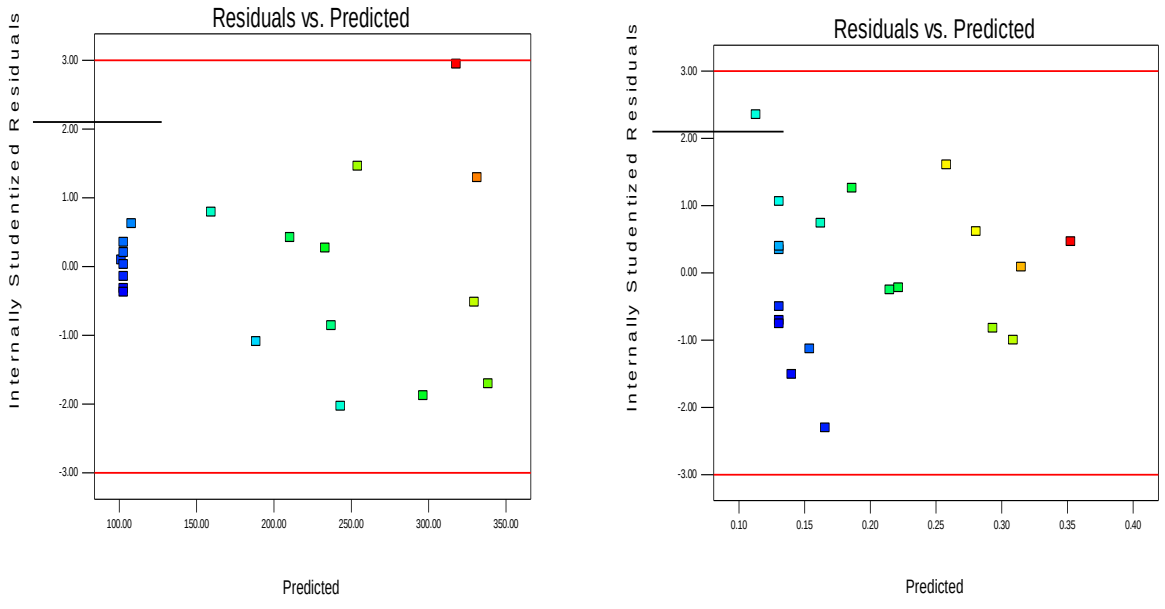

a b

Fig. 2: Plots of the residuals against predicted response for cassava SANPs a) particle size b) PDI

Appendix B

Calibration curve for Ibuprofen

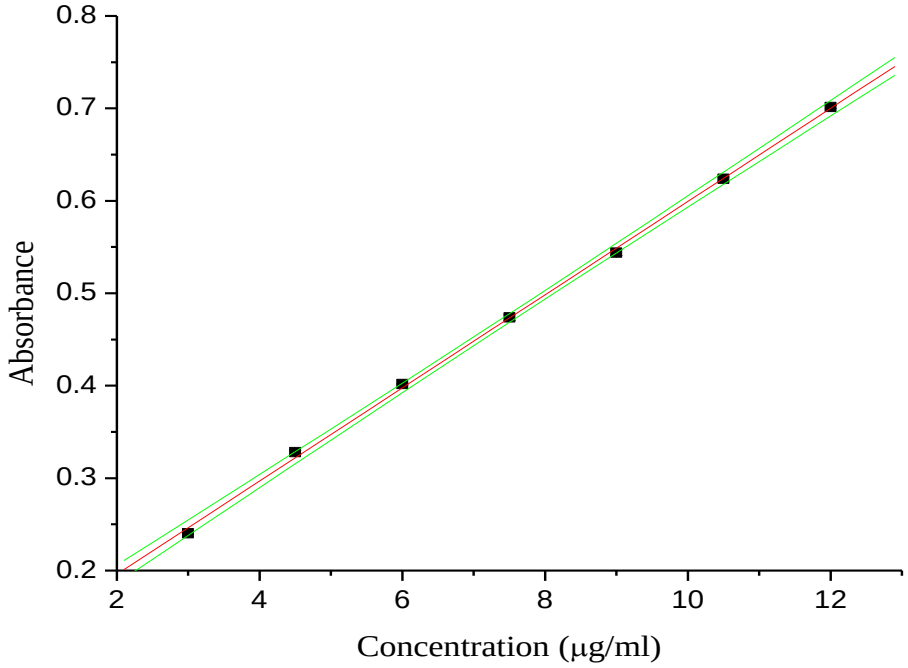

Fig. 1: The UV absorption calibration curve of ibuprofen in PBS (pH 7.4) at 221 nm with 95% confidence bands for mean, (r^2 = 0.9993).

Calibration curve for Acyclovir

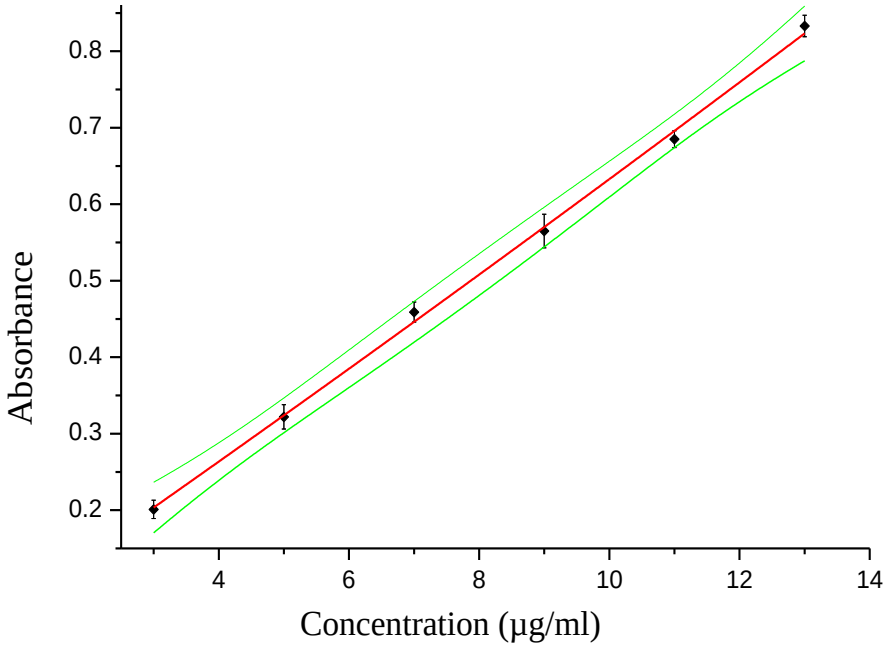

Fig. 2: The UV absorption calibration curve of acyclovir in PBS (pH 7.4) at 252 nm with 95% confidence bands for mean, (r^2 = 0.9983).

Calibration curve for Furosemide

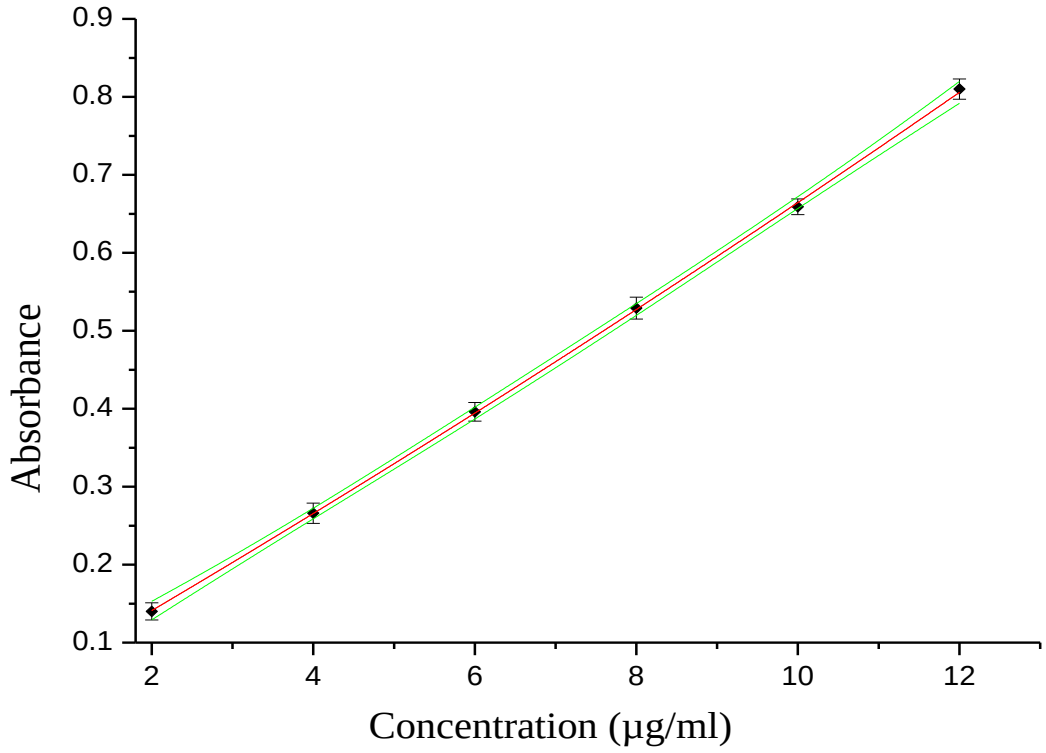

Figure 3: The UV absorption calibration curve of furosemide in PBS (pH 7.4) at 271 nm with 95% confidence bands for mean, (r^2 = 0.9992).

Appendix C

Cassava SA NPs

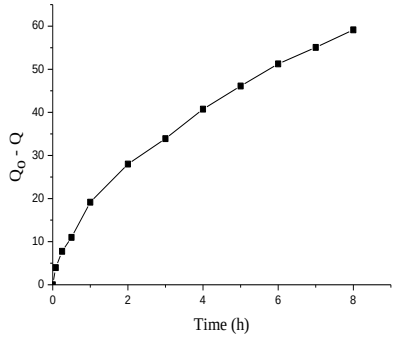

O-order release

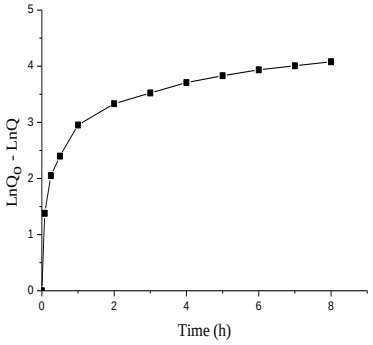

1st order release

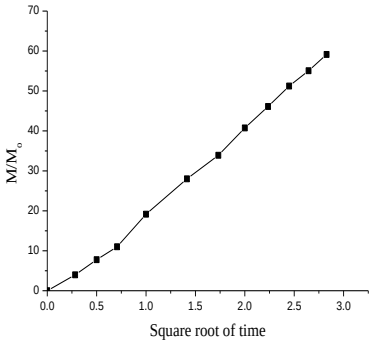

Higuchi release

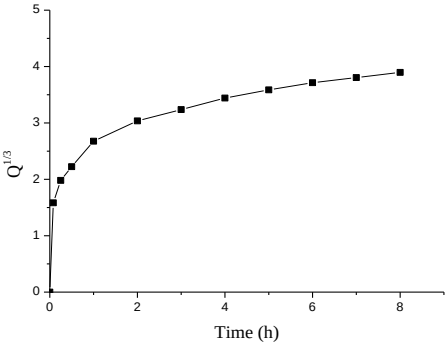

Hixson Crowell release

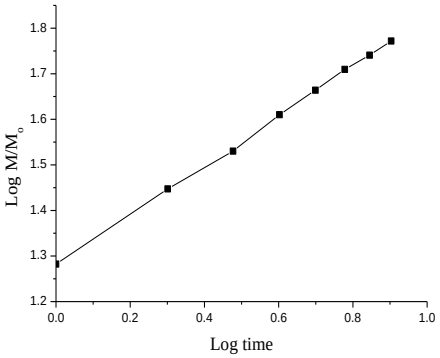

Korsmeyer-Peppas release

Dioscorea SA NPs

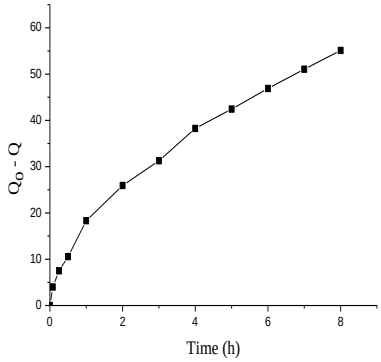

O-order release

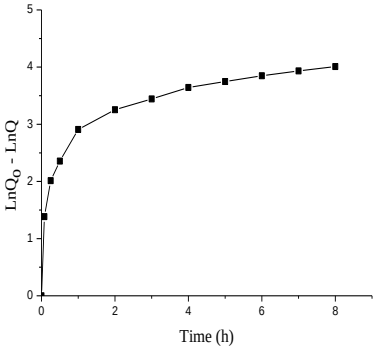

1st order release

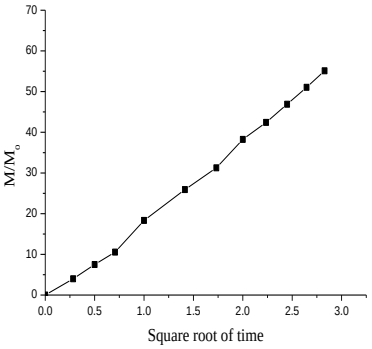

Higuchi release

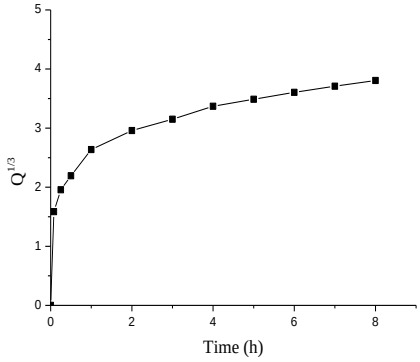

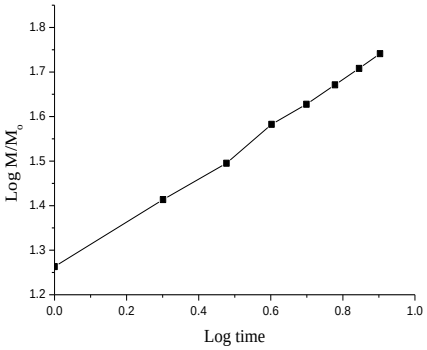

Hixson Crowell release) Korsmeyer-Peppas release

Enset SA NPs

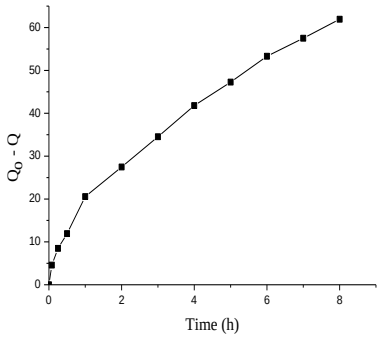

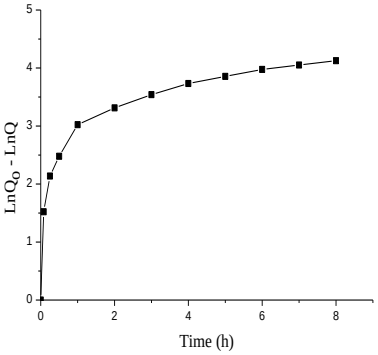

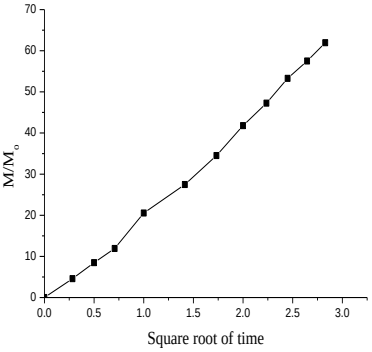

O-order release 1st order release Higuchi release

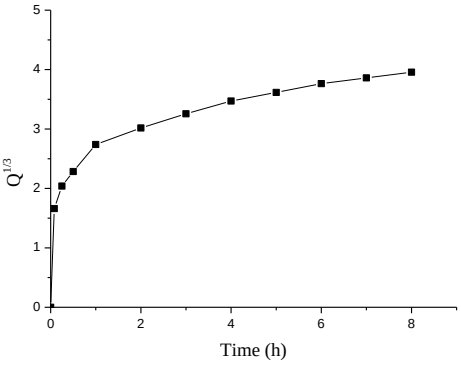

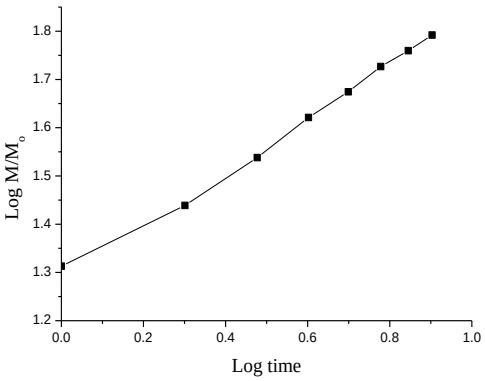

Hixson Crowell release) Korsmeyer-Peppas release

Maize SA NPs

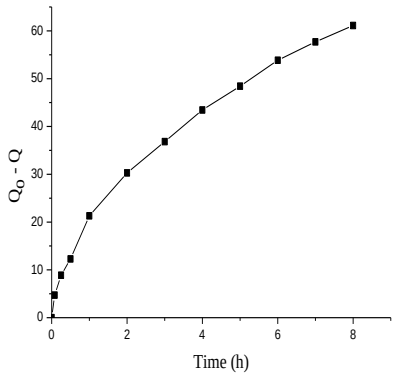

O-order release

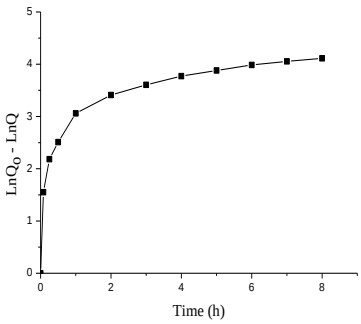

1st order release

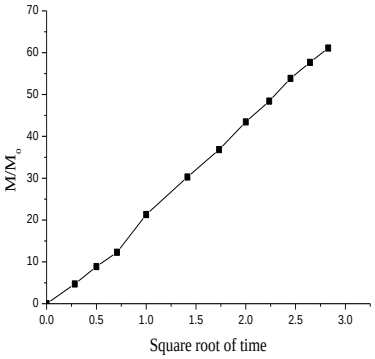

Higuchi release

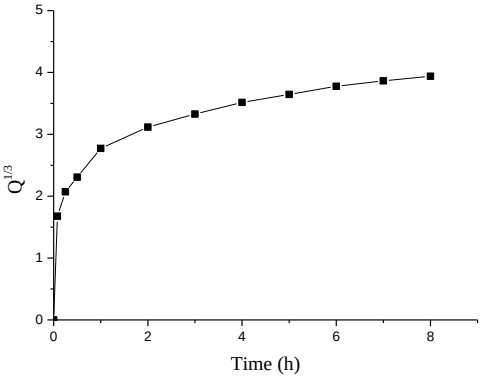

Hixson Crowell release)

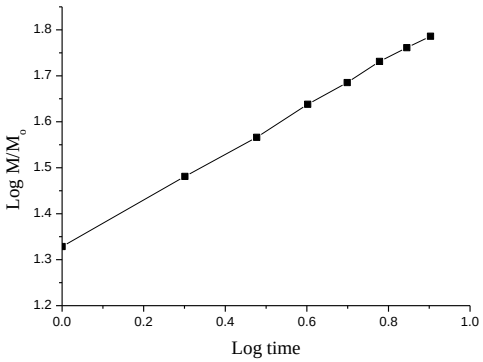

Korsmeyer-Peppas release

The various drug release kinetic models [zero order, first order, Higuchi, Hixson-Crowell and Korsmeyer-Peppas] of the SA nanoparticles studied.